Scheduling Strategies for Relay of Mars Rover data via Mars Orbiter and Earth Stations

Master's Thesis
to achieve the degree
Master of Science
in the SpaceMaster Program

handed in by

Jendrik Jördening
born on February 22nd 1993 in Braunschweig

Department of Control Engineering
Faculty of Electrical Engineering
Czech Technical University in Prague
2016

Co-funded by the
Erasmus+ Programme
of the European Union

Handed in on August 12th 2016

Supervisor at CTU Prague:	Antonin Novak
Supervisor at ESOC:	Adam Williams

Abstract: In this thesis, the relay communication between landed assets on the surface of Mars via a relay orbiter to Earth is studied for its latencies and the times which can be provided for the landed asset to work and for the ground to plan depending on the operational margins, the available ground station network and the available relay orbiters.

In this context, an automated solver is developed to evaluate a locally optimal strategy of relay pass assignment respecting the different constraints and is proven to provide a solution close to the globally optimal one. The solver is determining the link opportunities and reasons on them, by minimising a cost function for each relay pass and choosing the cheapest ones in an iterative process.

With this solver, it is shown that the best operational approach is to await commands confirmation and to provide the possibility of resending corrupted files. Moreover, it is shown that a 24/7 ground station coverage should be ideally provided, on which priority for booking should be given to relay missions since they depend on the actual timing of the orbiter overflights over the lander. Furthermore, it is shown that adding additional relay orbiters increases the solution space drastically, making it desirable to use them. The possibility to restrict cross-agency support is assessed, showing that cross-support is still eligible.

Finally, the data volume is shown to be sufficient to fulfil the ExoMars Rover and Surface Platform mission requirements, when using multiple orbiters, even though the solver itself would need extra capabilities to cope with allocating appropriate relay passes.

Czech Technical University in Prague
Faculty of Electrical Engineering

Department of Control Engineering

DIPLOMA THESIS ASSIGNMENT

Student: **Jendrik Jördening**

Study programme: Cybernetics and Robotics
Specialisation: Systems and Control

Title of Diploma Thesis: **Scheduling Strategies for Relay of Mars Rover data via Mars Orbiter and Earth Stations**

Guidelines:

The thesis aims on investigating and solving the scheduling problems introduced by a communication link to a mars rover via a Mars orbiting satellite. Hereby, ground station bookings and network latencies shall be minimised as possible and recommendations shall be provided for the future operations engineer.

1. Define the problem, study related literature and investigate current solution process for basic scenarios.
2. Propose and implement a solution for the problem of optimizing latencies in the overall network and station booking times.
3. Extend proposed solution to include multiple orbiters and ground stations.
4. Evaluate proposed solutions and discuss key parameters influences.

Bibliography/Sources:

[1] L. Barbulescu, J.-P. Watson, L. D. Whitley, and A. E. Howe, Scheduling space–ground communications for the air force satellite control network, Journal of Scheduling, vol. 7, no. 1, pp. 7-34, 2004.

[2] J. Y. Leung, Handbook of scheduling: algorithms, models, and performance analysis. CRC Press, 2004.

[3] L. Barbulescu, A. Howe, and D. Whitley, Afscn scheduling: How the problem and solution have evolved, Mathematical and Computer Modelling, vol. 43, no. 9, pp. 1023-1037, 2006.

[4] P. Brucker and P. Brucker, Scheduling algorithms, vol. 3. Springer, 2006.

Diploma Thesis Supervisor: Ing. Antonín Novák

Valid until the summer semester 2016/2017

L.S.

prof. Ing. Michael Šebek, Dr.Sc.
Head of Department

prof. Ing. Pavel Ripka, CSc.
Dean

Prague, February 24, 2016

Preface

I want to start by thanking all the people helping in any manner with this Master thesis.
Special thanks are going out to the ESOC staff, in particular to Tiago Loureiro and Adam Williams for making it possible to write this thesis in such a marvellous and friendly environment, with the most interesting tasks and the possibility to gather a tremendous amount of knowledge about space missions. Thank you as well for reading the thesis multiple times and pointing out the mistakes in it. Special thanks as well to Bruno Sousa for establishing the contact for this position. Moreover, I want to thank Johannes Bauer for introducing me to the basics of relay communication. In addition to that, I want to thank the whole ExoMars RSP FCT for supporting me with this thesis and doing the error correction for it. It is a pleasure to work with you!
Furthermore, I want to thank Tonda Novak for correcting this thesis and providing outstanding academic support for it. You resolved a lot of confusions and problems!
I want to thank all the other SpaceMaster students as well. It was a pleasure studying with you.
Thanks go as well out to the European Union and the European Space Agency. Without these institutions, neither my study program nor the mission on which my thesis based would exist.
In addition, I would like to thank for the support of the Education, Audiovisual and Culture Executive Agency of the Commission of the European Communities under the Erasmus Mundus Framework.
Finally, I want to thank my family, who always supported me, being it emotional, financial or in any other way. Without your support, this thesis would not exist.

Disclaimer

This project has been funded with support from the European Commission. This publication [communication] reflects the views only of the author, and the Commission cannot be held responsible for any use which may be made of the information contained therein.

Declaration of Authorship

I, J.Jördening, hereby declare that this thesis titled, *"Scheduling Strategies for Relay of Mars Rover data via Mars Orbiter and Earth Stations"* and the work presented in it are my own. I authored this thesis independently without prohibited help of third parties. Furthermore, I declare that all reference are marked as such. I confirm that:

- This work was done wholly or mainly while in candidature for a master degree at Czech Technical University.
- Where any part of this thesis has previously been submitted for a degree or any other qualification at this University or any other institution, this has been clearly stated.
- Where I have consulted the published work of others, this is always clearly attributed.
- Where I have quoted from the work of others, the source is always given. With the exception of such quotations, this thesis is entirely my own work.
- I have acknowledged all primary sources of help.
- Where the thesis is based on work done by myself jointly with others, I have made clear exactly what was done by others and what I have contributed myself.

Signature:

Date: August 12th 2016

Contents

1 Introduction

Since the beginning of time, humankind is fascinated by the night sky. Already in ancient times several lights in the sky were known to wander over it. One of the bright ones was named after the Roman war-god Mars, due to its reddish colour. With the rise of telescopes in the medieval age, the first scientific observations of its surface were performed by Galileo Galilei, who observed as well the varying phases of Mars in 1608 [1]. Many attempts were made to predict the Martian movement, but only the measurements of Tycho Brahe allowed Johannes Kepler to define his three Keplerian laws, describing the movement of the planets and their relative distance to each other [2]. This revealed that Mars is Earth's direct outer neighbour. This fact and the fact that the temperatures and pressures can be withstood by a typical spacecraft made it a desirable goal with the start of human spaceflight programmes in the late 1950s. These programs led to 40 Mars missions until today, of which 16 were successful. With the Viking program in the 1970s in the U.S. and the Mars program of the Soviet Union, a unique problem had to be solved: How to get data from another planet's surface back to Earth? For this two options are available. One is a direct communication link to Earth, making big antennae and transceivers necessary on the lander. The other is to position a relay orbiter around the other planet, communicating with the landed asset when flying over it and relaying the received data to Earth [3, 1]. Using a relay orbiter, it can be avoided to either land heavy and voluminous antenna on the other planet, or accepting lower data rates, due to a small signal to noise ratio. However, the timing of the overflights is problematic, since the communication times are short and depend on the orbit of the relay satellite. This problem increased even further when the landers got the capability to move with the launch of Mars Pathfinder and its rover Sojourner in 1996 [1]. Due to the movement, the data have to be counterchecked more often to avoid hitting obstacles and losing the rover or its movement capability. For Sojourner, the problem was still limited, since it only moved 100 m during the whole mission [1]. For the NASA rovers Spirit and Opportunity, launched in 2003 [1], the approach was to have a direct X-band link between Earth and a sun-synchronous relay orbiter, providing a relay pass at Martian morning and one at Martian evening [4]. This allows forwarding commands in the morning, working during daylight and getting the results for planning during the Martian night. This approach lead to 98% of the data being relayed instead of being directly transmitted [4].

The European Space Agency (ESA) and the Russian Space Agency (Roscosmos) are planning a joint mission, which shall deliver a rover and a surface platform to Mars in the frame of the ExoMars program. For this, the operations approach from Spirit and Opportunity can not be utilised, since the prime relay orbiter, the Trace Gas Orbiter (TGO), has a fixed, non-sun-synchronous science orbit and no direct link to Earth is available. Therefore, a more dynamic approach has to be taken, still allowing to work during Martian day and to plan during Martian night, even when the times of the overflights are varying over the whole day. It shall be as well possible to evaluate the necessary ground station bookings for the mission within this approach. Finally, the default operational procedure used

at ESOC shall be reviewed, with respect to the impact of it on the latency in the relay communication. An introduction to the theory of the problem is given in Chapter 2, followed by a definition of the problem and several sub-problems in Chapter 3. To solve this problem, the input data, provided by different entities, have to be prepared, which is explained in Chapter 4 and processed by a solver, which is described in Chapter 5. With this solver all sub-problems are solved their results are presented in Chapter 6 and the conclusions, which can be drawn from those, are shown in Chapter 7, providing recommendations on the overflight usage, the ground station bookings and the operational approach.

1.1 Contributions

This thesis is contributing to resolve the issue of scheduling relay data links via an orbiter to Mars by covering the following points:

- Defining the problem which has to be solved specifically and discussing why current methods can not be utilised for it.
- Providing an algorithm capable of determining a locally optimal trade-off between Rover Working Time (RWT) and Earth Planning Time (EPT), while keeping the overall latencies and ground station time as low as possible, being as well applicable on a problem horizon of several years, without requiring more computational resources than an average personal computer can offer.
- Extending the algorithm to provide multi-orbiter solutions.
- Extending the algorithm to provide multi-lander solutions.
- Showing that the performance of the solver is close to the global optimum
- Evaluating the key parameters and providing a recommendation on how they shall be chosen to solve this problem.
- Providing a solution for all landed assets at Mars, using all orbiters in circular orbits.

2 Preliminaries

This chapter offers an introduction to the theoretical background of this thesis. It provides the underlying ideas for the reasoning in this thesis. It starts with a presentation of the ExoMars RSP mission in Sec. 2.1, followed by a section on Mars with a particular focus on the definition of Martian time in Sec. 2.2. Afterwards, a general introduction to the operation of a spacecraft is provided in Sec. 2.3. Finally, the classification of scheduling problems is discussed in Sec. 2.4, the input sources used are described in Sec. 2.5 and a short introduction to Poincaré-Plots is given in Sec. 2.6.

2.1 The ExoMars RSP mission

The ExoMars RSP mission aka ExoMars 2020 is a joint ESA-Roscosmos mission, which shall land a surface platform and a rover on Mars. They are transported to Mars using a European carrier module, equipped with an X-band medium gain antenna [5] and separated shortly before entry into the Martian atmosphere. Afterwards, the Russian descent module is in charge of landing the composite of surface platform and rover at Mars. The current prime landing site for that is Oxia Planum at 18.20°N and −24.55°E and the secondary one to be selected from Mawrth Vallis at 22.16°N and −17.05°E and Aram Dorsum at 7.87°N and −11.22°E [6, 7]. Following separation, the only way of communicating with the surface platform and the rover is a relay link via an orbiter equipped with an Ultra High Frequency (UHF) radio, since neither of the assets is suited for deep-space communication. Via this relay link 150 Mbits have to be transmitted per sol and asset. [8, 9]

The Rover has the scientific goal to find well-preserved organic material and to investigate the physical and chemical properties of geological samples [9]. The rover is moving using six wheels, which can be steered independently of each other [10]. For navigation purposes, it is equipped with a panoramic camera to allow terrain mapping. Furthermore, it is fitted with a drill, capable of penetrating the Martian surface to a depth of 2 m. This drill includes a multispectral imager for investigation of the borehole walls. In addition, a small drill sample can be transported to the internal analytical laboratory for further analysis using four instruments. Moreover, it holds a spectrometer acquiring in the visible and infrared spectrum, a Raman spectrometer for the analysis of the mineralogical composition and the identification of organic pigments, an organic molecule analyser targeting biomarkers and a close-up imager to acquire high-resolution colour close-ups. To determine suitable positions for drilling, it is also equipped with an infrared spectrometer, determining the mineralogical composition of surface targets. This is supported by a ground penetrating radar and a neutron detector [11], providing information about the geological composition below the rover. [12]

The Surface Platform will remain at the landing site, taking context images and doing long-term atmosphere and climate observations. For this it is equipped with multiple instruments: A radio sci-

ence experiment, a habitability, brine irradiation and temperature package, a meteorological package, a magnetometer, a set of cameras, an Infrared Fourier spectrometer, an active neutron spectrometer and dosimeter, a Multi-channel Diode-Laser spectrometer, a radio thermometer for soil temperatures, a dust suite, a seismometer and a gas chromatography-mass spectrometer. [13]

2.2 Mars

Mars is the fourth inner planet of our solar system and therefore Earth's outer neighbour. With an equatorial radius of 3396.2 km it is half the size of Earth, while the distance to the sun is on average 1.523 AU, leading to a duration of a Martian year of 686.98 d and a One Way Light Time (OWLT) to Earth between 3.2 min and 22.3 min (Eqn.(2.18)). The Martian temperature is on average 210 K and the atmospheric pressure 6.36 mbar at the mean radius. Mars is orbited by two small moons called Phobos, with a subplanetary axis radius of 13.0 km and polar one of 9.1 km, and Deimos, with a subplanetary axis radius of 7.8 km and polar one of 5.1 km. [1, 2]

2.2.1 Martian Time

The ExoMars Rover has a desired RWT during the Martian day. Therefore, a definition of Martian time is necessary. For that, the Coordinated Mars Time (MTC) analogue to Earth's Coordinated Universal Time (UTC) was proposed. This is defined as the mean solar time measured at Martians prime meridian, which is going through the centre of the crater Airy-0 [7], and is given by Eqn.(2.3). In addition to that, it is necessary to determine the Mars time depending on the longitude, because Mars does not have any time zones. This time is the Local Mean Solar Time ($LMST$) and is given by Eqn.(2.4). In addition to that, the eccentric orbit of Mars leads to a shift of noon in the range of $[-50, 40]$ min. Since most missions depend on power provided by solar arrays, this is taken into account when defining the Local True Solar Time ($LTST$) in Eqn.(2.12). Finally, the length of the days varies due to the seasons on Mars. The Martian dusk and dawn are calculated using Eqn.(2.17). The formulae used for the derivations are hereby provided in [14].

The Coordinated Mars Time (MTC) can be retrieved by performing several steps. First, the Julian Date needs to be determined. This was done using the milliseconds elapsed since the 1st Jan 1970 (t_{unix}) and Eqn.(2.1), where the first summand gives the offset of the 1st Jan 1970 from Julian day zero. Since UTC does not take leap seconds into account, but the milliseconds are provided in it, the Terrestrial Time (TT) would go further and further ahead. By adding the leap seconds, using the USNO leap second tabular for dates after January 1st 1972, the Julian date in TT can be calculated with Eqn.(2.2). With this, the MTC can be determined, using the fact that on the January 6th 2000 midnight on Earth and Mars were only separated by 0.0009626 sol. This way the offset of JD_{TT} to that date can be divided by the length of the Martian day compared to the length of an Earth day, which is $1.0274912517\frac{\text{d}}{\text{sol}}$. To that number, 44796.0 sols are added to define the sol zero on Mars such that the first precisely dated measurements are afterwards. Then, the separation factor is subtracted. Finally, the result modulo 24 gives the Martian hour, leading to Eqn.(2.3).

$$JD_{\mathrm{UT}} = 2440587.5\,\mathrm{d} + \left(\frac{t_{\mathrm{unix}}}{8.64 \cdot 10^7 \frac{\mathrm{ms}}{\mathrm{d}}}\right) \tag{2.1}$$

$$JD_{\mathrm{TT}} = JD_{\mathrm{UT}} + \left(\frac{TT - UTC}{86400 \frac{\mathrm{s}}{\mathrm{d}}}\right) \tag{2.2}$$

$$MTC = \mathrm{mod}_{24}\left\{24\,\mathrm{h}\left(\frac{JD_{\mathrm{TT}} - 2451549.5\,\mathrm{d}}{1.0274912517\,\frac{\mathrm{d}}{\mathrm{sol}}} + 44796.0\,\mathrm{sol} - 0.0009626\,\mathrm{sol}\right)\right\} \tag{2.3}$$

The Local Mean Solar Time ($LMST$) can be directly derived from MTC using the longitude of the target (Λ) and Eqn.(2.4).

$$LMST = MTC - \Lambda\frac{1\,\mathrm{h}}{15^\circ} \tag{2.4}$$

The Local True Solar Time ($LTST$) has the property that noon is actually at the highest solar elevation. To derive it the time offset from the J2000 epoch ($\Delta t_{\mathrm{J2000}}$) has to be determined using Eqn.(2.5).

$$\Delta t_{\mathrm{J2000}} = JD_{\mathrm{TT}} - 2451545.0\,\mathrm{d} \tag{2.5}$$

With this offset Mars' orbital parameters can be determined, starting with the mean anomaly M applying Eqn.(2.6), the angle of the fiction mean sun α_{FMS} exploiting Eqn.2.7 and the perturbers PBS ,using Eqn.(2.8), with the parameters for the perturbers from Tab. 2.1.

$$M = 19.3871^\circ + \frac{0.52402073^\circ}{\mathrm{d}}\Delta t_{\mathrm{J2000}} \tag{2.6}$$

$$\alpha_{\mathrm{FMS}} = 270.3871^\circ + \frac{0.524038496^\circ}{\mathrm{d}}\,\Delta t_{\mathrm{J2000}} \tag{2.7}$$

$$PBS = \sum_{i=1}^{7} A_i \cos\left[\left(\frac{0.985626^\circ}{\mathrm{d}}\Delta t_{\mathrm{J2000}}/\tau_i\right) + \phi_i\right] \tag{2.8}$$

i	A_i	τ_i	ϕ_i
1	0.0071	2.2353	49.409
2	0.0057	2.7543	168.173
3	0.0039	1.1177	191.837
4	0.0037	15.7866	21.736
5	0.0021	2.1354	15.704
6	0.0020	2.4694	95.528
7	0.0018	32.8493	49.095

Table 2.1: The different perturbers for the Martian orbit

With these orbital parameters, the equation of centre can be defined as the difference between the true and mean anomaly to be Eqn.(2.9), from which the areocentric solar longitude (L_{s}) can be determined

with Eqn.(2.10). Using both, the equation of time (EOT) can be determined using Eqn.(2.11).

$$\begin{aligned}\nu - M = &\left(10.691^\circ + \frac{3.0^\circ}{\mathrm{d}} \cdot 10^{-7}\Delta t_{\mathrm{J2000}}\right)\sin M + 0.623^\circ \sin 2M \\ &+ 0.050^\circ \sin 3M + 0.005^\circ \sin 4M + 0.0005^\circ \sin 5M + PBS\end{aligned} \tag{2.9}$$

$$L_{\mathrm{S}} = \alpha_{\mathrm{FMS}} + (\nu - M) \tag{2.10}$$

$$EOT = 2.861^\circ \sin 2L_{\mathrm{S}} - 0.071^\circ sin4L_{\mathrm{S}} + 0.002^\circ \sin 6L_{\mathrm{S}} - (\nu - M) \tag{2.11}$$

Using the equation of time, the local true solar time is given as:

$$LTST = LMST + \frac{EOT\,\mathrm{h}}{15^\circ} \tag{2.12}$$

Dawn and Dusk can be as well determined using the orbital parameters of Mars. For that, the solar declination on Mars (δ_s) has to be determined using Eqn.(2.13). While knowing Λ and the planetographic latitude (ϕ) of the lander, the local solar azimuth (A) and zenith (Z) angle can be determined using Eqn.(2.14) and Eqn.(2.15). With latter, the dawn and dusk hour angle can be determined by setting the equation equal zero, leading to Eqn.(2.16) from which the actual time can be derived using Eqn.(2.17).

$$\delta_{\mathrm{S}} = \arcsin\{0.42565 \sin L_{\mathrm{S}}\} + 0.25^\circ \sin L_{\mathrm{S}} \tag{2.13}$$

$$A = \arctan(\sin H/(\cos\phi \tan\delta_{\mathrm{S}} - \sin\phi \cos H)) \tag{2.14}$$

$$Z = \arccos(\sin\delta_{\mathrm{S}} \sin\phi + \cos\delta_{\mathrm{S}} \cos\phi \cos H) \tag{2.15}$$

$$H_{\mathrm{d}} = \Lambda - \Lambda_{\mathrm{S}} = \pm(\arccos(-\tan\delta_{\mathrm{S}} \tan\phi)) \tag{2.16}$$

$$h_{\mathrm{d}} = 12\,\mathrm{h} - H_{\mathrm{d}}\frac{\mathrm{h}}{15^\circ} \tag{2.17}$$

2.3 Operation of Spacecraft

The operation of each spacecraft has the goal to "maximise [the] mission return" [15]. Amongst a lot of other necessities to reach this goal, a data link has to be established between the spacecraft and the operations centre. Its characteristics are described in Sec. 2.3.1. In the case of relay operations, an additional link has to be established between the spacecraft and the lander after uplinking the commands to and before downlinking them from the spacecraft. This link is described in detail in Sec. 2.3.2. Furthermore, a default operations procedure, providing the necessary steps and safety measures to operate a spacecraft, is defined by each agency operating spacecraft, depending on their experience. The default procedure at ESOC is described in Sec. 2.3.3.

2.3.1 Communication in Deep Space

Aside from the calculation of gains, including the design of antennae and transceivers for a mission, which are out of the scope of this thesis, there are several other important characteristics in deep space communication. The OWLT, describing the time light needs to travel until reaching a target, is discussed in Sec. 2.3.1.1. In addition to that, the solar conjunction, which is preventing communication, is described in Sec. 2.3.1.2. Finally, the ground station network used for this communication

is discussed in Sec. 2.3.1.3.

2.3.1.1 One Way Light Time

The OWLT is the time a signal propagating with the speed of light needs to reach a specific object in space. It can be calculated knowing the distance to the object (d) and the speed of light ($c = 299792458\frac{\mathrm{m}}{\mathrm{s}}$[16]) using Eqn.(2.18). It provides information about the time required to command a spacecraft or to receive a reply to a request from it. Since the OWLT is in the case of deep space missions a lot higher than the latency between the operations centre and the ground stations, it is a driving factor of latencies in a deep space communication.

$$\mathrm{OWLT} = \frac{d}{c} \tag{2.18}$$

2.3.1.2 Solar Conjunction

The Sun is a strong source of electromagnetic radiation. Therefore, it can disturb the communication link between a spacecraft and Earth when it is in a side lobe of the antenna radiation pattern. For parabolic antennae, which are typically used for communication on deep space spacecraft, the side lobes decrease drastically with the deviation from the nominal angle. Therefore, the disturbance increases as the angle between the Sun and the communication link is shrinking. Since this angle can be measured at two points, this leads to a separation of the problem depending on the reference point of view. One point of view is the angle between the sun and the communication link seen by Earth, and the other is the angle seen by the spacecraft. The angle seen by Earth is hereby the one which is more critical since the signal to noise ratio on the downlink is a lot lower than on the uplink. Thus, the noise introduced by the Sun impacts the downlink more than the uplink. Hereby, communication to spacecraft is stopped if the angle seen from Earth is smaller than three degrees. The angles from both points of view are provided by Flight Dynamics in the Eventfile described in Sec. 9.6.1.

2.3.1.3 Ground Station Network

The ground station network available for ESA missions can be seen in Fig. 2.1 from [17]. In this, a separation in three groups can be seen, core ESA network, cooperative network and augmented network. Since our goal is to command a spacecraft in deep space, the augmented network can be neglected since it provides only antennas which are too small to achieve the necessary gain. From the two other groups, the ESA core network describes antennae, which are always available to ESA spacecraft and are therefore only limited by the usage due to other ESA spacecraft. For using cooperative network antennae, a dedicated agreement has to be signed with the provider. On top of those restrictions, the mission we are interested in has a high distance to the Earth. Therefore, only the so-called Deep Space Antennae can establish a communication link with it. The deep space antennae of the core ESA network are New Norcia (NNO), Cebreros (CEB) and Malargüe (MLG), which are as well referred to as the ESTRACK deep space antennae. From the cooperative network Goldstone (GDS), Madrid (MAD) and Canberra (CAN) have this capability and are usually referred to as National Aeronautics and Space Administration (NASA) Deep Space Network (NASA DSN). In addition to those antennae, either the Bear Lakes (BLK) or Kalyazin antenna (KLZ) close to Moscow can be used. Since the TGO and ExoMars RSP are joint Roscosmos-ESA missions, they are allowed to use one of these stations

Figure 2.1: The ESTRACK network [17]

as the only missions coordinated from ESOC. Therefore, neither BLK nor KLZ is currently indicated in the ESTRACK map of cooperative networks. For all those stations there is a recommendation on the minimum elevation for communication with a spacecraft set by ESTRACK to be 10 degrees. This avoids ground-based radiation sources being in the side lobe of the antenna, guaranteeing a certain robustness on the downlink and avoids non-compliance with International Telecommunication Union (ITU) restrictions and clutter on the uplink.

ESTRACK Deep Space Antennae The ESTRACK network holds three Deep Space Antennae NNO, CEB and MLG. Being part of ESTRACK, those antennae can be booked to support the ExoMars RSP mission. Each booking is done in an iterative process with ESTRACK and other missions using it to avoid conflicts.

NNO is the Deep Space Antenna 1 near New Norcia, Australia, located at Long: 116° 11′ 29.40″ E and Lat: 31° 2′ 53.61″ S. It hosts an antenna dish with 35 m in diameter and can transceive in the S- and X-Band and can be seen in Fig. 2.2.[18]

CEB is the Deep Space Antenna 2 near Madrid, Spain, located at Long: 4° 22′ 09.68″ W and Lat: 40° 27′ 09.68″ N. It hosts an antenna dish with 35 m in diameter and can transceive in X-Band and receive in K_α-Band and can be seen in Fig. 2.3.[19]

MLG is the Deep Space Antenna 3 near Malargüe, Argentine, located at Long: 69° 23′ 53.31″ W and Lat: 35° 46′ 33.63″ S. It hosts an antenna dish with 35 m in diameter and can transceive in

X-Band and receive in K_α-Band and can be seen in Fig. 2.4.[20]
While transceiving data, all stations provide as well location and tracking capabilities to the ESOC Flight Dynamics Office.

Figure 2.2: The NNO deep space antenna [18]

Figure 2.3: The CEB deep space antenna [19]

Figure 2.4: The MLG deep space antenna [20]

Table 2.2: A Summary of the relay orbiters and their capabilities

NASA DSN The NASA DSN holds multiple deep space antennae spread over three sites, GDS, MAD and CAN. Each of those sites holds minimum antennae of the following diameters, three 34 m, one 26 m and one 70 m. GDS is hereby located in the U.S. Army's Fort Irwin Military Reservation, in the Mojave Desert, USA, at Long: 116° 53′ 24″W and Lat: 35° 25′ 36″N. MAD is located at Long: 4° 14′ 53″W and Lat: 40° 25′ 53″N. CAN is based on Long: 148° 58′ 54″E and Lat: 35° 24′ 05″S. [21]

BLK The Bear Lakes antenna is situated close to Moscow at Long: 37° 57′ 16″ E and Lat: 55° 55′ 59″ N [22]. It holds an antenna with 64 m in diameter, via which signals shall be transceived in S- and X-Band [23], in the year 2018. [24].

KLZ The Kalyazin antenna is similar to the BLK one and is situated close to Moscow as well at Long: 37° 56′ 42″ E and Lat: 57° 11′ 38″ N [22]. It holds an antenna with 64 m in diameter, via which signals shall be transceived in S- and X-Band [23], in the year 2018. Due to its similar position compared to BLK key parameters generated for BLK are nearly the same as for KLZ.

2.3.1.4 Allocation of ground station passes (booking)

When a ground station shall be booked by a mission several constraints have to be met. First of all, the bookings are scheduled in advance in communication with different missions to provide a conflict-free allocation. For this, internal priorities are given within each network to the missions depending on their scientific or commercial purpose and constraints. For the ESTRACK deep space antennae network, these allocations are typically fixed six to twelve months in advance with reconsiderations two months and two weeks in advance and two weeks in advance on the NASA DSN. The bookings made by spacecraft operated from ESOC are provided in the Planview file, which provides nearly the overall load on the ESTRACK deep space antennae. While allocating passes, the following constraints shall be respected:

- A deep space ground station needs 45 min in advance of the Acquisition of Signal (AOS) to be configured for the communication with the spacecraft
- It requires 15 min after Loss of Signal (LOS) to be deconfigured

Therefore, a station can only be used for tracking a spacecraft if it is free for the desired tracking time and 45 min before and 15 min after it. The whole time a station is booked is hereby referred to as activity time, while the time without configuration and deconfiguration times is referred to as tracking time.

2.3.2 Relay Communication

Due to the great distance between Mars and Earth and the corresponding high Free Space Path Loss (FSPL), big antennae and powerful transceivers are needed for communication between assets located at the different planets. Big antennae are however heavy and powerful transceivers require large solar panels to provide sufficient power to them. Getting those into orbit around Mars already requires a huge amount of fuel, but when landing them an extra $\Delta v \geq 3551.1\,\frac{\mathrm{m}}{\mathrm{s}}$ is needed, corresponding to the first orbital velocity calculated with Eqn.(2.23) from [25] using $r = r_{\mathrm{M,eq}}$. Some of this velocity can be provided using parachutes, but a lot of it has to be provided using fuel. Therefore, a relay communication via an orbiter around the planet can be established avoiding this costly landing. A sketch of such a link can be seen in Fig. 2.5. Two links can be provided in this setup, a forward link and a return link. A forward link describes the sending of commands from the lander operations centre via the orbiter operations centre and the ground station to the orbiter from which they are forwarded to the lander. A return link describes the inverse. The data are sent by the landed asset to the orbiter which downlinks them to a ground station from which they are forwarded via the orbiter operations centre to the lander operations centre. The orbiters available for such communications are listed and shortly described in Sec. 2.3.2.1 and the geometry and an estimate of the data rates can be determined using the equations derived in Sec. 2.3.2.2 and Sec. 2.3.2.3.

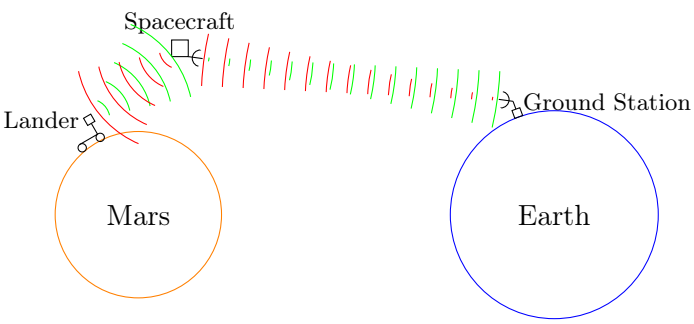

Figure 2.5: The sketch of a Mars-Earth transmission of information using a relay orbiter for telecommands (red) and telemetry (green)

2.3.2.1 Available Relay Orbiters

Currently, there are five satellites that might be available for relay communication when the RSP mission arrives at Mars. Those missions, their scientific objectives and orbits are described shortly in the following sections.

Trace Gas Orbiter (TGO) The joint ESA-Roscosmos TGO satellite is planned to be the prime relay service provider for the ExoMars RSP mission. It was launched on the 14th March 2016 [27]. Its mission objectives are "to search for evidence of methane and other trace atmospheric gases that could be signatures of active biological or geological processes on Mars" [28]. For this mission the spacecraft shall reach a circular orbit at an altitude of 400 km and an inclination of 74° after orbit insertion in October 2016 and an aerobraking phase starting in November 2016. The phasing of the orbit will hereby depend on the performance of the aerobraking. For the scope of this thesis, a phasing is assumed and propagated. The TGO is equipped with an Electra radio to communicate with landed assets providing Adaptable Datarates (ADR) to maximise the data return. It consists of an Electra UHF transceiver, coaxial cables and low-gain quadrifilar helix antennae [29] and is provided by the Jet Propulsion Laboratory (JPL). Finally, the TGO will require six hours of tracking time to downlink its scientific data. These can be shifted as required for the relay communication.

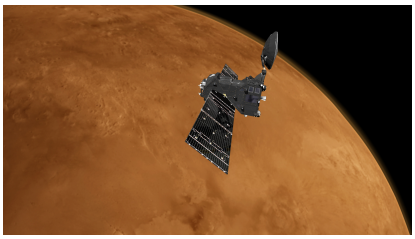

Figure 2.6: Artist's impression of the TGO at Mars [26]

Mars Atmospheric and Volatile Evolution Mission (MAVEN) The NASA MAVEN orbiter was launched on the 18th November 2013 and is currently in an elliptical orbit with perigee of 150 km altitude, an apogee of 6200 km and an inclination of 75° [31]. The missions objectives are to determine the role that losses of volatiles to space from the Martian surface played through time, the current state of the upper atmosphere and ionosphere and interactions with the solar wind, determining the current rates of escape of neutral gases and ions to space and determining the ratios of stable isotopes in the Martian atmosphere [29]. In addition to this MAVEN is equipped with an Electra radio to provide relay service with adaptable data rates.

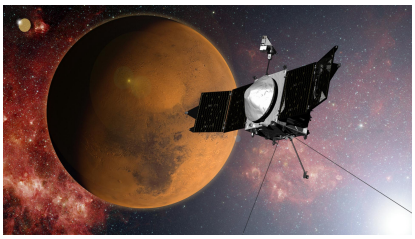

Figure 2.7: An Artist's impression of MAVEN at Mars [30]

Mars Reconnaissance Orbiter (MRO) The NASA MRO orbiter was launched on the 12th August 2005 and was the first Martian orbiter situated with an Electra radio. It is located in a slightly elliptical orbit with a perigee at 255 km altitude and an apogee at 320 km altitude. The orbit is inclined by 93° for sun-synchronisation. [31] Its scientific objective is to gather the history of water persistence on Mars by visually analysing minerals, looking for subsurface water and monitoring the global weather [33]. Multiple signs of instrument failures lead to a switch over to the redundant Inertial Measurement Unit (IMU) and the availability of only one travelling wave tube amplifier [31]. However, the orbiter is investigated for its capability for relaying for the RSP mission, since it might be available.

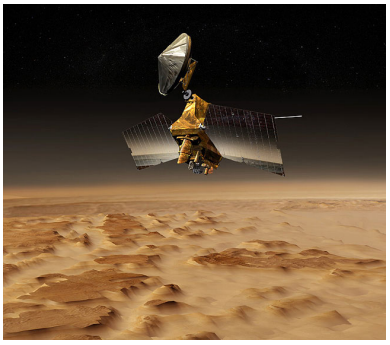

Figure 2.8: An Artist's impression of MRO at Mars [32]

Mars EXpress (MEX) The ESA MEX orbiter was launched on the 2nd June 2003 and is stationed in an elliptical orbit around Mars with an altitude of 330 km at perigee and 10530 km at apogee and an orbital inclination of 86.9°. MEX provided a multiplicity of scientific data throughout its mission, e.g. as probing of the polar regions of Mars, detection of hydrated minerals, including phyllosilicates and possible detection of methane in the atmosphere. Its current provisional mission end is the 31st December 2018, but the extension process is currently ongoing. The health status of the spacecraft gives an indication, that it will be available until 2022 from a technical point of view, so the orbiter is eventually available for relay services for the RSP mission [35] depending on the propellant left and the battery lifetime. Unlike MAVEN, TGO and MRO, MEX situates a Melacom transceiver, working with fixed data rates from 2 to 128 kbps, making it less suitable for relay operations than other orbiters.

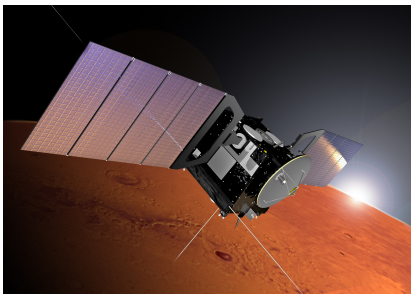

Figure 2.9: An Artist's impression of MEX at Mars [34]

Odyssey NASA's Odyssey orbiter, launched on the 7th April 2001, is currently the oldest of the spacecraft orbiting Mars [37]. Situated in a sun-synchronous orbit at 400 km altitude and an inclination of 93° [31]. Its main scientific mission is to determine the distribution of minerals, the presence of certain chemical elements in the surface and to study the radiation environment. Furthermore, it relayed over 95% of the Mars Exploration Rovers back to Earth [37]. For this relay operations, it is situated with a CE-505 transceiver with data rates up to 256 kbits. Depending on its further propellant consumption and the health of its reaction wheels, one of which is failed, Odyssey might be available for relay service for the RSP mission. [31]

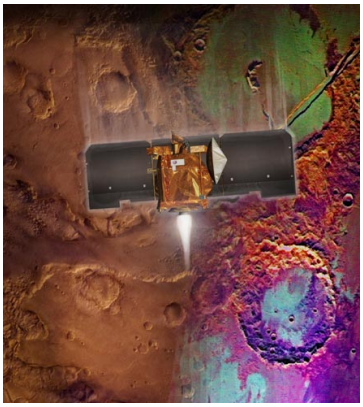

Figure 2.10: An Artist's impression of Odyssey at Mars orbit insertion [36]

Spacecraft	Orbit	Relay Radio	Health
TGO	400 km circular 74° inclination non-sun-synchronous	Electra 1-2048 kbps ADR	no issues on board
MAVEN	150 × 6200 km 75° inclination non-sun-synchronous	Electra 1-2048 kbps ADR	no issues on board
MRO	255 × 320 km 93° inclination sun-synchronous	Electra 1-2048 kbps ADR	using redundant IMU only one travelling wave tube amplifier available
MEX	330 × 10530 km 86.9° inclination non-sun-synchronous	Melacom 2-128 kbps	little propellant remaining battery lifetime
Odyssey	400 km circular 93° inclination sun-synchronous	CE-505 8-256 kbps	little propellant remaining one reaction wheel failed

Table 2.3: A summary of the different relay orbiter and their capabilities

2.3.2.2 Elevation and Azimuth Profile

In order to communicate with a lander via a satellite, a clear line-of-sight between those two is necessary during the communication time and the gain has to be high enough to transmit data. Furthermore, it is possible to change between landed assets during an overflight if the elevation is high enough for both of them and a 70 s switching time is provided to the Electra radio [38]. An illustration of an overflight over a single asset is sketched in Fig. 2.11. Hereby, the satellite needs to have a minimum elevation over the horizon, from the lander's perspective, in order to establish a communication link. This is indicated as the lander's horizon plane. The periods where the satellite is above this horizon plane are derived for specific minimum elevation values by the Flight Dynamics office, using the orbit of the satellite and the desired landing location, and are provided in the Eventfile. However, it is necessary to derive the elevation and azimuth profile during an overflight since those are required to calculate the link budget and data volume of the data link. For this, no formulae could be found in the literature which uses the overflight duration as a starting point. Therefore, a new approach is developed in this thesis, using the values for specific elevations from the Flight Dynamics office to countercheck the derived values.
For a satellite in a circular orbit, these can be derived assuming that the length of the semi-major axis of the satellites orbit (a), the inclination of it (i), the location of the landing site (Λ, Φ) and the overflight duration (T_{over}) are provided. Having this information, the orbital period can by directly calculated using Eqn.(2.19) from [25]. Afterwards, the velocity of the satellite with respect to the landing site has to be determined by splitting it into cartesian coordinates. Hereby, the z-axis is pointing upwards, the x-axis in the direction of the Martian rotation and the y-axis such that a right handed system is formed. This step is necessary since the overflight duration is determined in the rotating reference frame of Mars. This rotation is extending or shortening the overflight duration depending on the inclination of the satellites orbit. To perform this transformation the angle between the orbital plane of the satellite and the plane lander-centre of Mars, being the minimum nadir angle (η_{min}), has to be determined, using Eqn.(2.20). This formula can be derived using the triangle which is sketched purple-red-brown dashed lines in Fig. 2.11 and calculating its sides using the Pythagorean theorem. However, it can be seen, that Eqn.(2.20) depends on the velocity of the satellite in the horizontal plane. When deriving this velocity using the rotational speed of Mars at the landing site from Eqn.(2.21), the orbital angle of the satellite from Eqn.(2.22) (illustrated in Fig. 2.12) and parsing them into Eqn.(2.28), it can be seen that this velocity depends on the minimum nadir angle. This circular dependency can be resolved using Banach's fixed-point theorem, which states that:

Banach's fixed-point theorem. *"Let (X, d) be a non-empty complete metric space with a contraction mapping $T : X \to X$. Then T admits a unique fixed-point x^* in X (i.e. $T(x^*) = x^*$). Furthermore, x^* can be found as follows: start with an arbitrary element x_0 in X and define a sequence x_n by $x_n = T(x_{n\text{-}1})$, then $x_n \to x^*$."*

Since $\arctan(f(\eta_{\text{min}})) \in [-\pi, \pi]$ $\forall \eta_{\text{min}}$ the function obviously transfers every value from the interval $[-\pi, \pi]$ back to this interval. Furthermore, by using the metric $d = \sqrt{(x-y)^2}$ and the fact that $\frac{\mathrm{d}}{\mathrm{d}\eta} \arctan(x(\eta)) = \frac{1}{x^2+1} \frac{\mathrm{d}x}{\mathrm{d}\eta} < 1$ $\forall x$, it can be concluded that this function is a contraction. This and Banach's fixed-point theorem lead to the conclusion that for every arbitrary starting value for the minimum nadir and every overflight duration the actual minimum nadir can be found by repeatedly

solving the equation and taking the new value as the start value for the next iteration. It can be even found in a finite number of iterations when assuming a finite error.

$$T_{\text{sat}} = 2\pi\sqrt{\frac{a^3}{\mu_{\text{M}}}}\left(1+\frac{3}{2}\frac{J_{2,\text{M}}R_{\text{M}}^2}{a^2(1-e^2)}\left(\sqrt{1-e^2}\left(1-\frac{3}{2}\sin^2 i\right)+\left(2-\frac{5}{2}\sin^2 i\right)\right)\right) \tag{2.19}$$

$$\eta_{\text{min}} = \arctan\left(\frac{\sqrt{a^2-R_{\text{M}}^2-\frac{T_{\text{over}}^2\bar{v}_{\text{hor,corr}}^2}{4}}}{R_{\text{M}}}\right) \tag{2.20}$$

$$v_{\text{M}} = \frac{\sqrt{r_{\text{M,eq}}^2\cos^2\Phi + r_{\text{M,po}}^2\sin^2\Phi}}{T_{\text{M}}} \tag{2.21}$$

$$\beta(t) = \pi\frac{T'-2t}{T_{\text{sat}}} \tag{2.22}$$

$$v_{\text{sat}} = \frac{2\pi r_{\text{sat}}}{T_{\text{sat}}} = \sqrt{\frac{GM}{r_{\text{sat}}}} \tag{2.23}$$

$$v_{\text{vert}} = v_{\text{sat}}\cos\eta_{\text{min}}\sin\beta(t) \tag{2.24}$$

$$v_{\text{hor}} = v_{\text{sat}}\sqrt{\cos^2\eta_{\text{min}}\cos^2\beta(t)+\sin^2\eta_{\text{min}}} \tag{2.25}$$

$$\bar{v}_{\text{hor}} = \frac{1}{T}\int_0^T v_{\text{sat}}\sqrt{\cos^2\eta_{\text{min}}\cos^2\beta(t)+\sin^2\eta_{\text{min}}} \tag{2.26}$$

$$v_{\text{hor,corr}} = \sqrt{(v_{\text{hor}}\cos i - v_{\text{M}})^2 + v_{\text{hor}}^2\sin^2 i} \tag{2.27}$$

$$\bar{v}_{\text{hor,corr}} = \frac{1}{T}\int_0^T \sqrt{(v_{\text{hor}}\cos i - v_{\text{M}})^2 + v_{\text{hor}}^2\sin^2 i}\,\mathrm{d}t \tag{2.28}$$

$$corr = \sqrt{\left(\cos i - \frac{v_{\text{M}}}{\bar{v}_{\text{hor}}}\right)^2 + \sin^2 i} \tag{2.29}$$

$$\vec{v}_{\text{sat}} = \begin{pmatrix} v_{\text{hor}}\cos i - \frac{v_{\text{M}}}{v_{\text{sat}}} \\ v_{\text{hor}}\sin i \\ v_{\text{vert}} \end{pmatrix} \tag{2.30}$$

$$r_{\text{min}} = a\sin\eta_{\text{min}} \tag{2.31}$$

$$i_{\text{virtual}} = \arctan\left(\frac{v_{\text{hor}}\sin i}{v_{\text{hor}}\cos i - v_{\text{M}}}\right) \tag{2.32}$$

$$\vec{r}_{\text{rise}} = \int_0^{\frac{T_{\text{over}}}{2}} v_{\text{hor}}\ \mathrm{d}t \begin{pmatrix} \cos i_{\text{virtual}} \\ \sin i_{\text{virtual}} \\ 0 \end{pmatrix} + r_{\text{min}}\begin{pmatrix} \sin i_{\text{virtual}} \\ \cos i_{\text{virtual}} \\ 0 \end{pmatrix} \tag{2.33}$$

$$\vec{r}_{\text{sat}} = \int_0^{t'} \vec{v}_{\text{sat}}(\beta(t))\mathrm{d}t - \vec{r}_{\text{rise}} \tag{2.34}$$

$$\epsilon = \arctan\left(\frac{r_{\text{sat},z}}{r_{\text{sat},x}}\right) \tag{2.35}$$

$$\alpha = \arctan\left(\frac{r_{\text{sat},y}}{r_{\text{sat},x}}\right) - \alpha_{\text{rover}} \tag{2.36}$$

$$\eta = \arcsin\left(\frac{\sqrt{r_{\text{sat},x}^2 + r_{\text{sat},y}^2}}{r_{\text{sat},z}}\right) \tag{2.37}$$

Having the minimum nadir angle, the velocity parallel to the z-axis can be derived using Eqn.(2.24)

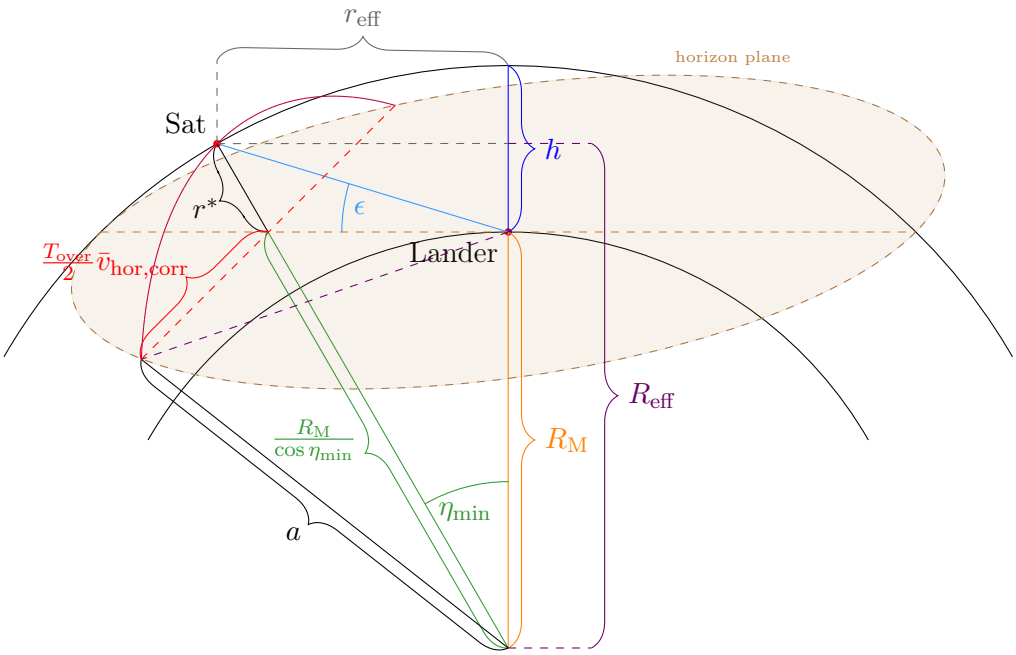

Figure 2.11: A possible overflight of the satellite, visible to the lander

and the one perpendicular to it using Eqn.(2.26). Then, the velocity vector can be derived using Eqn.(2.30). Integrating this about the time elapsed from the satellite crossing the horizontal plane and subtracting the distance of the rising point provides the position of the satellite in the frame of the lander as seen in Eqn.(2.34). The position of the rising point can be hereby determined using the inclination of the ground track which is provided by Eqn.(2.32) and the horizontal distance to the satellite at the closest approach which is given by Eqn.(2.31). With these, the horizontal distance can be split into the x and y-component. On this, the distance of the closest point is added after splitting it opposite to the horizontal distance covered, since it is orthogonal to it. This leads to the coordinates of the rise point stated in Eqn.(2.33). From this, the elevation and azimuth can be easily derived using Eqn.(2.35) and Eqn.(2.36). It shall be noted that this approach assumes that the ground track of the satellite is a straight line without any curvature. This is, however, an approximation and only reasonable when being close to the equator. This leads to relative errors compared to the absolute duration of the overflight of up to 10 % when evaluating the overflights at the most probable landing site Oxia Planum with a minimum elevation of 10° and crosschecking the derived values with the ones provided by Flight Dynamics. However, the overflights derived with both methods are the same, only varying in duration. Therefore, this approach is considered to be accurate enough, especially when considering the uncertainties on the gains and therefore the data volume. The code accomplishing the mentioned steps can be found in the *calculateCorrAndNadir()* function of the *LanderVisibility* class.

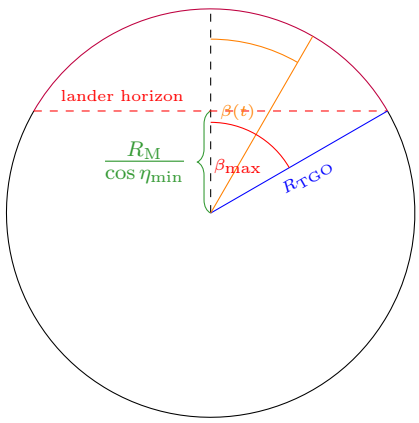

Figure 2.12: A sketch of the orbital angle, based on the lander's local horizontal plane

2.3.2.3 Data Volume

Since the prime relay orbiter for this mission works with an Electra radio, provided by NASA, which offers adaptable data rates, a look-up table [39], provided by JPL, has to be used to derive the data rate from the gain at the input of the radio. The input gain can be calculated using Eqn.(2.38). Hereby the FSPL can be determined using Eqn.(2.39) from [40] and the distance vector provided by Eqn.(2.34). The antenna gain for the rover can be determined by interpolating the values in Tab. 3-3 from [41] for the elevation and azimuth determined with Eqn.(2.35) and Eqn.(2.36). The gains for all other landers was assumed to be the same since no other data were available. The antenna gain for the satellite can be determined by interpolating the values in Tab. 4.3-4 from [39] for the nadir angle from Eqn.(2.37). The remaining values can be found in [41]. The actual values are not stated in this thesis for legal reasons. The data rate can be adapted every 10 s, requiring a 5 s period for reconfiguration [41] and in the beginning a hand-shake time of 20 s is needed [38]. The code calculating the data volume can be found in the *getDataVolume(long, long)* function of the *LanderVisibility* class.

$$\begin{aligned} G_{\text{input}} &= G_{\text{antenna,lander}} + 10\log_{10}(P_{\text{lander}}) + G_{\text{cable,lander}} + G_{\text{antenna, sat}} \\ &\quad - G_{\text{mod}} - G_{\text{imp}} - G_{\text{pol}} - \text{FSPL} \end{aligned} \tag{2.38}$$

$$\text{FSPL} = 20\log_{10}\left(|\vec{r}_{\text{sat}}|\right) + 20\log_{10}(f) - 147.55\,\text{dB} \tag{2.39}$$

2.3.3 Possible Operational Approaches

Due to the long transmission lengths in deep space communication, leading to small signal-to-noise ratios, errors are likely to appear when exchanging data with a spacecraft. Using convolutional coding a lot of errors, in particular bit errors, can be corrected directly by the Telemetry, Tracking and Command (TT&C) system. However, cosmic events, e.g. solar flares, can introduce burst errors which can not be corrected by the TT&C system. To counteract these errors, all commands files sent to the spacecraft are usually checked for validity on board of a satellite using Cyclic Redundancy Check (CRC). This way it is avoided that a spacecraft processes corrupted commands or files which could lead to an unpredictable behaviour. The process to send commands to the spacecraft and hoping that they arrive is equivalent to the situation in Fig. 2.13(a).

However, there is no knowledge if the commands arrived correctly or not. Therefore, the CRC replies to the ground if the check succeeded or not. The reply has to be however reflected by the ground system and therefore it is necessary that the telemetry of the spacecraft is still read, which requires a longer booking of a ground station. For that, it is necessary to wait for the data to travel from ground to the spacecraft and the reply to travel back which corresponds to two OWLT (the processing of the commands is assumed to take no time on the spacecraft, compared to the OWLT and sending of the data). The await of commands confirmation is reflected in Fig. 2.13(b).

If an error is detected, a request of a (partial) resend of the data from ground can be initiated by the spacecraft. The resend requires in total two extra OWLT for the commands to travel to the spacecraft and the reply to travel back, which is shown in Fig. 2.13(c).

To separate failures originating from processing the commands from the ones of the TT&C system, a ping can be sent to the spacecraft. This requires two additional OWLT before sending files, which can be seen in Fig. 2.13(d).

The whole process can be repeated as well to provide a countermeasure against a full pass failure,

referred to as prime uplink opportunity. It can be even forced to be on another ground station to avoid a single point of failure.
All these safety measures are of course nice to have, but they all cost extra ground station time when no data are returned from the spacecraft. Especially in deep space missions, which have high OWLT, these safety measures are altered to avoid blocking ground stations for all other missions. On e.g. Rosetta, which had a OWLT of up to 45 min, the reply of the ping was not awaited before sending the files [42]. This way it was confirmed that the TT&C system worked, by sending files over it.

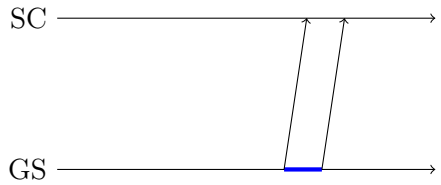

(a): Ground station time required (blue), when only transmitting commands

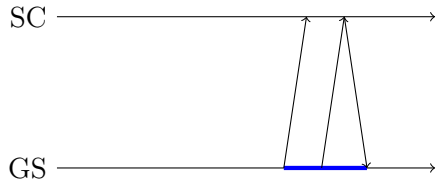

(b): Ground station time required (blue), when transmitting commands and waiting for the reply.

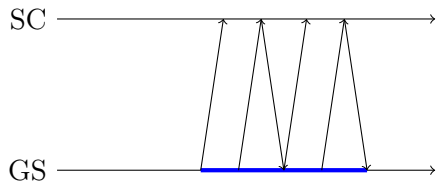

(c): Ground station time required (blue), when transmitting commands, waiting for the reply and providing a backup for this process.

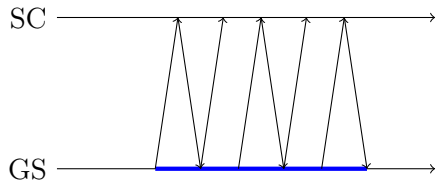

(d): Ground station time required (blue), when pinging the spacecraft and afterwards transmitting commands, waiting for the reply and providing a backup for the transmission process.

Figure 2.13: Sketches of the ground station booking requirements of different operational approaches

2.4 Classification of Scheduling Problems

A scheduling problem is present if m resources ($M_j(j = 1, ..., m)$) have to process n jobs ($J_i(i = 1, ..., n)$). Each of these J_i provides a number of l operations ($O_{i,k}(k = 1, ..., l)$). A release date (r_i) can be associated to each job which specifies the time at which the first operation of (J_i) is available. Finally, each job has an associated completion time (C_i) provided by the schedule, an associated cost function ($f_i(C_i)$), a processing time ($p_{i,j}$) and a processing speed ($s_{i,j}$). $s_{i,j}$ is describing hereby the number of jobs which can be processed in a unit of time and $p_{i,j}$ the time a job needs from the first operation performed on it until its completion. A schedule is defined as an allocation pattern of resource processing time for each of those jobs. The classification of a scheduling problem can then be determined by three characteristics, the resource environment (α), the job characteristics (β) and the optimality criterion (γ) and is noted as $\alpha|\beta|\gamma$. A more detailed description of classification of scheduling problems can be found in the subsection *"Notation"* of [43] and the section *"Classification of Scheduling Problems"* in [44] on which this section relies.

2.4.1 The Resource Environment

The resource environment (α) contains information about the characteristics of the resources, with $\alpha \in \{1, mP, mQ, mR, mO, mJ, mF\}$. m denotes the total number of resources. The meaning of the other part of α is:

- 1 - is the special case of having just one resource.
- P - the resources are identical parallel resources, meaning $p_{i,j} = p_i \forall M_j, J_i$. This requires each J_i to have only one operation which may be processed on any M_j.
- Q - the resources are uniform parallel resources, meaning $p_{i,j} = p_i/s_j$, where s_j denotes the speed of M_j
- R - the resources are unrelated parallel resources, meaning $p_{i,j} = p_i/s_{i,j}$, where $s_{i,j}$ denotes the speed of M_j for J_i.
- J - denotes a job shop. This implies a certain precedence relation, where each operation ($O_{i,j}$) has to be performed on a limited subset of $\{M_j\}$.
- F - denotes a flow shop. This is a job shop, with the restriction that $n_i = m$ and each operation ($O_{i,j}$) has to be processed on M_j.
- O - denotes an open shop. Here, each job must be processed once and only once on each resource.

2.4.2 The Job Characteristics

The job characteristic may contain multiple characteristics, with $\beta = \beta_1, \beta_2, \beta_3, \beta_4, \beta_5, \beta_6, \beta_7, \beta_8$. The meaning of the different β is:

- β_1 - states if preempting of jobs is allowed or not. If it is, then $\beta_1 = pmtn$, otherwise it is not included in β.
- β_2 - is for flow shops only and states if jobs can wait between two successive resources. If they are not allowed to wait $\beta_2 = nwt$, else it is omitted in β
- β_3 - states the precedence constraints for the different jobs. Possible options for it are:
  - *prec*, if the constraints are represented by an acyclic graph
  - *chains*, if each job has at most one successor and predecessor, respectively
  - *intree*, if each job has at most one successor
  - *outtree*, if each job has at most one predecessor
  - omitted, if there is no precedence given
- β_4 - denotes the release dates r_i of J_i. If all J_i can start immediately it is omitted.
- β_5 - gives the restriction on the number of jobs. Omitted, if no restriction is given.
- β_6 - is only for job shops and states the restriction on the number of operations per job. Omitted, if no restriction is given.

- β_7 - denotes the restriction on the processing time, if present. It states the number of units of one job's processing time.
- β_8 - denotes the deadlines $\tilde{\mathrm{d}}_i$ of J_i. If there are no deadlines it can be omitted.

2.4.3 The Cost Function

The cost function gives the costs for finishing a job, depending on its completion time, due date d_i and release date. It is mostly depending the lateness of a job Eqn.(2.40), the earliness Eqn.(2.41), or the processing time Eqn.(2.43) and is given as Eqn.(2.44) for sum objectives and Eqn.(2.45) for bottleneck problems.

$$L_i = d_i - C_i \tag{2.40}$$

$$E_i = \max\{0, C_i - d_i\} \tag{2.41}$$

$$T_i = \max\{d_i - C_i\} \tag{2.42}$$

$$p_i = C_i - r_i \tag{2.43}$$

$$\sum f_i(C) := \sum_{i=1}^{n} f_i(C_i) \tag{2.44}$$

$$f_{\max}(C) := \max\{f_i(C_i) | i = 1, ..., n\} \tag{2.45}$$

2.5 Input Sources

Two input sources were used, an Eventfile which provides the geometrical constraints, like visibilities and occultations, given by the orbital dynamics and a Planview file which provides the bookings on the ESTRACK network. Both documents are provided in XML format and are described in detail in the Appendix in Sec. 9.6.1 and Sec. 9.6.2.

2.6 Poincaré Plots

A Poincaré plot provides a special way to visualise time series data to extract dependencies in time domain from them. Hereby, the data are prepared such that a point is plotted for every (x_n, x_{n+1}) pair. This way it is possible to directly investigate timely dependencies between the data. An example can be found in Fig. 2.14 where the dependency of the elevation of an overflight on the previous can be seen. It is limited by two lines which are getting denser the closer one gets to the x and y-axis respectively indicating a dependency between the last elevation and the following one.

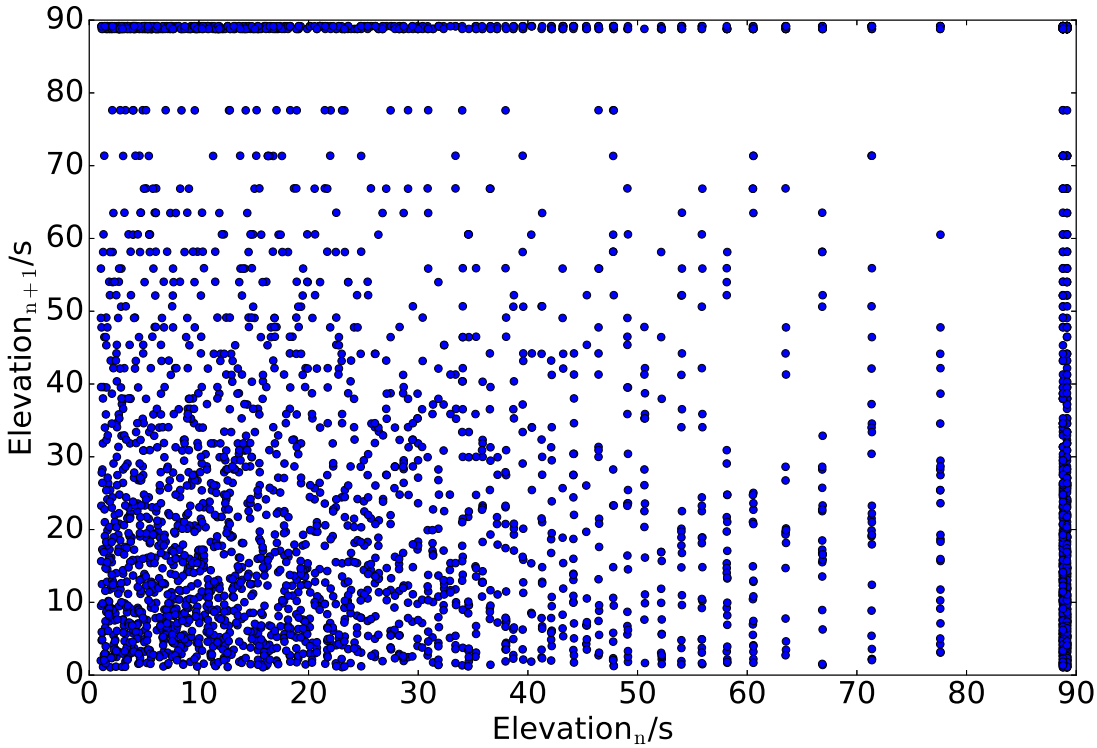

Figure 2.14: A Poincaré plot of the durations of the Odyssey overflights over EXM at 0° elevation

3 Problem Statement

As stated in Sec. 2.3 the aim of operating a spacecraft is to "maximise [the] mission return" [15]. For the ExoMars RSP mission, which is investigated in particular in this thesis, this statement means that the rover and surface platform shall work as long as possible on the surface of Mars. However, it is necessary to plan the activities of the rover depending on its location, environment and other scientific data, because it is not an entirely autonomous machine and certain scientific experiments can only be performed if the right conditions are given. The working time on the Martian surface is limited by daylight on Mars as explained in detail in Sec. 3.2.1. This is further constrained by the communication constraints a relay link has to meet as stated in Sec. 2.3.2 and requirements agreed upon to provide 150 Mbits return data volume to each rover and surface platform per sol [41] while the overflights require a minimum elevation of 10 degrees [8]. Therefore, a communication strategy has to be developed maximising the time for the rover to work (RWT) and the time to plan the rover's behaviour on the next sol on Earth (EPT), respectively, while respecting all constraints.
Similar missions and their communication strategy approaches are discussed in Sec. 3.1. However, it is shown in there that a new approach has to be taken. For this, a basic tool was available with a limited set of capabilities discussed in Sec. 3.1.4. This tool was completely redesigned keeping only its basic classes and functionalities.
To do this redesign, the desired cases of RWT and EPT are defined in Sec. 3.2.1 and Sec. 3.2.2. Furthermore, the scenarios are classified in Sec. 3.3 using the notation explained in Sec. 2.4.
In order to develop an in-depth understanding of the different parameters influencing the data link between rover and lander, on the one side, and the Earth, on the other, and therefore the RWT, EPT and data return several scenarios shall be investigated. For these investigations two periods are available, one spreading from 21st November 2017- 30th December 2019 and another spreading from 1st January 2020- 28th February 2023. This originates in a shift of the launch date for the RSP mission during the development of the tool. Hereby, the RSMs from the 1st February 2019 - 30th September 2019 and 21st March 2021- 30th October 2021 are of particular interest since they are (were) the planned minimum operational periods of the rover. The scenarios include the possibility of having different ground station networks, other missions blocking those ground stations, different operational margins, using multiple spacecraft orbiting Mars as relay satellites and serving multiple landers on the surface of Mars. This shall provide reliable recommendations to the mission's operation team on the resources necessary to fulfil this mission, the optimal operations margins, as introduced in Sec. 2.3.3, and the robustness of the relay link in general.

3.1 Related Work

In order to discuss related work, other missions using relay links and their operational approaches are presented here. First, missions having similar requirements on the commanding, as the Mars Exploration Rovers and the Mars Science Laboratory rover, are discussed and similarities and differences are shown. Then, a mission with similar communication capabilities, the Phoenix lander, is investigated for its similarities and difference.

3.1.1 Mars Exploration Rovers

The two Mars Exploration Rovers Spirit and Opportunity were capable of both relay communication and direct-to-Earth communication and were landed at (175.5°E,14.8°N) and (354.5°E,-1.9°N), respectively [4, 14]. This separation of 179° provided the opportunity of having the relay links for both of them just half an orbital period after each other. This allowed to use one satellite in a sun-synchronous orbit, namely Odyssey, to provide a forward link at dusk and a return link at dawn optimising RWT and EPT. This led to 98% of the data being returned via the relay link [4]. The direct-to-Earth link is mainly used to shift the planning periods to daytime to avoid costly night time shifts. These approaches can however not be utilised for the ExoMars RSP mission since the primary relay orbiter TGO has a non-sun-synchronous orbit and neither of the landed assets offers a direct-to-Earth link.

3.1.2 Mars Science Laboratory

For the Mars Science Laboratory rover, a communication strategy similar to the one of the Mars Exploration Rovers was used. The prime relay orbiter is in this case MRO, which is as well in a sun-synchronous orbit and had its overflights originally around 3 a.m. and 3 p.m., but a later orbit change shifted them to 4 a.m. and 4 p.m., leading to the direct-to-earth link being more utilised for the commanding. However, for the same reasons as for operations approach of the Mars Exploration Rovers, this one can not be utilised for the ExoMars RSP mission. [45]

3.1.3 Phoenix

The Phoenix landing platform was using a relay only communication. Hereby, Odyssey and MRO served both as relay orbiter. The overflights with the highest elevations were situated around 4 a.m. and 4 p.m.. However, a lot more overflights compared to all other landers were available since Phoenix landed at a latitude of 67.5°N. The relay concept can serve as a basis for the one of the ExoMars RSP, providing enough overflights to meet the data volume requirements while providing enough forward links for regular commanding. However, Phoenix had no other landed asset at the same location with which it needed to share passes and had two relay orbiters serving it. Therefore, the overflights for the ExoMars RSP mission have to be used more thoughtfully compared to the Phoenix lander. [46]

3.1.4 Summary

Compared to all missions mentioned above, the ExoMars RSP mission has to solve a unique problem since it can only be communicated with using relay passes while having an asset which can move. This requires a lot more regular contact and more dedicated planning making an optimisation of RWT and EPT as defined in Sec. 3.2.1 and Sec. 3.2.2 necessary. For this a starting point with an initial solver was available providing classes with the possibility to handle periods, calculating their intersections, unions and differences. Moreover, the read-in for Eventfiles and Planview files was available although without the capability of assessing the elevation and azimuth profiles of lander visibilities. In addition, an implementation of the Martian time was available excluding the capability of assessing dusk and dawn. Furthermore, an investigation of the overflights was done taking the simplified assumption that an uplink pass has to be before noon and a downlink not between dawn and noon not respecting their influence on the EPT. This investigation was as well performed with a fixed set of operational constraints and only one orbiter. This is extended to an approach allowing to make a tread-off between RWT and EPT with the possibility to put constraints on the minimum length for both of them. Furthermore, the possibility of using multiple orbiters and serving multiple landers is assessed. Finally, the possibility to determine the approximate data volume is provided.

3.2 Key Parameters for Investigation

As stated earlier, it is a key goal to maximise RWT and EPT, respectively, which are explained in Sec. 3.2.1 and Sec. 3.2.2. However, there are other driving factors which play a role when reasoning on the scenarios' solution. First of all, there are the forward link and return link latency which are directly influencing the RWT and EPT, since the latencies cannot be used for either of them. The definition of those can be found in Sec. 3.2.3 and Sec. 3.2.4. In addition to that, the data return volume has to be kept high enough, because the data collected during the RWT have to be returned. This is discussed in Sec. 3.2.5.

3.2.1 Rover Working Time

The RWT is defined as the time a landed asset can work following a plan which is specifically planned based on the last scientific data downlinked. The natural limit for the RWT is the time of dawn and dusk since the Sun provides the energy to the rover's systems. However, the rover has a minimum input power necessary to operate which coincides with a minimum elevation of the Sun of 10° (RO-GN-130 in [8]), since the power provided by the solar cells increases with the sinus of the Sun's elevation. This leads to a definition of the theoretical start and stop points of the RWT by the Sun crossing the minimum elevation. However, it is necessary that there are specific commands available for the sol as well. Therefore, a forward link has to happen before the RWT is assumed to start. Furthermore, the RWT is assumed to stop as soon as a return link of the data from the rover happens. This leads to four possible cases indicated in Fig. 3.1. The RWT provides four key parameters, the total RWT over the RSM, the average RWT in hours per sol, the one sigma deviation from the average and the percentage of RWT used, compared to the theoretically available one. The theoretical one is given by the time the Sun is high enough to provide enough power to work. The ratio of RWT/theoretical RWT is referred to as RRWT.

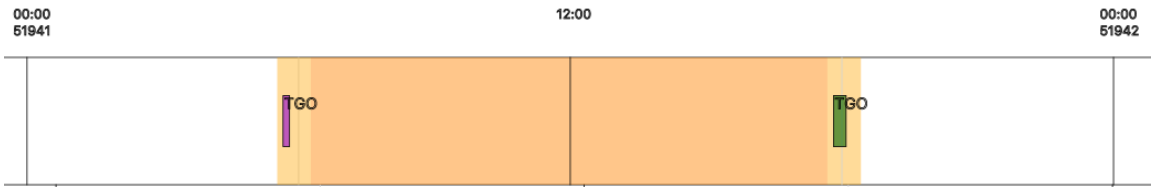

(a): An example, where the RWT is only limited by the minimum elevation of the Sun, necessary to operate the rover.

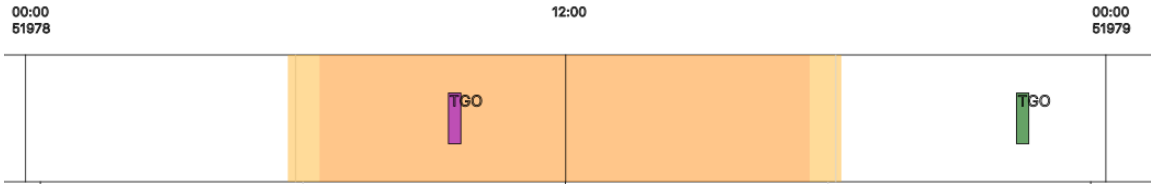

(b): An example, where the RWT is limited by the necessity of uplinking data in advance.

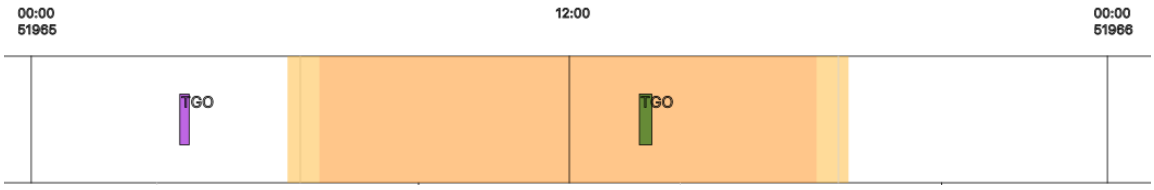

(c): An example, where the RWT is limited by the data being downlinked before dusk.

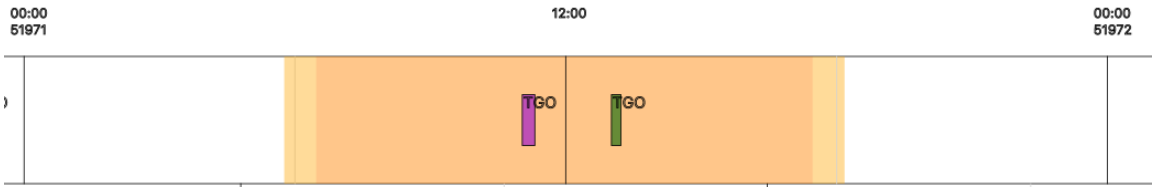

(d): An example, where the RWT is limited by both, the necessity of uplinking data in advance and the downlinking of them before dusk.

Figure 3.1: The different cases of RWT restrictions, which can appear on one sol, displayed on an event timeline. Here, white background indicates Martian night, light orange the time when the Sun is above zero degrees elevation and the darker orange, the time when the Sun is above the minimum required elevation. A purple box indicates a forward link and a green one a return link.

3.2.2 Earth Planning Time

The EPT can be defined as the time from returning telemetry to Earth until the time the lander operations centre has to deliver the new commands to the orbiter operations centre. This time is defined by taking the last uplink opportunity to the spacecraft, subtracting the time required for the different operational margins, as discussed in Sec. 2.3.3 and shifting it further forward to respect a margin set by the orbiter operations centre, which is referred to as Rover Operations Control Centre (ROCC)-Deadline. This time is necessary to pre-process the files provided by the lander operations centre (ROCC in the case of the rover) at ESOC and preparing the uplink of them. Of particular interest are hereby the cases where the lander operations centre has less than 4 or 6 h EPT, respectively, since this gives an indicator to the centre how it has to perform its strategic planning to keep to the constraints set by the EPT. However, the average EPT with a one sigma deviation is provided as well giving a general idea of the range in which it normally lies.

3.2.3 Forward Link Latency

The forward link latency shall be defined as the time between the end of the EPT and the start of the RWT. It is the time which is required to get the commands defined by the lander operations centre, via the satellite operations centre, a ground station and an orbiter, to the landed asset. Since this time can not be used for either planning or working, it is a key driving factor for the RWT and EPT. Its value is provided as the average latency in hours per forward link and its one sigma deviation referred to as $\overline{\lambda_{\mathrm{FWD}}}$.

3.2.4 Return Link Latency

The return link latency can be seen as the complement of the forward link latency and is the time between the end of the RWT and the start of the EPT. It is the time needed to get the data from a landed asset, via an orbiter, a ground station and the satellite operations centre, to the lander operation centre. Since it is again not possible to either work or plan during this time, it is another driving factor for the RWT and EPT. Its value is provided as the average latency in hours per return link and its one sigma deviation referred to as $\overline{\lambda_{\mathrm{RET}}}$.

3.2.5 Data Volume

Since the amount of data volume returned has to be 150 MBits/sol for the rover and the surface platform, respectively, (RO-CO-35 in [8]) it is a driving factor for reasoning on the scenarios and it shall be fulfilled even when splitting passes between the surface platform and the rover. The data volume provides two key parameters: the average data volume per pass and the days at which the requirement of 150 Mbits/sol can not be fulfilled. The data volumes are hereby computed using the optimal headings for the overflights as discussed in [47].

3.3 Classification of the Scenarios

The crucial part of all the scenarios is, on the one hand, to provide enough telecommands to the rover so it can perform science operations during the whole Martian day and, on the other hand, to return those data to Earth in order to plan the next working day depending on the current conditions. Hereby, the EPT and RWT should be maximised, meaning that the forward link and return link latencies shall be minimised, while keeping the requirements on the return data volume. The RWT and EPT times depend hereby only on the time of the forward link and return link. Those are defined as the jobs J_i which have to be performed. From these facts, the resource environment and the job characteristics, the key parameters for the cost functions can be derived.

The Resource Environment The resources M_j for the J_i are the data links over the orbiters since those are the only systems which can process the J_i. This decision originates in the fact that it is not of detailed concern, for the scheduling, what is happening on the way from the ground station to the landed asset as long as the processing time and availability is known. Therefore, the data link can be assumed to be a black box with several options providing the processing times for the job depending on those options. The number of resources m equals the number of orbiters around Mars since each of them can provide one data relay link. The resources are hereby unrelated ones, because the processing

time varies from satellite to satellite due to the different orbits and depends as well on the time at which the job is processed due to the changing geometry. Therefore, the resource environment can be characterised as mR.

The Job Characteristics The definition of the jobs to be the forward link and return link introduces constraints on the processing of the jobs for each individual landed asset, owing to the fact that a return link job always requires a forward link job happening before it and vice versa. This leads to the conclusion that $\beta_3 = chains$.

The Cost Function Since Martian night shall be used for planning and daylight for working it can be concluded that every forward link job shall be finished at the time when the landed asset can start working and every return link when the landed asset stops working. These two times provide the due dates for the related job and one cost factor for the cost function, which is the tardiness of the job, as defined in Eqn. 2.42. In addition to this, the time before the due date shall be used for RWT or EPT, respectively, until a certain maximum, implying a second cost factor to be $\max\{0, t_{\max} - (C_i - p_i - r_i)\}$. Finally, the processing time itself shall be minimised since it can neither be used for RWT nor EPT.

Summary In [48] it is shown, that already the problem $1||\sum \omega_i T_i$ is strongly NP-hard. Therefore, even a pseudo-polynomial algorithm does not exist to find a solution for this problem. Since the problem presented in this thesis is even more complicated, a new solving algorithm had to be developed which can be found in Sec. 5.

3.3.1 Processing Time and Speed

The availability of each resource, its processing speed and processing time can be determined using the ground station visibilities, the lander visibilities, the bookings of the ground stations, the bookings of the link by other landers, the occultations based on all bodies passing the line of sight between orbiter and Earth and the landing site of the lander. Since the processing speed varies with every link anyway it is not calculated separately, but instead, the processing time is determined directly for every job. Hereby, the landing site for the rover and the surface platform is always assumed to be Oxia Planum. To reflect the different restrictions on the jobs, the processing time shall be denoted as $p_{i,j} = p_{i,j,lander,network,elevation,missions,landers,margins}$. In this context, *elevation* states the minimum elevation in degrees required to establish a communication link between a lander and a satellite. *networks* refers to the ground station network used and can have the following values:

- E for the ESTRACK deep space antennae, consisting of MLG, CEB and NNO
- $E + B$ for the ESTRACK deep space antennae and BLK as ground station network
- $E + B + D$ for the ESTRACK deep space antennae, BLK and the NASA DSN, consisting of MAD, GDS and CAN, as ground station network
- $M + B$ MLG + BLK as ground station network

Missions is depending on other missions using the same ground station network or parts of it. It can be omitted if no other missions are assumed or can be every value or a sum of:

- $nL1$ for n missions stationed around the first Lagrangian point of Earth
- $nL2$ for n missions stationed around the second Lagrangian point of Earth
- nR for n missions with nearly randomised bookings

The *landers* attribute is depending on the landers serviced by the same orbiter. It can be every value or a sum of:

- EXM for the European rover of the RSP mission
- RUS for the Russian landing platform of the RSP mission
- MSL for the American rover "Mars Science Laboratory"
- NSY for the American landing platform "InSight"
- MRB for the American rover "Opportunity"

Finally, the *margins* attribute states the safety margins. If none are provided the symbol is omitted, otherwise it is one or a combination of:

- *pi* indicates that dummy commands are used to ping the spacecraft before transmitting any data.
- *pu* indicates that an extra visibility is used to have a safety if the TC-commanding fails.
- *cc* indicates that a confirmation of telecommands is necessary.
- *rot* indicates that a deadline of t h was set for the ROCC to transmit the TC files before the last uplink opportunity.
- *rt* indicates that a retransmission of the commands needs to be possible.
- *dl* indicates that a downlink is necessary for each overflight.
- *ul* indicates that an uplink is necessary for each overflight.

From these operational margins, the following ones were considered as possible desired options:

- $ro2$ as it is a margin demanded by ESOC for relay communication
- $cc, ro2$ since it adds the information of the safe arrival of the commands on board.
- $cc, pi, ro2$ as the margins with the smallest demands, which provide any certainty that the orbiter is available before sending commands to it.
- $cc, rt, ro2$ since this way, a backup possibility of sending the commands to the orbiter is provided requiring a minimal extra ground station time
- $cc, pu, rt, ro2$ as the margins with the smallest demands providing a safety against a complete pass failure

Not considered were:

- $cc, pi, rt, ro2$, since a ping followed by a transmission and a retransmission opportunity require five OWLT of pass duration, which is longer than a considerable number of visibilities between Mars occultations.

- A prime uplink opportunity on another station, since this would already imply regular latencies of 8 h, due to the separation of most ground stations being 120°, which is too high for working on every sol.

3.3.2 One Orbiter Scenarios

Every one-orbiter scenario can be described as $1|chains|\sum f_i(C_i, d_i, r_i)$, using the notation given in Sec. 2.4. Nevertheless, this scenario contains an infinite number of sub-scenarios, because the processing speed of the resource depends on the environment as described in Sec. 3.3.1. These sub-scenarios shall be investigated to provide a reasoning on the different operational constraints that can be applied to the RSP mission without decreasing the key parameters too much, as well as on the ground station network being necessary to support the RSP mission. In this case, the following speeds shall be investigated for the TGO:

a) $p_{i,j} = p_{i,j,EXM,B+M,10}$ to have a baseline scenario for the originally proposed ground station network MLG+BLK. It provides the best case solution, due to having the least restrictions, for all other scenarios with the MLG+BLK network and is further referred to as scenario 1a. It contains sub-scenarios to investigate the influence of the different margins on it.

   i) $p_{i,j} = p_{i,j,EXM,B+M,10,ro2}$ to provide an analysis of the geometrical constraints when adding a deadline for handing the commands of the landed asset to the orbiter operations centre. It is further referred to as scenario 1a i.

   ii) $p_{i,j} = p_{i,j,EXM,B+M,10,cc+ro2}$ to determine the influence of requiring command confirmation on each uplink to the orbiter. It is further referred to as scenario 1a ii.

   iii) $p_{i,j} = p_{i,j,EXM,B+M,10,cc+pi+ro2}$ to provide an analysis of demanding ping, before sending commands to the orbiter, to check its availability. It is further referred to as scenario 1a iii.

   iv) $p_{i,j} = p_{i,j,EXM,B+M,10,cc+ro2+rt}$ to determine the difference between demanding a ping and a retransmission opportunity. It is further referred to as scenario 1a iv.

   v) $p_{i,j} = p_{i,j,EXM,B+M,cc+pu+ro2+rt}$ to provide an analysis of the originally intended operations. It is further referred to as scenario 1a v.

b) $p_{i,j} = p_{i,j,EXM,E,10}$ to provide the best case solution for all other scenarios with the ESTRACK deep space antennae. It is further referred to as scenario 1b.

   i) $p_{i,j} = p_{i,j,EXM,E,10,cc+ro2+rt}$ to have a baseline scenario with the most probable margins for all scenarios with the ESTRACK network. It is further referred to as scenario 1b i.

   ii) $p_{i,j} = p_{i,j,EXM,E,10,1L1+1L2+2R,cc+ro2+rt}$ to get an idea how bookings influence the solution on the ESTRACK network. It is further referred to as scenario 1b ii.

c) $p_{i,j} = p_{i,j,EXM,E+B,10}$ to provide the best case solution for all other scenarios with the ESTRACK+BLK network. It is further referred to as scenario 1c. For this scenario, there are

as well several sub-scenarios analysed to retrieve the influence of the different possible margins on a scenario with a ground station coverage mainly constrained by occultations. Those sub-scenarios are:

i) $p_{i,j} = p_{i,j,EXM,B+E,10,ro2}$ in order to retrieve the influence on scenario 1c when introducing a deadline to hand the commands for the landed asset to the orbiter operation centre. It is further referred to as scenario 1c i.

ii) $p_{i,j} = p_{i,j,EXM,B+E,10,cc+ro2}$ in order to retrieve the influence on scenario 1c i, when making the confirmation of all commands necessary. It is further referred to as scenario 1c ii.

iii) $p_{i,j} = p_{i,j,EXM,B+E,10,cc+pi+ro2}$ in order to retrieve the influence on scenario 1c ii when sending a ping before actually sending telecommands. It is further referred to as scenario 1c iii.

iv) $p_{i,j} = p_{i,j,EXM,B+E,10,cc+ro2+rt}$ in order to retrieve the influence on scenario 1c ii, when demanding a retransmission opportunity for the telecommands. Within this scenario, the sensitivity to the ratio of the RWT and EPT cost factors shall be determined as well. It is further referred to as scenario 1c iv.

v) $p_{i,j} = p_{i,j,EXM,B+E,10,cc+dl+ro2+rt}$ in order to retrieve the influence on scenario 1c iv when demanding a downlink for every overflight. It is further referred to as scenario 1c v.

vi) $p_{i,j} = p_{i,j,EXM,B+E,10,rt+cc+ro2+dl+ul}$ in order to retrieve the influence on scenario 1c iv when demanding an uplink and a downlink on every overflight. It is further referred to as scenario 1c vi.

vii) $p_{i,j} = p_{i,j,EXM,B+E,10,cc+pu+ro2+rt}$ to determine the influence of demanding a prime uplink opportunity on scenario 1c iv. It is further referred to as scenario 1c vii.

viii) $p_{i,j} = p_{i,j,EXM,B+E,10,1L1+1L2+2R,cc+dl+ro2}$ to get an idea how bookings influence the solution on the ESTRACK+BLK network. It is further referred to as scenario 1c viii.

d) $p_{i,j} = p_{i,j,EXM,B+D+E,10}$ to have a baseline scenario providing the best case solution for all other scenarios with the ESTRACK+BLK+NASA DSN network. Hereby, the cost for the NASA DSN shall be kept so high that they are only used when really required since they are external entities. It is further referred to as scenario 1d.

i) $p_{i,j} = p_{i,j,EXM,B+D+E,10,cc+ro2+rt}$ to have a baseline scenario with the most probable margins for all scenarios with the ESTRACK+BLK+NASA DSN network. It is further referred to as scenario 1d i.

ii) $p_{i,j} = p_{i,j,EXM,B+D+E,10,1L1+1L2+2R,cc+ro2+rt}$ to get an idea how an optimistic assumption of bookings influences the solution on the ESTRACK+BLK+NASA DSN network. It is further referred to as scenario 1d ii.

e) $p_{i,j} = p_{i,j,EXM+RUS,B+E,10,rt+cc+ro2}$ to investigate the influence of solving a multiple-landers problem with the ESTRACK+BLK network to determine a solution acceptable for both landed assets. This is of particular importance when respecting the result on the remaining data volume, if all passes of the RSP mission are allocated only respecting the requirements of the rover, in Sec. 7.2. Hereby, the solution shall still be constrained to the baseline resources for the RSP mission, but the multiple lander solver described in Sec. 5.3.2 is used to provide passes to both the rover and the

surface platform. Furthermore, a sensitivity analysis on the cost factors of the individual landers is performed, as well as changing the focus of importance between rover and surface platform. For this scenario, the optimisation focus is kept on the rover. It is further referred to as scenario 1e.

i) $p_{i,j} = p_{i,j,EXM+RUS,B+E,10,cc+ro2+rt}$ as a scenario with the same constraints as scenario 1e but setting the optimisation focus equally to surface platform and rover. It is further referred to as scenario 1e i.

ii) $p_{i,j} = p_{i,j,EXM+RUS,B+E,10,cc+ro2+rt}$ as a scenario with the same constraints as scenario 1e but setting the optimisation focus on the surface platform instead of the rover. It is further referred to as scenario 1e ii.

iii) $p_{i,j} = p_{i,j,EXM+RUS,B+E,10,cc+dl+ro2+rt}$ to investigate the influence of demanding a downlink on every overflight. It is further referred to as scenario 1e iii.

iv) $p_{i,j} = p_{i,j,EXM+RUS,B+E,10,cc+dl+ro2+rt+ul}$ to investigate the influence of demanding a downlink and an uplink on every overflight. It is further referred to as scenario 1e iv.

3.3.3 Multiple Orbiter Scenarios

Using multiple orbiters adds additional resources to the system which can be reflected, using the notation from Sec. 2.4, as $mR|chains|\sum f_i(C_i, d_i, p_i, r_i)$. The possible orbiters are stated in Sec. 2.3.2.1. From those, MRO is of particular interest, since it provides regular patterns due to its circular, sun-synchronous orbit and the high data rates of the Electra radio on board. Furthermore, Odyssey shall be investigated as yet another orbiter in a circular orbit. However, in all the scenarios TGO shall remain the prime spacecraft as it is supposed to be the prime relay satellite for the RSP mission. This is achieved by assigning penalties to the overflights which would use other orbiters. The influence of this penalty is investigated within the individual scenarios. A further constraint is that the orbits provided by JPL to ESOC start first in May 2021 which is two months after the start of the RSM. Therefore, only the impact on the time afterwards can be investigated. The scenarios investigated are:

a) TGO+MRO, $p_{i,j} = p_{i,j,EXM,B+E,10,cc+ro2+rt}$, to determine the influence of another orbiter available to solve a scenario, with the most probable ground station network and operational constraints. It is further referred to as scenario 2a.

   i) TGO+MRO, $p_{i,j} = p_{i,j,EXM+RUS,B+E,10,cc+ro2+rt}$, to determine the influence of another orbiter available to solve the scenario for both landed assets of the RSP mission, using the multiple lander solver and respecting the most probable ground station network and operational constraints. It is further referred to as scenario 2a i.

b) TGO+MRO, $p_{i,j} = p_{i,j,EXM,B+D+E,10}$, to determine the influence of another orbiter available to solve a scenario, with unconstraint ground station coverage and nominal operational constraints. It is further referred to as scenario 2b.

   i) TGO+MRO, $p_{i,j} = p_{i,j,EXM+RUS,B+D+E,10,cc+ro2+rt}$, to determine the influence of another orbiter available to solve the scenario for both landed assets of the RSP mission, using the multiple lander solver, unlimited ground station coverage and the desired operational constraints. It is further referred to as scenario 2b i.

c) TGO+MRO+Odyssey, $p_{i,j} = p_{i,j,EXM,B+E,10,cc+ro2+rt}$, to determine the influence of a third orbiter available to solve a scenario, with the most probable ground station network and operational margins. It is further referred to as scenario 3a.

   i) TGO+MRO+Odyssey, $p_{i,j} = p_{i,j,EXM+RUS,B+E,10,cc+ro2+rt}$, to determine the influence of a third orbiter available to solve the scenario for both landed assets of the RSP mission, with the most probable ground station network and operational constraints and the multiple lander solver. It is further referred to as scenario 3a i.

d) TGO+MRO+Odyssey, $p_{i,j} = p_{i,j,EXM,B+D+E,10,cc+ro2+rt}$, to determine the influence of a third orbiter available to solve a scenario, with nearly unrestricted ground station visibility and the desired operational margins. It is further referred to as scenario 3b.

e) TGO+MRO+Odyssey, $p_{i,j} = p_{i,j,EXM+RUS+MRB+MSL+NSY,B+D+E,10,cc+ro2+rt}$, to determine a solution for all assets, which will be most probable operational at the arrival of the RSP mission, using all orbiters in a circular orbit and the single and multiple lander solver as necessary. Hereby, it shall be respected, that cross-support from an agency to another is an adverse manner and shall be avoided. It is further referred to as scenario 3c.

3.4 Comparison to 2018 launch

The RSP mission was delayed to a launch date in 2020 during the writing time of this thesis. Therefore, a comparison analysis of the 2018 launch date can be provided and investigated, handing new information for probable future missions. For that scenario 1e was investigated for the 2018 launch date as well, to show the differences to the 2020 launch date.

4 Data Preparation

In order to provide processable input to the solver, the input files have to be prepared. The processing of the bookings, provided by the Planview file, is discussed in Sec. 4.1. The preparation of the Eventfile data is straightforward and is just a conversion to Java classes. The only special conversion is the one of the overflights over the landers where the elevation and azimuth profiles are determined. This is discussed in Sec. 4.2.

4.1 Booking Simulation

Since the available Planview file is covering the period from the 8th March 2016 - 1st January 2017 a simulation of the bookings is required to evaluate them for the RSMs, which takes place long after. In order to provide a good simulation of typical bookings the ones existing in the Planview file are divided into three groups:

- Missions which are related to the position of a celestial object, e.g. Mars.
- Missions which are related to the length of a synodical day. Such missions are missions at L1 and L2.
- Missions which do not fit in any of the above groups.

For the missions in the first group, the simulation requires the visibility of the related body on the different ground stations and is described in detail in Sec. 4.1.1. The second group can be modelled for the desired time period by shifting them by full days. The procedure to do this is described in Sec. 4.1.2. The third group can be assumed to perform relatively random bookings since they are not related to any orbital events. Therefore, modelling those can be done as preferred and in this particular case it is performed as the modelling of the missions related to the synodical day. By choosing missions from the three different groups, a load on the ESTRACK stations can be simulated. For future developments of the tool, it might be worth replacing it by a load factor and allow the tool to determine the necessary bookings depending on their duration.

4.1.1 Planetary Missions

For missions targeting planets other than Earth, a Planview file for the evaluation period is required, since the station visibilities and therefore the bookings change with the propagation of the planets on their orbits. Therefore, those missions were till now neglected when the bookings were investigated, since the Planview file available at the earliest one year in advance.
For missions orbiting Mars, this can be justified since the prioritisation between ESA Mars missions can be handled internally in ESOC easily, because they are situated in the same division.

4.1.2 Synodical Day Missions

For those missions, the simulation is quite straightforward. Since the missions remain at the same spot with respect to Earth, the booking can be assumed to be the same every day of the year. Therefore, the first midnight of the Planview file can simply be shifted to the first midnight which appears in the Eventfile. Afterwards, the bookings for all missions which are repeating with the synodical are pasted into the scenario. However, the Planview file only provides bookings for six months. In order to have bookings after those six months, the first midnight in the Planview file is set to the first midnight in the scenario which does not contain bookings yet. Then the bookings are pasted again and the procedure is repeated until the bookings spread over a period longer than the scenario.

4.2 Elevation and Azimuth Profiles

In order to calculate the data volume for each pass the elevation and azimuth profiles have to be determined using the derivation provided in Sec. 2.3.2.2. From this preparation of the data, the following overflight patterns appear for each of the orbiters in a circular orbit. Since they do not change with the different scenarios, they are already discussed here and conclusions drawn from them are provided in Sec. 7.1. An assessment of orbiters in elliptical orbits has to follow up, as soon as orbit files are available for them.

4.2.1 TGO

For the European TGO, it can be seen that the elevation depends exponentially on the duration in Fig. 4.2(a), which should hold as well for every other satellite in a circular orbit due to the conserved geometry. Plotting the elevation in a histogram in Fig. 4.2(b) shows that the number of passes with a maximum elevation is given by an inverse exponential function. For both plots, it shall be noted that the cluster close to 90 degrees originates in the algorithm used to determine the elevation from the duration. When assuming no minimum elevation the pattern of overflights consists of two consecutive overflights with a separation of one orbital period repeating every 12 hours as visible in Fig. 4.1. This

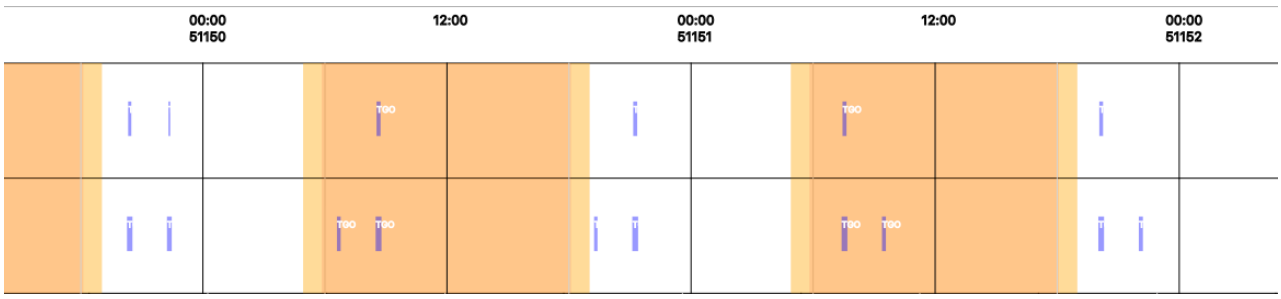

Figure 4.1: The pattern of overflights with a minimum elevation of 10° in the upper column and with no minimum elevation in the lower one displayed on an event timeline. A blue box indicates hereby an overflight, while text in it just refers to the orbiter that can see the lander, which is fixed in this case as TGO.

separation of 12 h leads to a shift of the passes with respect to the landing sites $LTST$, with a period of approximately 48 d, leading to an occurrence of the passes over the whole day as visible in Fig. 4.2(d). The Poincaré plot of the elevation of the overflights in Fig. 4.2(c) is limited by two lines, which are

getting denser, the closer one gets to the x and y-axis, respectively. From this, it can be derived that in regular cases, a high elevation overflight is followed by a low elevation one and vice versa. This is of particular importance when taking into account that the rover needs a minimum elevation of 10 degrees for a communication link with the orbiter. The pattern of a low and high elevation overflight guarantees that at least one of two consecutive ones can provide a communication link. A similar behaviour can be as well spotted for smaller elevations. However, it can be seen as well, that some discrete elevation values appear more often. This is originating from the algorithm determining the elevation and could be resolved using orbit files.

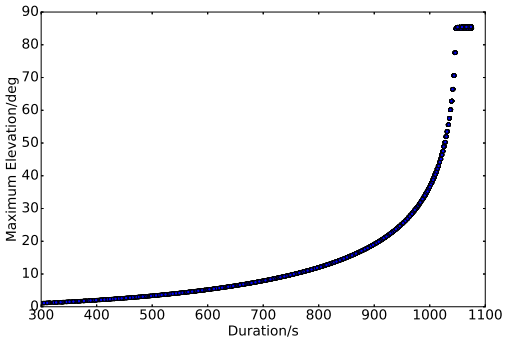

(a): The elevation as a function of the duration

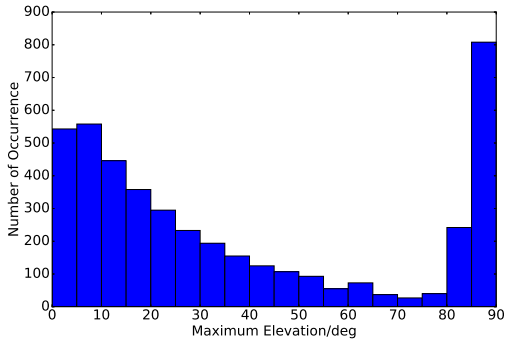

(b): The appearance of the different elevations

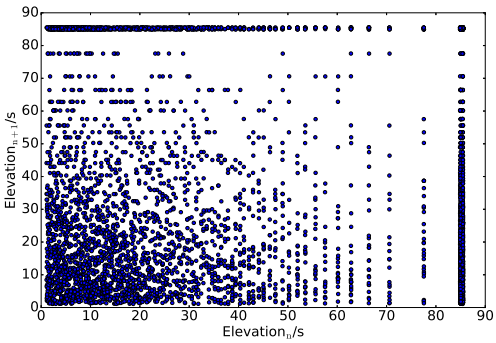

(c): A Point-Careé plot of the durations at 0° elevation

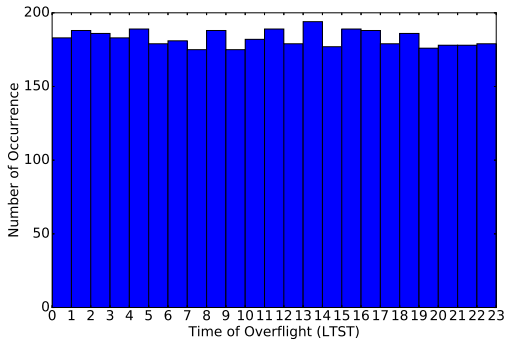

(d): The timely occurrence of the overflights on Mars in *LTST*

Figure 4.2: The elevation, duration and timing properties of the overflights for TGO

4.2.2 MRO

Since MRO is as well in a nearly circular orbit with a smaller semi-major axis than TGO the elevation is a bit higher for the same duration of an overflight as visible in Fig. 4.3(a). This is originating in the higher orbital velocity on the lower orbit. The elevation distribution, however, is basically the same as for the TGO which is visible in Fig. 4.3(b). The pattern in the Poincaré plot of the elevation is as well similar to the one of the TGO. The timing of the overflights is however completely different to the one of the TGO. This is originating in the sun-synchronous orbit of MRO leading to an appearance of the overflights around 4 a.m. and 4 p.m. *LTST* with some deviation due to the equation of time and the duration of a sol not being a multiple of the orbital period. This can be as well spotted in the overflight pattern in Fig. 4.4 where, assuming no minimum elevation, the pattern of overflights

consists of two consecutive ones with a separation of one orbital period, or a single one, which are always appearing around the stated times.

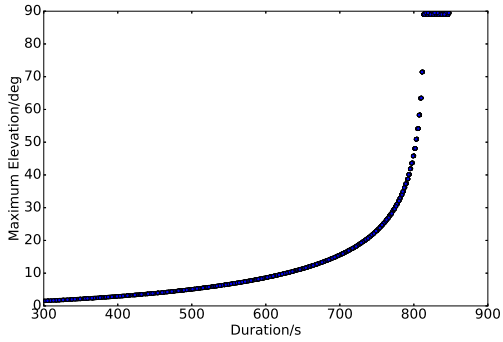

(a): The elevation as a function of the duration

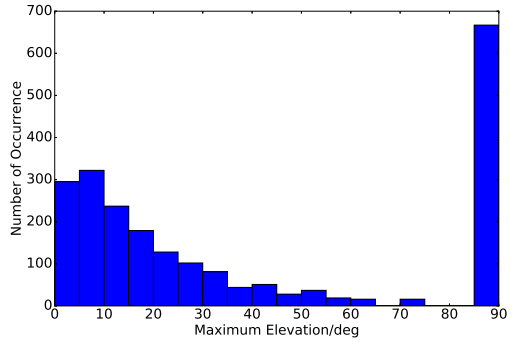

(b): The appearance of the different elevations

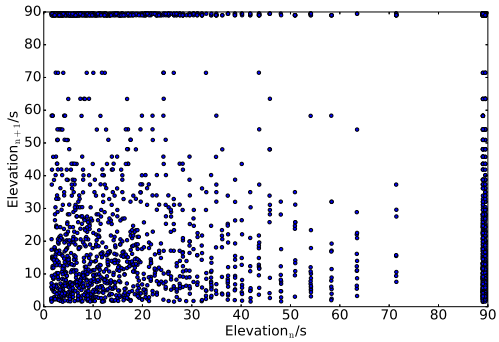

(c): A Point-Carée plot of the durations at 0° elevation

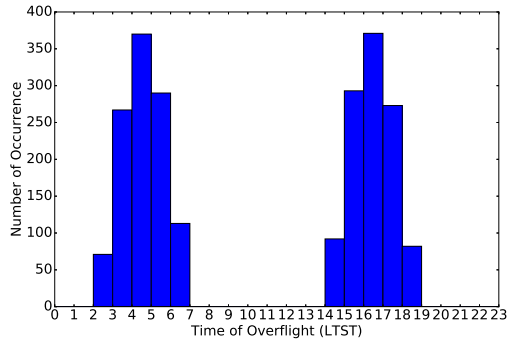

(d): The timely occurrence of the overflights on Mars in *LTST*

Figure 4.3: The elevation, duration and timing properties of the overflights for MRO

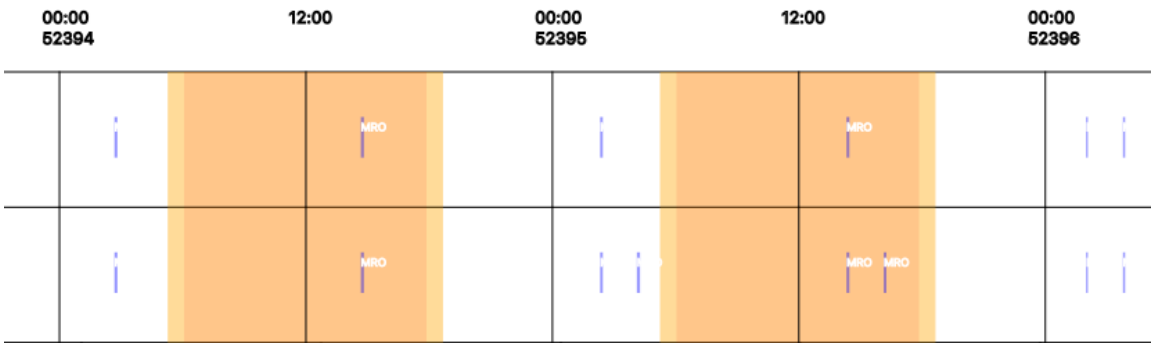

Figure 4.4: The pattern of overflights with a minimum elevation of 10° in the upper column and with no minimum elevation in the lower one displayed on an event timeline. A blue box indicates hereby an overflight, while the text in it just refers to the orbiter that can see the lander, which is fixed in this case as MRO.

4.2.3 Odyssey

Situated in a sun-synchronous orbit with the semi-major axis as TGO the duration-elevation dependency and the elevation occurrence is the exact same as for TGO, as visible in Fig. 4.5(a) and

Fig. 4.5(b). Furthermore, the dependence of the elevation of one overflight on the previous one is as well similar as visible in Fig. 4.5(c). However, the timing of the overflights is fixed, similar to the one of MRO with the only difference that the ones of Odyssey are situated around 8 a.m. and 8 p.m. which can be seen in Fig. 4.5(d). This can be as well spotted in the overflight pattern in Fig. 4.6 where, assuming no minimum elevation, the pattern of overflights consists of two consecutive ones, with a separation of one orbital period, or a single one, which are always appearing around the stated times.

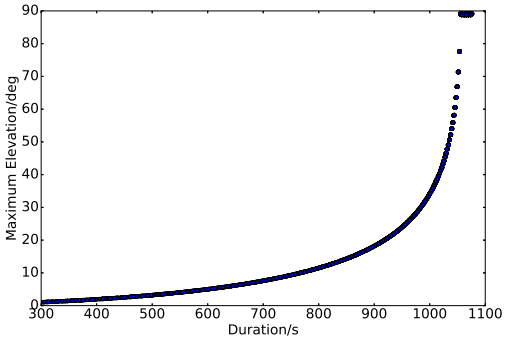

(a): The elevation as a function of the duration

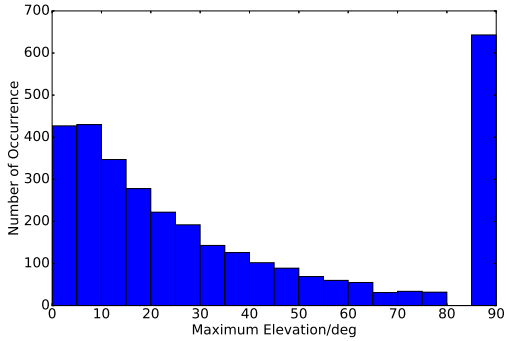

(b): The appearance of the different elevations

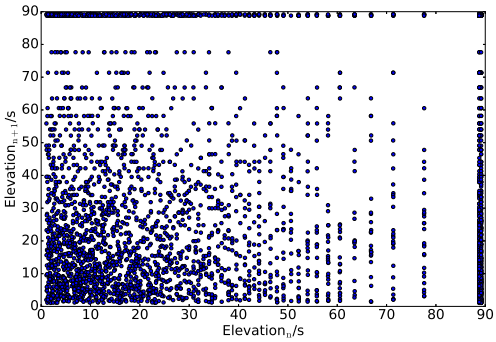

(c): A Point-Carée plot of the durations at 0° elevation

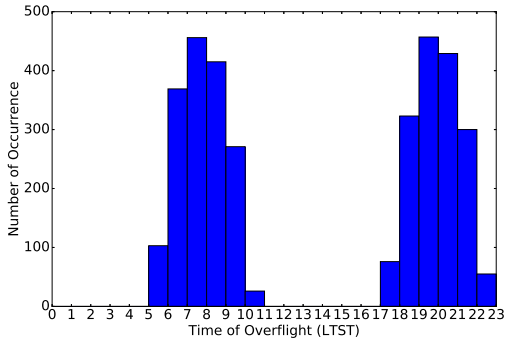

(d): The timely occurrence of the overflights on Mars in *LTST*

Figure 4.5: The elevation, duration and timing properties of the overflights for Odyssey

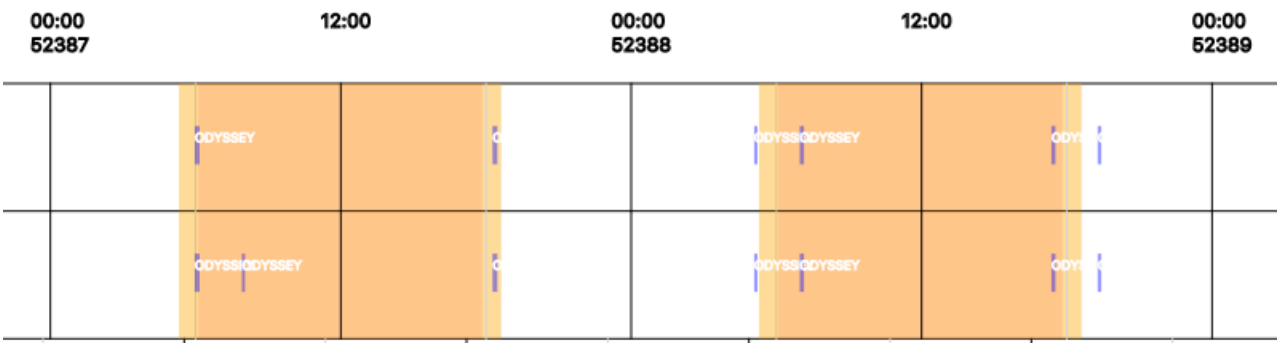

Figure 4.6: The pattern of overflights with a minimum elevation of 10° in the upper column and with no minimum elevation in the lower one displayed on an event timeline. A blue box indicates hereby an overflight, while text in it just refers to the orbiter that can see the lander, which is fixed in this case as Odyssey.

5 Solution Approach

To solve the problem, a local optimisation was chosen to keep the computational resources required small. The local optimum is determined by minimising the cost function Eqn.(5.2) or Eqn.(5.3) for each overflight depending on the current type of communication required. Before the cost function can be evaluated several steps have to be performed. First of all the simulation of all external bookings has to be done, which is described in Sec. 4.1. With these and the input of one Eventfile per satellite, described in Sec. 9.6.1, the available communication opportunities from Earth to each orbiter have to be determined. The process doing this is described in detail in Sec. 5.1. With these, the downlink and uplink opportunities from each ground station to each satellite are determined, which are closest to each of the overflights over each lander. This is described in detail in Sec. 5.2. Finally, the algorithm determines the locally optimal usage for the overflights to be forward link or return link to bring/return data to/from the rover or to remain idle by minimising the related cost function. With the determination of the cost function, the optimal ground station pass to uplink or downlink data to the satellite is evaluated. This reasoning is described in detail in Sec. 5.3.

5.1 Determining available Ground Communication Windows

To determine the pure geometrical constraints, the ESOC Flight Dynamics office provides dedicated Eventfiles, described in Sec. 9.6.1, for each orbiter. Using this and the Planview file, described in Sec. 9.6.2, giving the bookings of the different ground stations, the communication windows which each satellite can actually use for communication with Earth can be determined. While explaining the algorithm step by step a simplified example shows the changes on timelines during each step in Fig. 5.1. Furthermore, pseudo-code performing these steps is shown in algorithm 5.1 and the Java code for it can be found in the *run()* function of the *OrbiterGSAllocation* class. In (1) the visibilities of one ground station (GS1) can be seen. In addition to those, a number of bookings for the ground station (2) and occultations (3) are given. Hereby, it has to be taken into account that the data provided by the ESOC Flight Dynamics only provide the geometrical visibility. To retrieve the visibilities for downlink and uplink the geometrical ones have to be shifted by a OWLT to the future or past, respectively. This way, the downlink (4) and uplink (5) visibilities can be determined from (1). Afterwards, those windows are cut by the occultations, which are as well shifted according to the kind of visibility. Doing this, it has to be taken into account, that the OWLT for the moon is nearly zero, while the ones for Phobos and Deimos are close to the one from Mars. One special occultation is the one from the Sun which is not shifted since the OWLT is included in the margin of the definition of the solar conjunction.

Performing the mentioned cut, the visibilities for downlink (6) and uplink (7) are left. Now, the bookings from the Planview file are taken into account. With those, the times in which each ground station is free for tracking can be derived by taken the inverse of the bookings timeline. Hereby, the

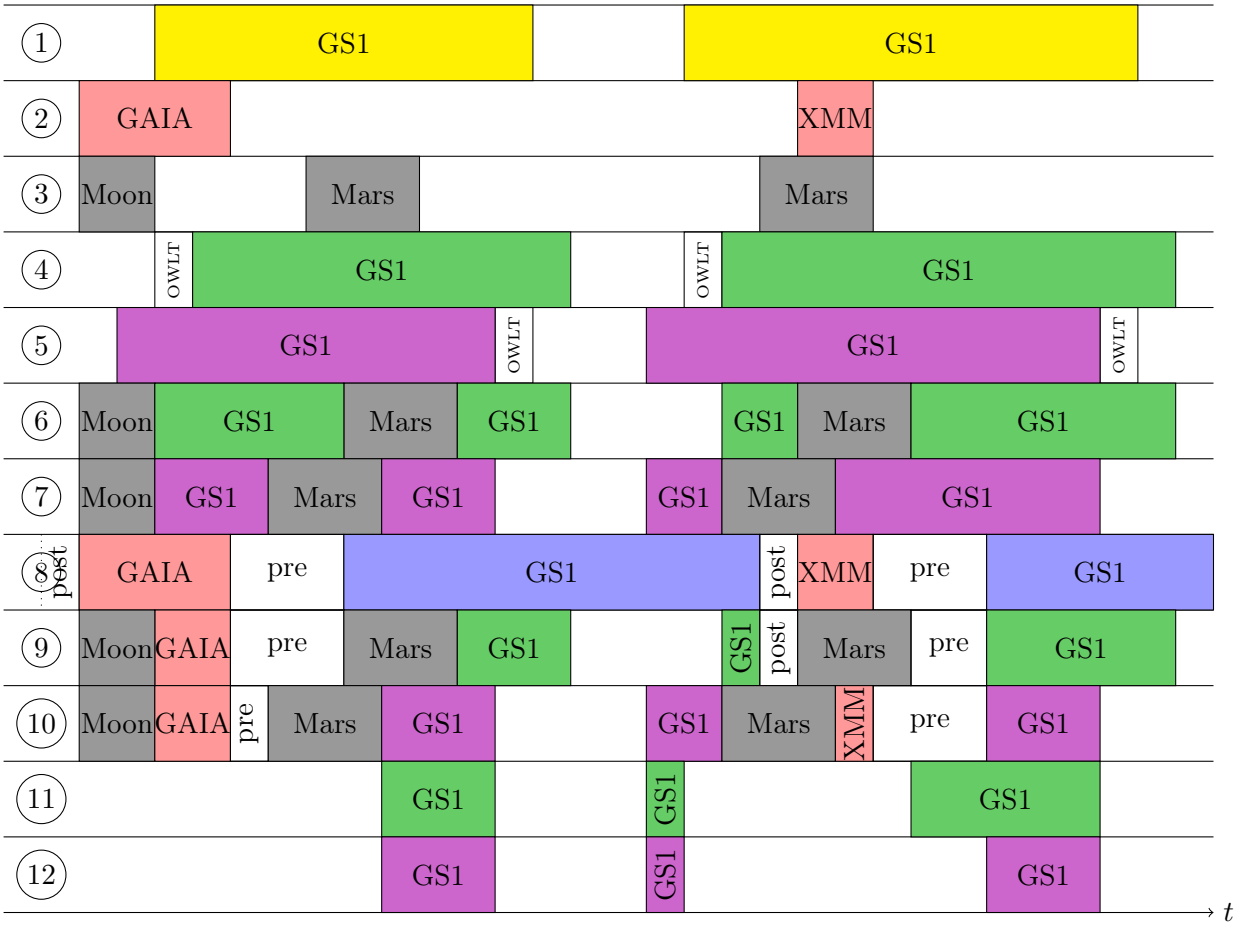

Figure 5.1: The algorithm to determine the available communication windows and the timelines originating from its steps. Tracking and visibility based windows are hereby indicated yellow, downlink based ones green, uplink based ones purple, booking based ones red, occultations based ones grey and the ones based on the left-overs from other bookings blue.

time necessary to set up the ground station for a pass needs to be added at the end of each booking and the one for performing after-pass actions, to the start of it. Doing this and taking the inverse leads to (8). If reallocating bookings from other missions is prohibited the intersection of periods in (8) with the periods in (6) and (7) give the newly available windows for downlink (9) and uplink (10). In the case of a confirmation of the telecommands is required the downlink visibilities are shifted two OWLT to the past (11) and the intersection of this with (10) forms the telecommunication windows which provide telecommand confirmation (12). This gives us the final uplink windows in which the ground station is visible, no other spacecraft is using the station and the commands send to the spacecraft can be as well confirmed by receiving an answer from it two OWLT after sending it. Performing this algorithm for each ground station (9) and (12) of each station provide the basis for the next step, if telecommand confirmation is needed otherwise, (9) and (10) provide the basis. In this next step, the algorithm chooses the opportunities on each ground station, which can be used for uplink and downlink depending on the different overflights over the rover. It is described in Sec. 5.2.

Algorithm 5.1: The algorithm to determine the available ground station communication windows

```
Data: visibilities, occultations (2), bookings (3)
Result: commsWindowsUl, commsWindowsDl
for station in visibilites.keySet() do
    visibility ← visibilities.get(station) (1)
    tmVisbility ← shift visibilities by a OWLT to the future (4)
    tcVisbility ← shift visibilities by a OWLT to the past (5)
    for occ in occultations do
        if occ.getBody() = MOON or occ.getBody() = SUN then
            tmVisibility ← tmVisbility\occ (6)
            tcVisibility ← tcVisbility\occ (7)
        else
            tmVisibility ← tmVisbility\occ shifted a OWLT to the future (6)
            tcVisibility ← tcVisbility\occ shifted a OWLT to the past (7)
        end
    end
    stationUnavailable ← booking.toStationOccupation() (8)
    tmVisibility ← tmVisbility\stationUnavailable (9)
    tcVisibility ← tmVisbility\stationUnavailable (10)
    commsWindowsDl.add(station, tmVisibility)
    if Commands Confirmation Required then
        commsWindowsUl.add(station, tmVisibility shifted by 2 OWLT to the past (11)∩tcVisbility)
        (12)
    else
        commsWindowsUl.add(station, tcVisibility)
    end
end
```

5.2 Determining data link Opportunities

With the windows determined using the procedure described in Sec. 5.1 the actual opportunities for a data link to the lander shall be determined. Meaning that data can be transmitted from a ground station, via a satellite, to a landed asset or vice versa. Hereby, the time between an uplink and the forward link and a return link and a downlink shall be as small as possible, while all of them have to provide enough time for the necessary transmissions and, in the case of forward links, the operational margins. These data link opportunities are determined for each lander visibility window and each ground station. The procedure for one example shall be discussed in detail and is shown in Fig. 5.2, in pseudo-code in algorithm 5.2 and can be found as Java code in the *call()* function of the *LanderTask* class. Starting with an overflight visibility (in this case from the TGO) (1) the downlink (2) and uplink (3) windows on a ground station can be determined in the following way. For the uplink, the first window prior to the overflight is investigated and selected if it is long enough to hold an uplink with the necessary operational margins. Otherwise, the window previous to that window is investigated. Afterwards, the uplink window is saved as an uplink opportunity for this particular overflight. In the case of telecommand confirmation being required it is as well extended by two

OWLT to receive it. Hereby, the step in the prior section, of overlaying the uplink windows with the shifted downlink windows, ensures that the extension by two OWLT actually allocates a window with telemetry visibility. The same procedure is done after the overflight for the downlink windows, except for the confirmation since it is not required for a downlink. This means that the first downlink window after the pass is investigated and selected if it is long enough to hold a downlink pass. If not, the investigation is continued on the window after the currently selected one. This leads to a dedicated downlink (4) and uplink (5) opportunity on each ground station for each overflight. Having those, the overflights can be optimised, using the procedure described in Sec. 5.3.

Algorithm 5.2: The algorithm to determine for each overflight the uplink and downlink pass on every ground station closest to it and long enough to fit the operational margins

```
Data: overflights (1), commsWindows (2) (3)
Result: overflights
for overflight in overflights do
    for station in commsWindows.keySet() do
        tcWindow ← commsWindow.get(station).before(overflight shifted a OWLT to the past)
        while tcWindow.isToShort() do
            tcWindow ← commsWindow.get(station).before(tcWindow)
        end
        tmWindow ← commsWindow.get(station).after(overflight shifted a OWLT to the future)
        while tmWindow.isToShort() do
            tmWindow ← commsWindow.get(station).after(tmWindow)
        end
        overflight.addPossibleUlWindow(station, tcWindow) (5)
        overflight.addPossibleDlWindow(station, tmWindow) (4)
    end
end
```

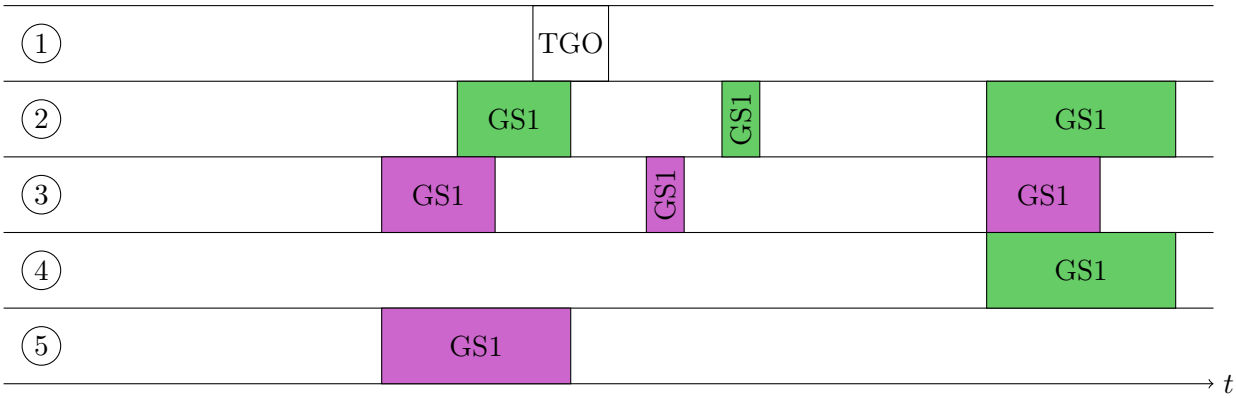

Figure 5.2: The algorithm to choose the data link opportunities and its different steps indicated with timelines. Downlink based opportunities are indicated green and uplink based ones purple.

5.3 Optimisation of data link Opportunities

With the windows retrieved, using the steps stated in Sec. 5.2, the optimisation to maximise RWT and EPT can be performed. The pseudo-code for this can be found in algorithm 5.3 and the Java code

for it can be found in the *findOptimizedSelectionOfRelayPasses()* function of the *Optimizer* class. For the optimisation, an initial forward link has to be found. This is assumed to be the first overflight happening before noon of a sol for which minimum one uplink opportunity exists. Afterwards, an iterative process takes place. A cost function explained in Sec. 5.3.1 is applied to the next twenty overflights over the landed asset. Twenty is hereby assumed to keep the computation power needed small, while not neglecting overflights. This can be guaranteed since twenty overflights correspond to minimum five sols. Therefore, taking the last pass would already correspond to a loss of four days RWT which is already unacceptably high. While calculating the costs, the cost function for the job opposite to the last one is taken. If the last pass was a forward link, the next one is assumed to be a return link and vice versa. This assumption is taken, since it is not useful to send new commands without having new information and it is neither useful to return data if the rover had no commands to work. The cost functions for each of the jobs are explained in detail in Sec. 5.3.1.2 and Sec. 5.3.1.3. From the twenty passes considered, the one with the smallest cost is chosen and serves as starting point for the next iteration. Hereby, taking the cheapest guarantees a local optimisation of the parameters chosen, because every undesired behaviour leads to a higher value of the cost function. This procedure is repeated until the number of remaining overflights is smaller than twenty. This way the whole RSM is covered.

Algorithm 5.3: The algorithm to determine the cheapest overflights and their related ground station passes.

```
Data: overflights
Result: optimisedOverflights
lastOverflight ← overflights.first()
while lastOverflight.isAfterNoon() do
    lastOverflight ← overflights.next(lastOverflight)
end
index ← lastOverflight.index()
while overflights.size() - index > 20 do
    cheapestCost ← -1
    for i in [index; index+20) do
        if lastOverflight.getCommsType == UPLINK then
            cost, gsWindow ← CostFunctionReturnLink(overflights.get(i))
        else
            cost, gsWindow ← CostFunctionForwardLink(overflights.get(i))
        end
        if cheapestCost < 0 or cost< cheapestCost then
            cheapestCost ← cost
            cheapestOverflight ← overflight
            cheapestGsWindow ← gsWindow
        end
    end
    cheapestOverflight.addGsWindow(cheapestGSWindow)
    optimisedOverflights.add(cheapestOverflight)
    index ← cheapestOverflight.index()
    lastOverflight ← cheapestOverflight
end
```

5.3.1 Cost Functions

In order to find a locally optimal solution, the cost function for the related job shall be minimised for every allocation. The cost functions for the jobs are different, leading to the usage of an individual cost function for each the forward link and return link. Hence, for a forward link job Eqn. (5.2) shall be minimised and for a return link Eqn. (5.3). However, the factors for losing either EPT or RWT are the same. The same applies to the costs of the allocation of ground station time. Thereby, the allocation of one hour of ground station time serves as the identity value. The cost factors themselves are adjustable to retrieve the different influences of the parameters. The factors are:

- ω denotes the costs for the loss of one hour of RWT on the surface of Mars. The assumptions for lost hour of RWT are indicated in the individual cost function. Its default value is 10000 for rovers and 100 for surface platforms.
- ρ denotes the costs for the loss of one hour of EPT. The assumptions for lost hour of EPT are indicated in the individual cost function. Its default value is 10000 for rovers and 100 for surface platforms.
- γ_{GS} denotes the costs for the allocation of one hour tracking time on the ground station GS containing penalties for agency cross-support and an individual factor. Those are by default 500 and 1.
- γ_{SAT} denotes the costs for the allocation of a satellite for relay operations. It depends on the agencies the lander and the orbiter belong to and an individual factor, which can be set according to the properties of the orbiter (e.g Electra radio available or not). The default values for this are 10000 for cross-support and 10000 for the orbiter if it does not hold an Electra radio, 0 otherwise.
- ξ denotes the costs when downlink and uplink happen on different stations. It is set by default to the allocation cost for the newly allocated station.
- μ denotes the costs of an omitted uplink. It is set by default to 0 to avoid uplinks which are not required.
- δ denotes the costs of an omitted downlink. It is set by default to 0 to avoid downlinks which are not required.

While adjusting those parameters, ω and ρ should be kept minimum two orders of magnitude higher than all others, since RWT and EPT are valued a lot higher than blocking a ground station, because the TGO requires six hours tracking time. These two orders of magnitude ensure that losing either EPT or RWT changes the minimum of the cost function a lot more than the ground station allocation costs. μ and δ provide the possibility to set a cost constraint on additional uplinks or downlinks. This way, they are only booked if they can be achieved without adding more costs than μ or δ, respectively.

5.3.1.1 Ground Station Costs

The costs for the ground station allocation is basically the same for both forward link and return link and can be seen in Eqn.(5.1). It only differs in the necessity of uplink and downlink. The first one is

required for all forward link passes, while latter is optional if not specifically indicated. For the return link, it is the exact opposite.
To retrieve the ground station costs for an overflight the number of allocation hours for each ground station has to be derived. It depends on the time at which the job is processed, since the OWLT changes, and is represented as $H(C_i)_{\mathrm{GS}}$. It is evaluated by the solver by taking the allocations necessary to serve a pass and summing those up.
Furthermore, it depends on the minimum uplink ($t_{\mathrm{ul,min}}$) and downlink ($t_{\mathrm{dl,min}}$) time. Hereby, the minimum time for each required link is multiplied with the γ_{GS} for the station on which it happens and is assumed to state the costs for the pass. Every pass which is longer than that is assumed to save $1/\gamma_{GS}$ general hours of ground station allocation and is considered beneficial.
In addition to that an extra penalty (ξ) is added if the downlink happens on another station than the uplink since this causes an extra configuration to happen. In addition to those, there are several options in the tool which can lead to extra factors. If the uplink is not required on each pass, an additional penalty is added if it is omitted (μ). This way, a return link gets an uplink allocated if the costs for that are smaller than μ. The same reasoning applies for the downlink on a forward link and δ. This way passes which could provide an uplink and downlink can be preferred.

$$\begin{aligned} g(C_i) = {} & \gamma_{\mathrm{GS_{dl}}} t_{\mathrm{dl,min}} - \frac{H(C_i)_{\mathrm{GS_{dl}}} - t_{\mathrm{dl,min}}}{\gamma_{\mathrm{GS_{dl}}}} + \gamma_{\mathrm{GS_{ul}}} t_{\mathrm{ul,min}} - \frac{H(C_i)_{\mathrm{GS_{ul}}} - t_{\mathrm{ul,min}}}{\gamma_{\mathrm{GS_{ul}}}} \\ & + \xi + \mu + \delta \end{aligned} \tag{5.1}$$

5.3.1.2 Forward Link Jobs

The cost function for the forward link job can be seen in Eqn.(5.2). Hereby it is taken into account, that the idle time ($C_i - p_i - r_i$) before the job, composed of the job completion time (C_i), its release date (r_i) and processing time (p_i), is used as EPT and is therefore desired up to a maximum of eight hours. These eight hours were chosen after discussion with the ROCC. After that point, it is assumed that there is no extra benefit in adding further EPT since it directly reduces RWT. In addition, the forward link latency given by the processing time p_i has to be added as lost planning time, since a shorter latency allows more time for planning. Furthermore, the difference of the completion time of the job to dawn plus the rover warm-up time, which is assumed to be the due date (d_i), is added if the forward link happens during daylight. This is done because those hours indicate a loss of RWT. In addition to those costs, the costs for the ground stations ($g(C_i)$) are added as discussed in Sec. 5.3.1.1. Hereby, the cost function is calculated for each ground station pass available and the ground station providing the smallest value is chosen. The Java code for the forward link cost function can be found in the *getCheapestUplinkPass()* function of the related *Optimizer* class used.

$$f_i(C_i) = \omega \max\{0, C_i - d_i\} + \rho p_i + \rho \max\{0, 8 - (C_i - p_i - r_i)\} + g(C_i) + \gamma_{\mathrm{SAT}} \tag{5.2}$$

5.3.1.3 Return Link Jobs

The cost function for return link jobs can be seen in Eqn.(5.3). For this, the idle time before the job ($C_i - p_i - r_i$), composed of the job completion time (C_i), its release date (r_i) and processing time

(p_i), is used as RWT and is desired until a maximum of the Martian day length (t_{md}), reflecting a full working day. Hereby, an extra factor normalising the length of a Martian day to 12 Martian hours is added. This way, RWT is considered more valuable during winter at the landing site, since less of it is available. In addition to that, the difference of the return link to dusk is added, if the return link happens during Martian night because the earth planning is preferably done during Martian night to save the day for working. Therefore, the Martian dusk after the release date is assumed as due date (d_i) for the process. This loss has however always a lower boundary being p_i the return link latency since this is the minimum loss of EPT even if the downlink happens during Martian day. In addition to those costs, the costs for the ground stations ($g(C_i)$) are added as discussed in Sec. 5.3.1.1. Hereby, the cost function is calculated for each ground station pass available and the ground station providing the smallest value is chosen.The Java code for the return link cost function can be found in the *getCheapestDownlinkPass()* function of the related *Optimizer* class used.

$$f_i(C_i) = \rho \max\{p_i, C_i - d_i\} + \omega \frac{12}{t_{\mathrm{md}}} \min\{t_{\mathrm{md}}, t_{\mathrm{md}} - (C_i - p_i - r_i)\} + g(C_i) + \gamma_{\mathrm{SAT}} \tag{5.3}$$

5.3.2 Multiple Landed Assets

When having multiple landed assets close to each other, or a satellite flying at a high altitude, the visibilities of the landers can overlap. This is particularly the case for the RSP mission, where the rover and the surface platform land at the same location and even though the rover is moving the overflights remain basically the same throughout the whole mission time. There are several ways to cope with this problem. One is to have a solver, which is solving one landed asset after each other handing the constraints from all previously processed landed assets to the solving process of the following ones. In order to provide a more flexible solution approach for landed assets with the same location, those are solved by a separate solver. This allows sharing overflights, if they are long enough, between both assets and only book one ground station pass for them, which the single solver can not cope with.
For assigning relay overflights, the cost function for each one is determined using the cost function approach of the single solver. The cheapest overflight is determined for each landed asset, collected and sorted by their start date. Afterwards, three different cases can appear. Those are sketched for the case of the rover and the surface platform in Fig. 5.3. In the first case, the overflights are after each other as visible in (1) and (2). In this case, the earlier overflight is allocated, resulting in (3), and the solving algorithm starts again to determine the costs for the overflights, respecting the newly allocated one.
In the second case, the overflights are overlapping each other as sketched in (4) and (5), but the overflight is too short to be shared. In this case, the overflight is allocated for the landed asset with the higher cost function, since a pass is more pressing for this asset. In the example, the pass then might be given to the rover, since it is more constrained regarding RWT and EPT, leading to the booking in (6).
The last case can be seen in (7) and (8). The two overflights overlap, but this time, they are long enough to be shared. In this case, the pass is cut into halves, on the end of the first half and the start of the second half the time required for switching between the assets is subtracted and the overflights are allocated, leading to (9). The Java code for this can be found in the *findOptimizedSelectionOfRe-*

layPasses() function of the *MultipleLanderOptimizer* class.

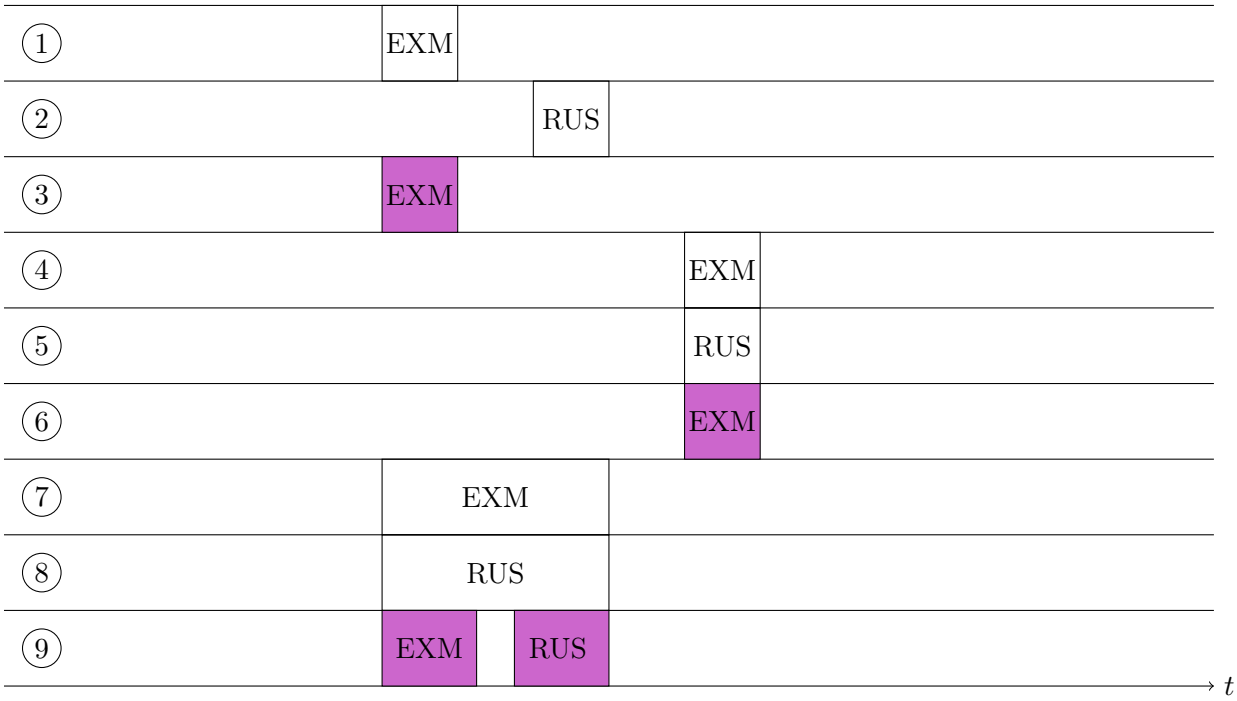

Figure 5.3: The different overflights patterns, which can appear while solving a scenario for multiple landers and the allocations following from them, indicated as timelines.

5.4 Summary

Performing the steps mentioned above provides the possibility of processing information handed to the tool in the form of an Eventfile and Planview file such, that a locally optimal allocation of overflights and an optimal allocation of the ground station passes can be performed for each landed asset.

6 Results

After applying the solver on the scenarios, discussed in Sec. 3, the following results were found. The results are ordered similar to the presentation of the scenarios in Sec. 3, starting with the one orbiter scenarios and their results in Sec. 6.1, followed by the multiple orbiter scenario in Sec. 6.2 and the comparison to the 2018 launch data in Sec. 6.3.

6.1 One Orbiter Scenarios

Since the baseline for the ExoMars RSP mission is the usage of one orbiter, it shall be discussed in detail with different ground station networks, operational constraints and the possibility of sharing overflights to provide an in-depth understanding of it.

6.1.1 Scenario 1a

Scenario 1a: Geometrical Constraints $(TGO, EXM, BLK + MLG, 10)$
This scenario, being a fully theoretical, best case solution with no operational margins at all, which is using the BLK+MLG network, provides 1839.3 h EPT and 1670.5 h RWT during the RSM. These values correspond to an average of 9.5 h EPT and 8.4 h RWT, while 2 % of the passes provide an EPT of less than four hours and 12 % an EPT of less than six hours.

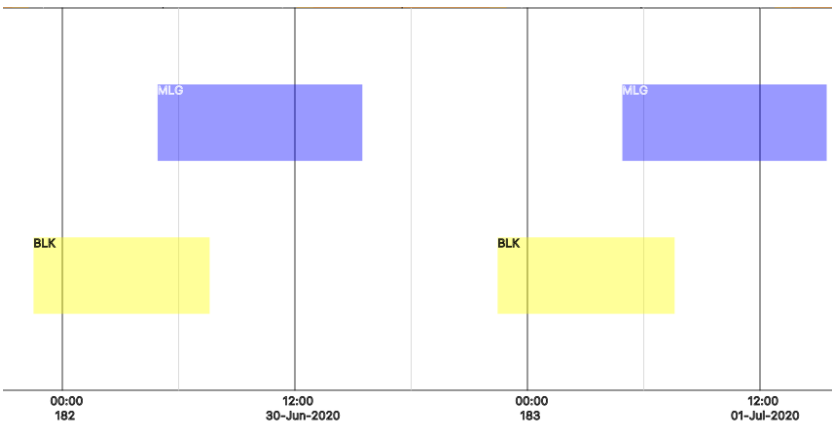

Figure 6.1: An example of repeating visibility gap between MLG and BLK. Hereby every ground station's timeline is displayed on a different y-level for better visibility.

Investigating the RWT in Fig. 6.5, two repeating patterns with a period of approximately two months and two years can be spotted. The shorter one originates in the repeating pattern of overflights of the TGO over the landing site and is quite stable since the TGO's ascending node orbits Mars once every 24 h leading to the overflights being shifted by approximately 30 mins every sol. If they are situated around dawn and dusk, the full time in-between them can be filled with RWT, leading to a maximum corresponding to the time of Sun being above the minimum elevation on the sol. If they are then getting shifted, the time from dawn till

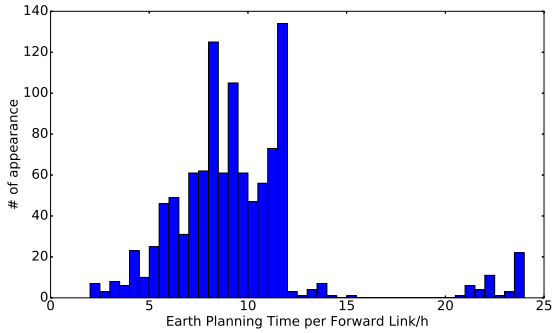

Figure 6.2: The distribution of EPT within the evaluated period

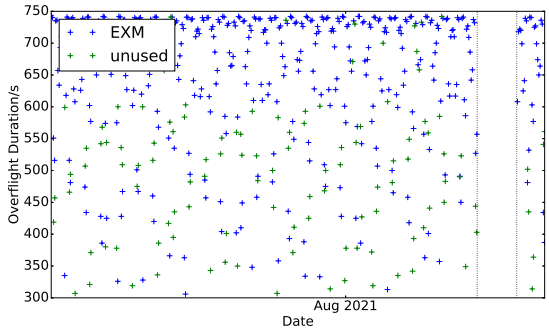

Figure 6.3: The overflights over the rover and their assignment

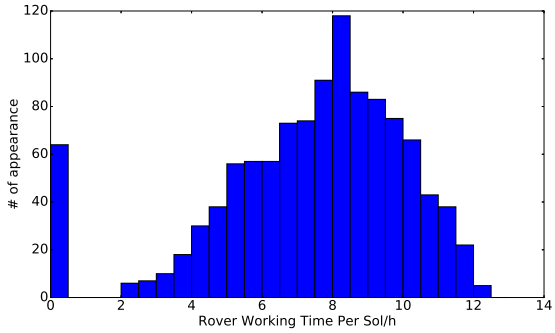

Figure 6.4: The distribution of RWT within the evaluated period

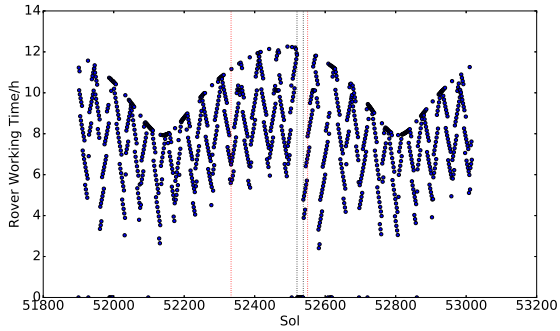

Figure 6.5: The RWT available on each sol

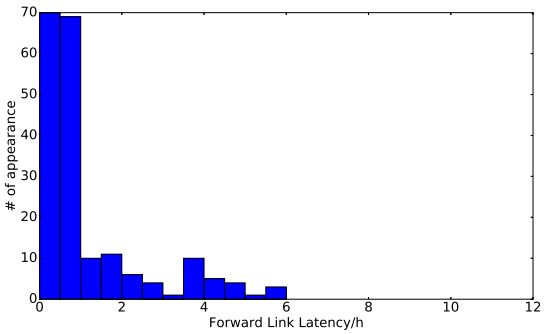

Figure 6.6: The distribution of the forward link latencies within the evaluated period

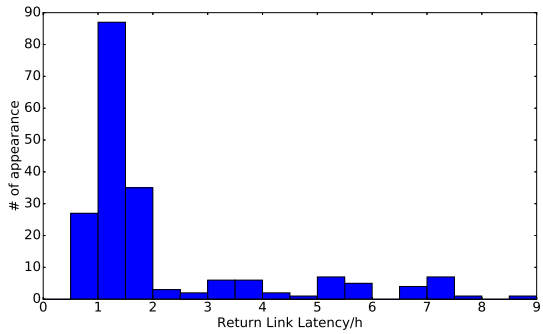

Figure 6.7: The distribution of the return link latencies within the evaluated period

Table 6.1: The parameters evaluated for TGO,EXM,BLK+MLG,10. The dotted red lines are indicating the borders of the RSM and the black ones the borders of the conjunction.

the return link decreases and therefore the RWT decreases until a minimum of half the time of the Sun being above the minimum required elevation. Afterwards, it is more beneficial to use the day pass as a forward link and work till dusk. With the propagation of time, the overflights get shifted further, leading back to the first case of the whole time of the Sun being above the minimum required elevation being used as RWT. This shift of the pattern has a magnitude of a bit less than 30 min per sol, which leads to a pattern period of a bit more than 48 days. The pattern can hereby be altered if two consecutive overflights are available to choose from. On top of this, there are some minor influences on the minimisation of the cost function if the uplink latency

increases drastically, which can lead to a jump to the next overflight. Therefore, there are some cases where the actual RWT deviates from this pattern. Moreover, there is a sinusoidal modulation of the pattern with a period of approximately two years, which is the orbital period of Mars around the Sun. This is originating from the seasonal effects of the non-equatorial landing site. During the RSM it is summer at Oxia Planum, offering longer daylight and therefore more RWT. These two patterns provide as well an upper boundary for the theoretically achievable RRWT, with the latter pattern giving the maximum theoretical RWT in total and the first one an idea of the constraint due to the overflights. When subtracting from the maximum achievable RWT the solar conjunction, only 92 % of theoretically available RRWT remain. Assuming an average fraction of 75 % of the sol being between two overflights of TGO, the theoretically achievable RRWT is around 69 %. Comparing this with the RRWT provided by the BLK+MLG network, being 65%, it can be seen that the solution is already close to the optimum from the RWT perspective when neglecting operational margins.
Investigating the EPT, indicated in Fig. 6.2, a high deviation from the average can be spotted leading to undesirable cases of having less than six hours of EPT. The reason for this is that a gap between the visibilities on BLK and MLG appears every day. An example of the gap can be seen in Fig. 6.1. It is a result of Earth shadowing the TGO from the ground stations, leading to high forward link and return link latencies visible in Fig. 6.6 and Fig. 6.7. This problem can only be solved by having three ground stations with a separation of 120° situated at Earth's equator since the shadow of Earth is a bit more than 180° at each location depending on the local geography. This separation is approximately fulfilled by the ESTRACK network.
Investigating the overflights during the RSM in Fig. 6.3, it can be seen that 79 % of the overflights are allocated for the rover, which leaves only 14.6 h for the surface platform during the RSM. This is too short to transmit all data back even if the highest data rate available could be used all the time. Since a further optimisation of the data link to Earth would lower the amount of overflights available for the surface platform even more, a sharing of the overflights between the rover and surface platform should be considered. However, in the summary table (Tab. 6.3) it can be seen that the requirement of returning 150 Mbits/sol is fulfilled on all of the sols with an average of 659.7 Mbit/sol. This is somewhat similar to earlier studies regarding the link budget, which led to an average of 672.9 Mbit/sol [47]. However, an in-depth investigation of the data volume during overflight sharing is performed in Sec. 6.1.5 to investigate the impact of the surface platform on the data volume.

Scenario 1a i: Submission Deadline $(TGO, EXM, BLK + MLG, 10, ro2)$

When demanding a transmission of the commands from the lander operations centre to the orbiter operations

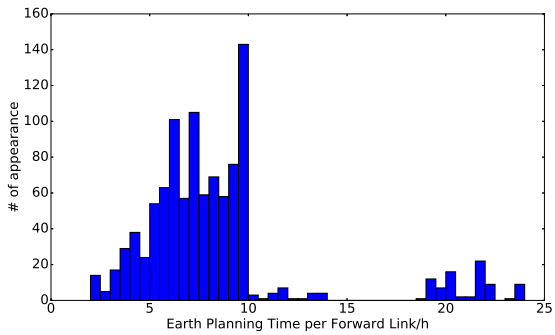

Figure 6.8: The distribution of EPT within the evaluated period of scenario 1a i

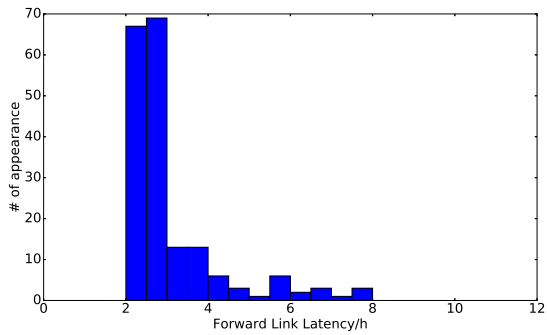

Figure 6.9: The distribution of the forward link latencies within the evaluated period of scenario 1a i

centre 2 h in advance of the uplink, 1627.7 h of RWT and 1546.7 h of EPT can be provided during the RSM. Those are corresponding to an average of 8.3 h of EPT and 8.1 h of RWT. These values indicate an average loss of 1.2 h of EPT and 0.3 h of RWT compared to the geometrical scenario. The reason for this loss can be seen, when comparing the forward link latencies of this scenario in Fig. 6.9, with the one of the geometrically

constrained one in Fig. 6.6. There it can be seen that the average forward link latency is increased by 1.9 h. The reason for the loss being a bit less than the 2 h of the deadline is that there are now more cases where the desired EPT is not reached and therefore the pass allocation is altered a bit compared to scenario 1a, leading to an alternating latency while keeping the cost functions minimised.

Scenario 1a ii: Command Confirmation $(TGO, EXM, BLK + MLG, 10, cc, ro2)$
Requiring commands confirmation does not alter the RWT nor the EPT compared with only requiring a submission deadline. However, the ground station time required is increased, since the ground stations have to be booked for two additional OWLT. The small impacts originate in the fact that the two OWLT only require telemetry visibility, which is only unavailable when Moon occultations take place and those are quite rare phenomena. In all other cases, the visibility for telemetry is always two OWLT longer than the one for telecommands. Therefore, waiting for a confirmation only extends the ground station pass and the impact on the rest of the scenario is rather small.

Scenario 1a iii: Ping $(TGO, EXM, BLK + MLG, 10, cc, pi, ro2)$
If a ping is required as well before sending commands to the orbiter, the RWT decreases to 1552.8 h and the EPT increases to 1557.7 h. The decrement originates from the ping extending the ground station passes by two OWLT, which are not added to the forward link latency since the ping does not require to have the commands for the lander available. This is only impacting, similar to the commands confirmation, the allocation of the overflights which are established on the edge of ground station visibilities. However, in this case, the two OWLT require as well telecommand visibility, which shifts the passes to the past when occultations take place, altering the selection of relay passes if not enough EPT can be provided. Therefore, the RWT decreases and the EPT increases, since several sols are skipped, which counters the loss of EPT on other occasions, being as well indicated by the increased average EPT.

Scenario 1a iv: Retransmission $(TGO, EXM, BLK + MLG, 10, cc, ro2, rt)$
If instead of a ping, a retransmission opportunity is granted, the file is required two OWLT earlier compared

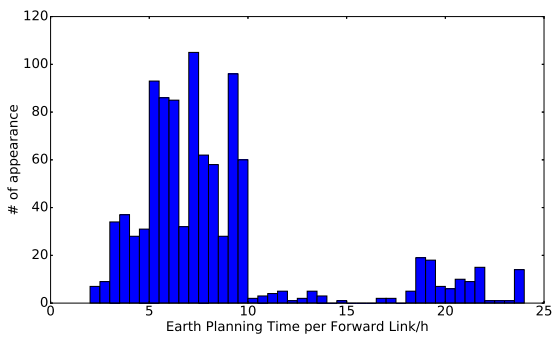

Figure 6.10: The distribution of EPT within the evaluated period of scenario 1a iv

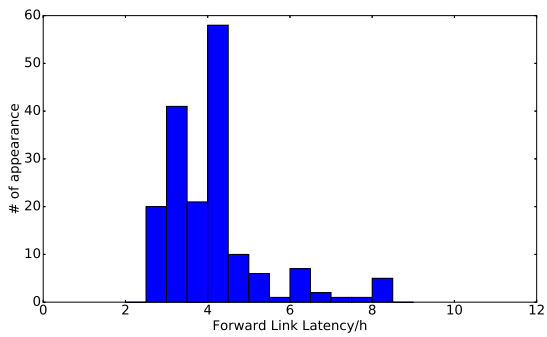

Figure 6.11: The distribution of the forward link latencies within the evaluated period of scenario 1a iv

to the usage of a ping only. When evaluating this possibility, 1473.6 h of EPT and 1536.9 h of RWT remain. This indicates a loss of half an hour EPT on each overflight compared to the ping case, being approximately the average of two OWLT during the RSM. The decrement of the RWT originates in altered reasoning on consecutive overflights.
This set of operational constraints is further referred to as desired operations, for reasons which are stated in the conclusions in Sec. 7.2.

Scenario 1a v: Prime Uplink $(TGO, EXM, BLK + MLG, 10, cc, pu, ro2, rt)$

Requiring a prime uplink opportunity on top of the retransmission requirement, a further decrement of the

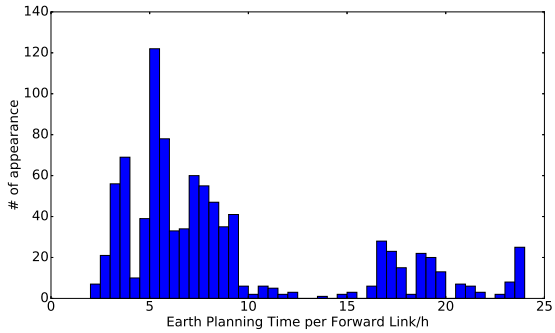

Figure 6.12: The distribution of EPT within the evaluated period

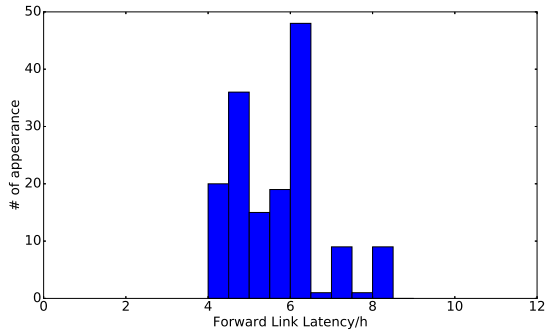

Figure 6.13: The distribution of the forward link latencies within the evaluated period

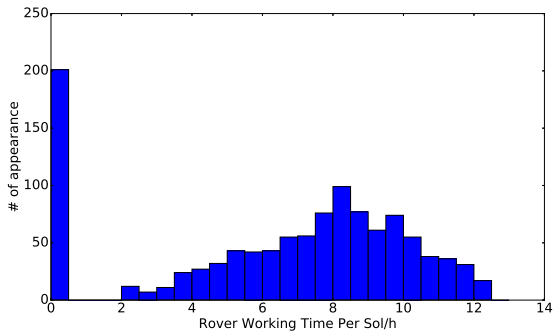

Figure 6.14: The distribution of RWT/sol within the evaluated period

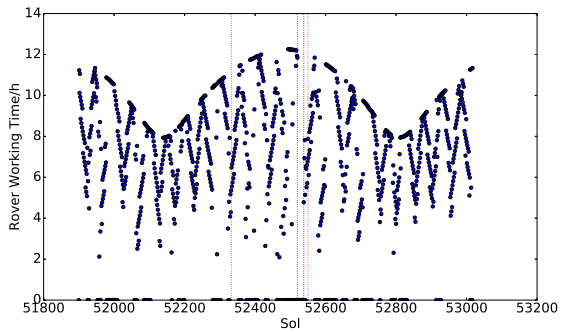

Figure 6.15: The RWT available on each sol

Table 6.2: The parameters evaluated for scenario 1a v. The dotted red lines are indicating the borders of the RSM and the black ones the borders of the conjunction.

EPT to 1386.8 h and of the RWT to 1428.8 h is observed. The average of the EPT is hereby 8.8 h and the one of the RWT 7.1 h. The reason for the absolute EPT to decrement can be spotted when comparing Fig. 6.12 and Fig. 6.10. There it can be spotted that this scenario holds a lot more cases where the EPT is higher than 15 h, indicating that a complete sol was skipped. This can be as well spotted in Fig. 6.15 and is a highly adverse case. It originates from the high increment of the forward link latency which can be spotted when comparing Fig. 6.13 with Fig. 6.11. The decrement of the RWT is owed to the fact that complete sols are skipped as well as the solver is trying to counter the loss of EPT by changing the overflight pattern cutting into the RWT.

Scenario	RWT/h	$\overline{\text{RWT}}$/h	RRWT	$\overline{\lambda_{\text{FWD}}}$/h	$\overline{\text{EPT}}$/h	<4 h EPT	<6 h EPT	<150 MBit
1a	1670.5	8.4 ± 2.7	65%	1.2 ± 1.3	9.5 ± 3.4	2 %	12 %	0 %
1a i	1627.7	8.1 ± 3.2	63%	3.1 ± 1.2	8.3 ± 3.7	6 %	23 %	0 %
1a ii	1627.7	8.1 ± 3.2	63%	3.1 ± 1.2	8.3 ± 3.7	6 %	23 %	0 %
1a iii	1552.8	7.8 ± 3.8	60%	3.6 ± 1.2	9.0 ± 4.9	7 %	31 %	0 %
1a iv	1536.9	7.7 ± 3.9	60%	4.2 ± 1.1	8.5 ± 5.0	9 %	32 %	0 %
1a v	1428.8	7.1 ± 4.4	55%	6.3 ± 1.9	8.8 ± 5.8	20 %	48 %	0 %

Table 6.3: Summary of all variations of Scenario 1a

6.1.2 Scenario 1b

Scenario 1b: Geometrical Constraint $(TGO, EXM, ESTRACK, 10)$

When using the ESTRACK network as ground station network, the amount of RWT during the RSM is 1767.0 h and the one of EPT is 2014.4 h. Compared to the BLK+MLG network, using the ESTRACK network marks a gain of 96.5 h of RWT and 121.1 h EPT. This leads to an average of 10.1 h EPT and 8.8 h of RWT. The difference to scenario 1a can be immediately determined when comparing Fig. 6.17 and Fig. 6.6. There it can be directly seen that the scenario 1a contains a lot more cases with uplink latencies higher than 3 h which originate in visibility gaps. These high latencies result, either in the overflights being shifted and cutting the RWT or in cutting the EPT. This is solved in this scenario by providing a nearly gapless coverage with ground station visibility leading to an average forward link latency of only 42 min.

In addition to the patterns in the RWT, another pattern can be spotted in the EPT in Fig. 6.16, but it

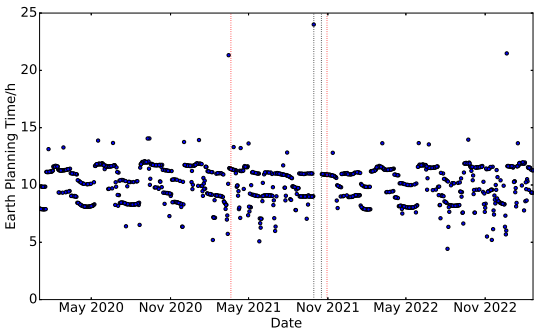

Figure 6.16: The EPT available on each date for scenario 1b. The red lines are indicating the borders of the RSM and the black ones the one of the solar conjunction.

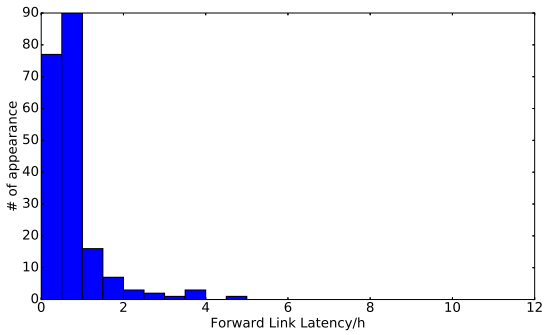

Figure 6.17: The distribution of the forward link latencies within the evaluated period of scenario 1b

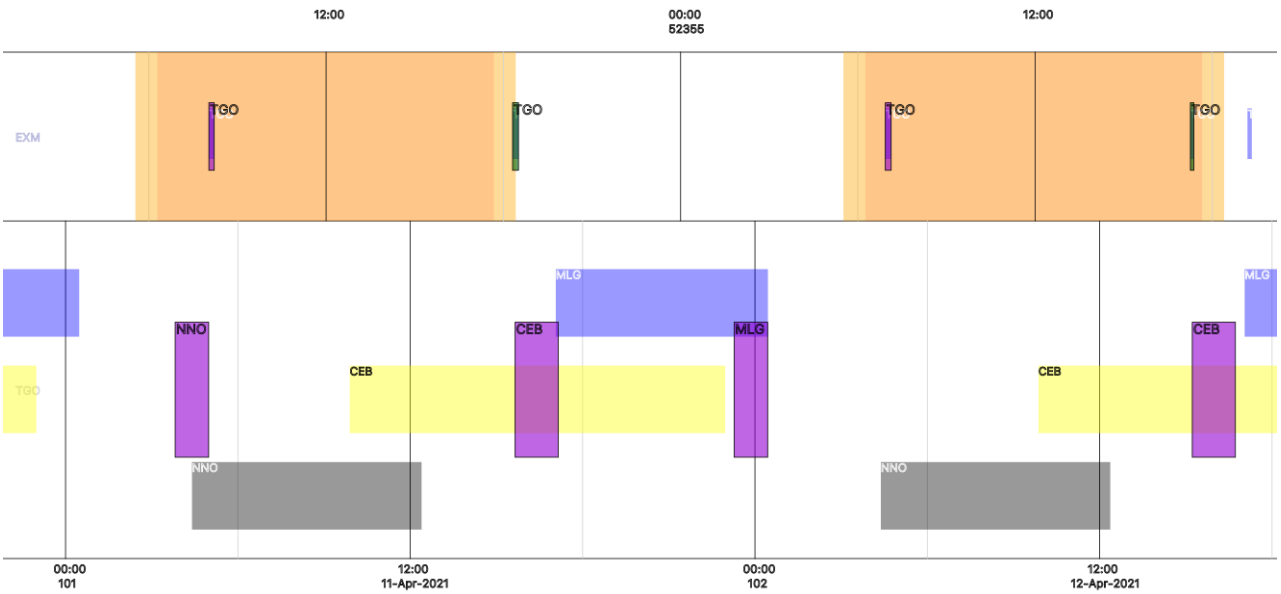

Figure 6.18: An example of the possible gap between the two ground stations NNO and MLG when Mars is north of the ecliptic plane. The upper row indicates Martian time and events occurring on Mars on a timeline, while the lower row shows UTC and events happening on Earth. Hereby every ground station's timeline is displayed on a different y-level for better visibility, while the actual passes are displayed on top of them.

scatters around May 2021. The scattering is due to Mars being situated furthest in the northern hemisphere of Earth at that time, leading to shorter visibilities for all ground stations on Earth's southern half. Since the chosen network contains two stations situated below the equator, MLG and NNO, both ground stations have shortened visibilities during this period. This leads to a gap between the stations' visibility periods. Furthermore, the fact that Mars is far away from Earth at that time leads to a high OWLT. In Fig. 6.18 it is visible that a pass in the visibility gap between NNO and MLG has a high forward link latency due to the missing coverage. The high latency shrinks the available EPT, breaking the usual pattern.
Finally, the amount of passes allocated to the rover increased further to 79 %, while on all the sols the data volume requirement is fulfilled for the rover. The RRWT is with 68 % close to the determined theoretical limit.

Scenario 1b i: Desired Operations $(TGO, EXM, ESTRACK, 10, cc, ro2, rt)$
If this network is used with the desired operational margins, it provides 1419.0 h EPT and 1730.0 h RWT. The reasoning is the same as it is for the retransmission case in scenario 1a. However, it can be seen that both, RWT and EPT, are higher and the cases with <4 h and <6 h EPT decreased to 7% and 25%, respectively. Finally, the RRWT marks 67 %, being still close to the theoretical limit even when respecting the operational margins.

Scenario 1b ii: Loaded $(TGO, EXM, ESTRACK, 10, cc, loCL2 + GAIA + LIPF + XMM, ro2, rt)$
If the scenario is loaded with bookings made by other missions, 1468.5 h EPT and 1552.2 h RWT can be provided. The decrement of the RWT is due to the fact that not all overflights can be serviced with short enough latencies anymore. The longer latencies originate hereby from the effective available visibility now having gaps again, due to the bookings. The delay of the forward links increases, however, the EPT in case it is not leading to a higher uplink latency.

Scenario	RWT/h	$\overline{\text{RWT}}$/h	RRWT	$\overline{\lambda_{\text{FWD}}}$/h	$\overline{\text{EPT}}$/h	<4 h EPT	<6 h EPT	<150 MBit
1b	1767.0	8.8 ± 2.0	68%	0.7 ± 0.6	10.1 ± 1.7	0 %	1 %	0 %
1b i	1730.0	8.7 ± 2.3	67%	4.1 ± 0.9	7.2 ± 2.5	5 %	23 %	0 %
1b ii	1552.2	7.8 ± 3.8	60%	4.3 ± 1.3	8.5 ± 5.1	15 %	30 %	0 %

Table 6.4: Summary of all variations of Scenario 1b

6.1.3 Scenario 1c

Scenario 1c: Geometrical Constraint $(TGO, EXM, BLK + ESTRACK, 10)$
This scenario, where ESTRACK and BLK are used as ground station network, provides a total number of 2014.4 h of EPT and 1767.0 h RWT, being the same as for scenario 1b since the visibility is not increasing effectively, only an alternative to certain visibility periods is offered.

Scenario 1c i: Submission Deadline $(TGO, EXM, BLK + ESTRACK, 10, ro2)$
Requiring a submission deadline in this scenario leads to a RWT of 1762.9 h and an EPT of 1638.1 h. Comparing this with scenario 1a i, it can be seen that 135.2 h more of RWT and 91.4 h more of EPT can be provided. The reason for that can be spotted when comparing Fig. 6.9 with Fig. 6.20. There it can be seen that the forward link latency is on average 24 min shorter and its deviation is smaller as well. Furthermore, it can be seen that Fig. 6.19 only has one case where the EPT is higher than 15 h meaning that a sol for working is skipped.

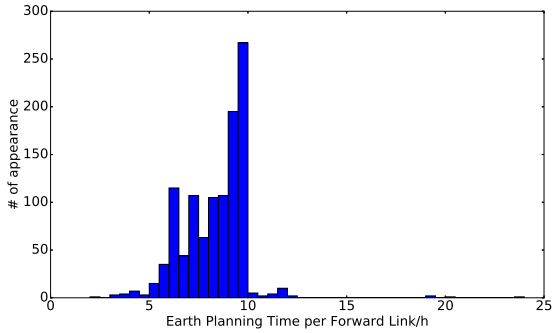

Figure 6.19: The distribution of EPT within the evaluated period of scenario 1c i

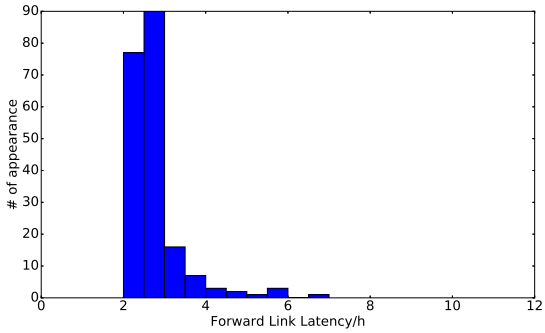

Figure 6.20: The distribution of the forward link latencies within the evaluated period of scenario 1c i

Scenario 1c ii: Command Confirmation $(TGO, EXM, BLK + ESTRACK, 10, cc, ro2)$
Similar to 1a ii, including a command confirmation on each forward link does not alter the results for the same reasons as stated for scenario 1a ii.

Scenario 1c iii: Ping $(TGO, EXM, BLK + ESTRACK, 10, cc, pi, ro2)$
Requiring a ping before uplinking commands to the orbiter, the RWT remaining is 1733.7 h and the EPT 1541.0 h. The reasoning is hereby comparable to the one of scenario 1a iii and the better key parameters originate only from the better visibility.

Scenario 1c iv: Desired Operations $(TGO, EXM, BLK + ESTRACK, 10, cc, ro2, rt)$
Similar to scenario 1a iv, the RWT and EPT are decreasing as well. Due to the better visibilities 1730.0 h RWT and 1419.0 h EPT can be provided while the same reasoning as for scenario 1a iv holds. To cover these operations on ground, 780.3 h of ground station time have to be booked during the RSM, corresponding approximately to 3.9 h per sol excluding the sols during conjunction. This ground station time includes preparation and deconfiguration times. The effective tracking time is 386.3 h, giving an average of 1.9 h per sol, which is just a third of the time the TGO requires anyway.
Varying the weighting of RWT and EPT leads to a decrement of the key parameters originating in the limited solution space and local optimisation approach. Altering the factors leads to different cost function minima and to different switching points where the forward link is shifted to daylight.
When increasing the cost factor for a lost hour of RWT, referred to as scenario 1c iv RWT, this switching is done earlier, leading to the forward link being afternoon for a long time until the pattern shifts. Furthermore, the selection of one of the consecutive overflights is always favouring RWT which as well decreases the EPT.
When increasing the EPT factor, referred to as scenario 1c iv EPT, the impact on the RWT is even higher compared to the case where RWT factor is increased. This is again originating in the altered switching point as well as favouring EPT on consecutive passes. However, the EPT conditions got better, since on consecutive overflights the EPT is favoured.

Scenario 1c v: Demanding Downlink $(TGO, EXM, BLK + ESTRACK, 10, cc, dl, ro2, rt)$
When demanding a downlink for every overflight, neither the RWT nor the EPT changes, since the only thing required for a downlink on every overflight is more ground station time. This increases, however, the required ground station hours from 780.3 h to 1039.6 h, leading to an average of 5.2 h per sol. Hereby, 514.6 h are effective tracking time, corresponding to an average of 2.6 h per sol, which is nearly half of the time the TGO requires.

Scenario 1c vi: Demanding Uplink $(TGO, EXM, BLK + ESTRACK, 10, cc, dl, ro2, rt, ul)$
When demanding an uplink for every overflight on top of the downlink, the ground station time is further increased from 1039.6 h to 1451.2 h, corresponding to 7.3 h per sol. The effective tracking time is hereby 871.2 h, leading to an average of 4.4 h per sol, which is already close to the requirements of TGO.

Scenario 1c vii: Prime Uplink $(TGO, EXM, BLK + ESTRACK, 10, cc, pu, ro2, rt)$
Demanding a prime uplink opportunity decreases the EPT and RWT even further to 1201.6 h and 1624.4 h, respectively. This is expected given the results from scenario 1a v and applying the same reasoning.

Scenario 1c viii: Loaded
$(TGO, EXM, BLK + ESTRACK, 10, cc, loCL2 + GAIA + LIPF + XMM, ro2, rt)$
When loading the scenario with bookings from other missions and using the desired operational constraints, the RWT that can be provided is 1592.4 h and the EPT 1495.3 h. Comparing this with scenario 1b ii it can be seen that both, RWT and EPT, are increased. This can be explained looking at the BLK passes while making the cost for it higher than for other ground stations, so it is only used if really necessary to increase RWT or EPT. Doing that, it can be seen that 72 BLK passes are used compared to none in the unloaded case, indicating that BLK can lower the impact of bookings on the ESTRACK network. It has to be however taken into account that this mission has to have priority on BLK. Otherwise, bookings on BLK would need to be included as well.

Scenario	RWT/h	$\overline{\text{RWT}}$/h	RRWT	$\overline{\lambda_{\text{FWD}}}$/h	$\overline{\text{EPT}}$/h	<4 h EPT	<6 h EPT	<150 MBit
1c	1767.0	8.8 ± 2.0	68%	0.7 ± 0.6	10.1 ± 1.7	0 %	1 %	0 %
1c i	1762.9	8.8 ± 2.0	68%	2.7 ± 0.6	8.2 ± 1.8	1 %	8 %	0 %
1c ii	1762.9	8.8 ± 2.0	68%	2.7 ± 0.6	8.2 ± 1.8	1 %	8 %	0 %
1c iii	1733.7	8.7 ± 2.3	67%	3.5 ± 1.0	7.8 ± 2.5	4 %	21 %	0 %
1c iv	1730.0	8.7 ± 2.3	67%	4.1 ± 0.9	7.2 ± 2.5	5 %	23 %	0 %
1c iv RWT	1722.9	8.6 ± 2.6	67%	4.2 ± 1.0	7.3 ± 3.1	5 %	26 %	0 %
1c iv EPT	1687.1	8.4 ± 2.4	65%	4.0 ± 0.7	7.4 ± 2.5	2 %	18 %	0 %
1c v	1730.0	8.7 ± 2.3	67%	4.1 ± 0.9	7.2 ± 2.5	5 %	23 %	0 %
1c vi	1730.0	8.7 ± 2.3	67%	4.1 ± 0.9	7.2 ± 2.5	5 %	23 %	0 %
1c vii	1624.4	8.1 ± 3.3	63%	5.8 ± 1.0	6.6 ± 4.1	18 %	66 %	0 %
1c viii	1592.4	8.0 ± 3.6	62%	4.1 ± 1.0	8.3 ± 4.2	3 %	21 %	0 %

Table 6.5: Summary of all variations of Scenario 1c

6.1.4 Scenario 1d

Scenario 1d: Geometrical Constraints $(TGO, EXM, BLK + DSN + ESTRACK, 10)$
To avoid cross-support between different agencies, which is always an extra effort, the cost of acquiring foreign stations was set to 500, while the one for a lost RWT and EPT hour was kept at 10000. With this increased cost factor, NASA DSN stations are only used for European orbiters when approximately six mins of RWT or EPT can be gained. This lead to an amount of 1774.6 h of RWT and 2086.5 h of EPT and the usage of 50 GDS passes. Apart from that station, NASA DSN is never used. Comparing the pattern of the EPT in Fig. 6.16 with the one in Fig. 6.21, it can be seen that the problems when Mars is situated in the northern hemisphere can be completely solved using GDS leading to a pattern only having minor deviations. This pattern originates in the distance between the overflights of the TGO over the rover subtracting the time required for the forward link latency. The reason for that pattern being stable can be seen, when investigating the forward link latency

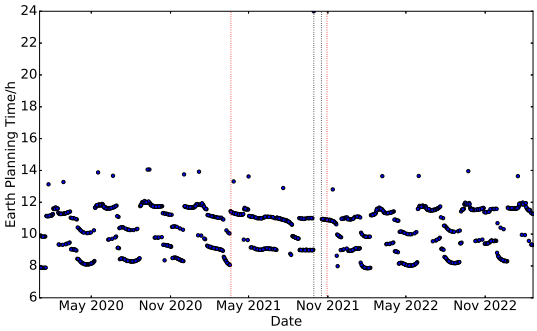

Figure 6.21: The EPT available on each date of scenario 1d

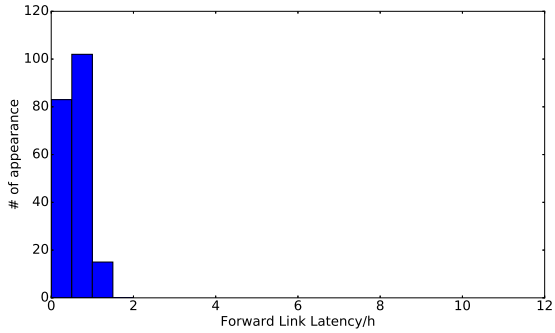

Figure 6.22: The distribution of the forward link latencies within the evaluated period of scenario 1d

in Fig. 6.22. There it can be seen that the average decreased as well as the deviation. The small deviation leads to the pattern being so stable, since all other parameters are nearly constant or, in the case of the overflights, jumping between three different values. These three values can be seen as the three levels between which the EPT jumps.

Scenario 1d i: Desired Operations $(TGO, EXM, BLK + DSN + ESTRACK, 10, cc, ro2, rt)$

When applying the desired operational margins the RWT provided is 1759.8 h while the EPT is 1470.4 h marking an average of 8.8 h and 7.4 h, respectively. However, this requires already 55 GDS passes during the RSM, but it provides the necessity to only plan in less than 6 h in 11% of the cases compared to 23% in scenario 1c iv without GDS. In addition, it as well decreased the cases of less the 4 h EPT from 5% to 0% while even increasing the RWT compared to scenario 1c iv. Finally, the RRWT provided is 68 % which is nearly the theoretical boundary determined for the one orbiter case.

Scenario 1d ii: Loaded

$(TGO, EXM, BLK + DSN + ESTRACK, 10, cc, loCL2 + LIPF + GAIA + XMM, ro2, rt)$

When applying bookings on the ESTRACK network, the key parameters stay the same. This can be explained, since the amount of the NASA DSN station bookings increases such that CAN is booked 11 times and GDS 71 times, while MAD remains still unused. Compared to 55 GDS in the unloaded case, this corresponds to an increase of 11 CAN passes and 16 GDS passes. These increments originate in BLK compensating bookings made on CEB. Therefore MAD is not necessary as an option. However, bookings on NNO and MLG can not always be resolved using another ESTRACK station or BLK. Therefore, CAN or GDS are used to avoid conflicts. This way the key parameters can be kept the same.

Scenario	RWT/h	$\overline{\text{RWT}}$/h	RRWT	$\overline{\lambda_{\text{FWD}}}$/h	$\overline{\text{EPT}}$/h	<4 h EPT	<6 h EPT	<150 MBit
1d	1768.2	8.8 ± 2.1	68%	0.6 ± 0.2	10.5 ± 1.4	0 %	0 %	0 %
1d i	1759.8	8.8 ± 2.0	68%	3.9 ± 0.6	7.4 ± 1.6	0 %	11 %	0 %
1d ii	1759.8	8.8 ± 2.0	68%	3.9 ± 0.6	7.4 ± 1.6	0 %	11 %	0 %

Table 6.6: Summary of all variations of Scenario 1d

6.1.5 Scenario 1e

Scenario 1e: Rover Favoured $(TGO, EXM + RUS, BLK + ESTRACK, 10, cc, ro2, rt)$
When allowing overflights which are longer than 10 min to be shared, leading to two passes with approximately

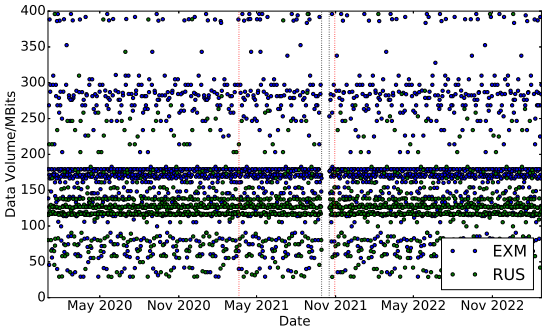

Figure 6.23: The data volume of all overflights allocated in scenario 1e, with the red lines indicating the borders of the RSM and the black ones the one of the solar conunction.

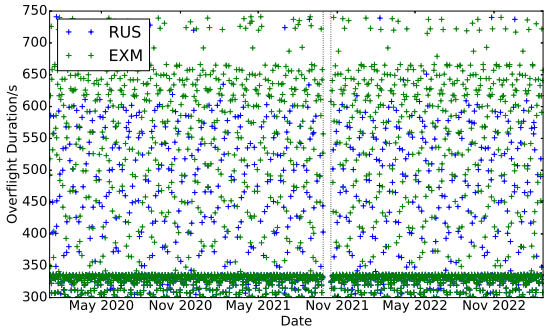

Figure 6.24: The duration of all overflights allocated in scenario 1e. The black lines are indicating the borders of the solar conjunction.

4 min of active transmission time, and keeping the optimisation with a focus on the rover, by setting the cost factors of it to 10000 each while the ones of the surface platform are kept at 100 each, the RWT provided to the rover is 1736.3 h with an EPT of 1419.0 h. This indicates a gain of 6.3 h of RWT compared to the case, where everything is allocated to the rover. The gain of RWT can be explained by the fact that the forward links end earlier due to the sharing, which allows the rover to work ≈ 6 min more per shared overflight.
For the surface platform, the RWT is 1318.0 h and the EPT 1466.0 h. At the same time, the average data volume per sol provided to the rover is 379.4 MBits and the one for the surface platform is 201.3 MBits. The amount of sols on which the requirement on the data return can not be fulfilled is now 2 % for the rover and 38 % for the surface platform, even though it is fulfilled on average. Furthermore, it can be shown that the RWT for the surface platform is lower than for the rover originating from keeping the optimisation focus on the rover.

Scenario 1e i: Equal Cost Factors When setting the cost factors for both assets equally, denoted as scenario 1e i, the RWT that can be provided to the rover is 1377.2 h and the EPT provided to it is 1512.5 h. The RWT for the surface platform is hereby 1507.7 h and the EPT 1484.5 h. This can be assumed to be equal when considering the limited solution space. The huge decrement of the rover's key parameters compared to the minor improvement of the surface platform's can be explained by the overflight pattern avoiding the splitting of some overflights. This leads to a break of the earlier assignment of having a forward link in the morning and a return link in the evening, making the allocation unfavourable for both assets. The data volume, which can be returned on average for the rover on each sol is hereby decreased to 326.0 MBit and the one for the surface platform increased to 262.5 MBit. The inequality in the data volumes originates from the asymmetric radiation pattern of the rover, which is used for the surface platform as well since no alternative is available. This has a considerably smaller gain on the descending flank than on the ascending one, which leads to different data volumes even though an overflight might be split half in time. The difference between splitting a pass by data volume or by duration can be seen when comparing Fig. 6.23 with Fig. 6.24. There it can be seen that even though the passes are split equally in time the data volume for the surface platform passes is considerably smaller. This could be resolved by splitting passes half in data volume and not in time.

Scenario 1e ii: Surface Platform Favoured When putting the optimisation focus on the surface platform by setting its cost factors to 10000 and the one from the rover to 100, denoted as scenario 1e ii, the RWT that can be provided to the rover is 1320.7 h and the EPT provided to it is 1466.0 h. The one for the surface platform are 1734.0 h RWT and 1419.0 h EPT. The average return volume for the rover is 264.4 MBit and for the surface platform 320.0 MBit. These key parameters can be interpreted as a nearly perfect inverse of favouring the rover with the discussed asymmetry in the data volume. The ground station time required in all the cases is 1008.5 h, giving an average of 5.0 h per sol. The effective tracking time is 538.5 h, giving an average of 2.7 h per sol, which less than half of the tracking time the TGO requires.

Scenario 1e iii: Demanding Downlink $(TGO, EXM + RUS, BLK + ESTRACK, 10, cc, dl, ro2, rt)$
Demanding a downlink on every overflight leads to an increment of the required ground station time to 1263.3 h, corresponding to an average of 6.3 h per sol. From that, the effective tracking time is 664.3 h, giving an average of 3.3 h per sol, which is a bit more than half of what TGO requires.The reason of the increment to be lower than in scenario 1c v is that the shared overflights are sometimes a forward link and return link which already have a downlink and uplink. All other key parameters remain the same.

Scenario 1e iv: Demanding Uplink $(TGO, EXM + RUS, BLK + ESTRACK, 10, cc, dl, ro2, rt, ul)$
Demanding an uplink on every overflight increments the required ground station time further to 1670.7 corresponding to an average of 8.4 h per sol. From that the effective tracking time is 1046.7 h, giving an average of 5.2 h per sol, which is quite close to the actual requirements of the TGO. Hereby the same reasoning regarding the smaller increment compared to scenario 1c vi as for the downlink applies. All other key parameters remain the same.

Scenario	RWT/h	$\overline{\text{RWT}}$/h	RRWT	$\overline{\lambda_{\text{FWD}}}$/h	$\overline{\text{EPT}}$/h	<4 h EPT	<6 h EPT	<150 MBit
1e rov.	1736.3	8.7 ± 2.3	67%	4.1 ± 0.9	7.2 ± 2.5	5 %	23 %	2 %
1e plat.	1318.0	6.6 ± 4.5	51%	4.1 ± 0.9	9.6 ± 6.2	3 %	28 %	38 %
1e i rov.	1377.2	6.9 ± 4.1	53%	4.0 ± 0.9	9.1 ± 5.4	4 %	24 %	8 %
1e i plat.	1507.7	7.5 ± 3.9	58%	4.2 ± 1.1	8.6 ± 5.0	5 %	29 %	22%
1e ii rov.	1320.7	6.6 ± 4.5	51%	4.0 ± 0.9	9.6 ± 6.2	3 %	28 %	16 %
1e ii plat.	1734.0	8.7 ± 2.3	67%	4.2 ± 0.9	7.2 ± 2.5	5 %	23 %	5 %
1e iii rov.	1736.3	8.7 ± 2.3	67%	4.1 ± 0.9	7.2 ± 2.5	5 %	23 %	2 %
1e iii plat.	1318.0	6.6 ± 4.5	51%	4.1 ± 0.9	9.6 ± 6.2	3 %	28 %	38 %
1e iv rov.	1736.3	8.7 ± 2.3	67%	4.1 ± 0.9	7.2 ± 2.5	5 %	23 %	2 %
1e iv plat.	1318.0	6.6 ± 4.5	51%	4.1 ± 0.9	9.6 ± 6.2	3 %	28 %	38 %

Table 6.7: Summary of all variations of Scenario 1e

6.2 Multiple Orbiter Scenarios

6.2.1 Scenario 2a

Scenario 2a: Desired Operations $(MRO + TGO, EXM, BLK + ESTRACK, 10, cc, ro2, rt)$
Allowing the usage of the MRO without any cost factor penalty on it, referred to as scenario 2a un., the RWT provided is 1887.7 h and the EPT 1504.0 h. Compared with scenario 1c iv, this marks an increase of 157.7 h of RWT and 85.0 h of EPT using 228 TGO and 170 MRO overflights.
Since MRO is a NASA mission, it shall only be used if it is really required. Therefore, a second investigation was done applying a cross-agency support penalty of 10000. With this penalty MRO is only used when it can

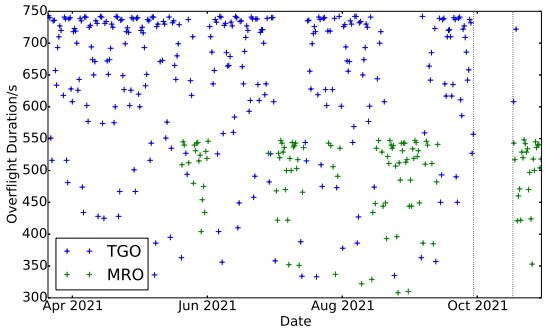

Figure 6.25: The overflights during the RSM marked by the orbiter used for them. Between the black lines is the time of solar conjunction.

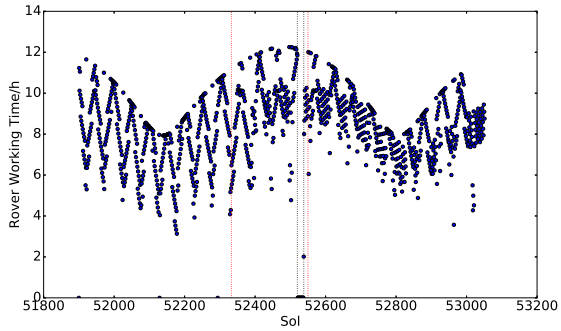

Figure 6.26: The RWT available on each sol in scenario 2a con., with the RSM being between the red lines and the solar conjunction between the black ones.

gain more than an hour EPT or RWT. It is referred to as scenario 2a con. and leads to a RWT of 1863.6 h, an EPT of 1520.6 h and 280 TGO and 118 MRO overflights ones being used. The reason for the improvement of the key parameters compared to scenario 1c iv can be seen in two figures. When investigating the RWT in Fig. 6.26, it can be seen that the pattern with a period of 48 d changes shortly after the start of the RSM, when the overflights of MRO become available. This is due the fact that the MRO passes are always located around 4 a.m. and 4 p.m., making them favourable when the TGO's are located around noon and midnight. In Fig. 6.25 it can be spotted that the MRO passes are exclusively used every 48 d for $\approx$ 15 d, solving the issue of the most unfavourable cases of the TGO overflights. The penalty value of 10000 is hereby somewhat arbitrary. Increasing it leads to less MRO overflights, but as well less RWT and EPT. Furthermore, its impact depends on the weighting of RWT to EPT, originating in higher loss costs making it easier to reach the cost gap for allocating overflights at MRO. This can be shown by setting the EPT cost factor to 12000 to counter the uneven distribution of RWT and EPT. The key parameters for that can be found in Tab. 6.8 referred to as scenario 2a con. e.
The altered weighting leads to a RWT of 1837.4 h and an EPT of 1562.7 h using 264 TGO relay passes and 132 MRO ones. It can already be seen, that MRO is allocated more often since the increased cost factor increases the base costs for the passes.

Scenario 2a i: Allocation for both assets
$(MRO + TGO, EXM + RUS, BLK + ESTRACK, 10, cc, ro2, rt)$
When allocating overflights for both surface platform and rover while keeping the optimisation focus on the rover, as in scenario 1e, the rover can be provided with 1832.5 h RWT and 1545.6 EPT while the surface platform is served with 1357.3 h RWT and 1454.6 h EPT. Comparing this with scenario 1e, the key parameters for the rover can be shown to increase a lot more than the one of the surface platform, which originates from the fact that the optimisation focus is kept on the rover. Due to that, the cost factors for the surface platform are a lot smaller than the cost of using MRO, which avoids an allocation of MRO by the surface platform. Therefore, the increment of the surface platform's parameters originates from the overflights of the TGO, which are not used by the rover. Finally, it can be seen that the cases of sols where the requirement on the data volume can not be fulfilled decreased to none for the rover and 19% for the platform.

Scenario 2a ii: Equal Cost Factors When setting the loss costs for each asset, for EPT and RWT, to 10000, referred to as scenario 2a ii, the RWT provided to rover is 1600.4 h and the EPT 1509.7 h while the

platform is served with 1642.9 h RWT and 1510.2 h EPT. For that 582 TGO and 164 MRO relay passes are used. The increment of the MRO passes originates in the surface platform allocating MRO as well. The uneven distribution of the RWT and EPT between rover and surface platform is smaller than in scenario 1e due to the solution space being increased. However, the impair of the rover's solution is still higher than the improvement of the surface platform's solution.

Scenario	RWT/h	$\overline{\text{RWT}}$/h	RRWT	$\overline{\lambda_{\text{FWD}}}$/h	$\overline{\text{EPT}}$/h	<4 h EPT	<6 h EPT	<150 MBit
2a un.	1887.7	9.4 ± 1.9	73%	3.7 ± 0.9	7.5 ± 2.3	6 %	18 %	0 %
2a con.	1863.6	9.3 ± 1.9	72%	3.7 ± 0.9	7.6 ± 2.3	3 %	17 %	0 %
2a con. e	1837.4	9.2 ± 2.1	71%	3.6 ± 0.7	7.9 ± 2.3	2 %	13 %	0 %
2a i rov.	1832.5	9.2 ± 2.2	71%	3.8 ± 0.9	7.7 ± 2.6	4 %	18 %	0 %
2a i plat.	1357.3	6.8 ± 4.3	53%	4.1 ± 0.8	9.1 ± 5.8	4 %	28 %	19 %
2a ii rov.	1600.4	8.0 ± 3.6	62%	3.8 ± 0.8	8.0 ± 3.8	5 %	27 %	2 %
2a ii plat.	1642.9	8.2 ± 3.6	64%	4.0 ± 1.0	8.1 ± 4.0	5 %	23 %	14 %

Table 6.8: Summary of all variations of Scenario 2a

6.2.2 Scenario 2b

Scenario 2b: Desired Operations

$(MRO + TGO, EXM, BLK + DSN + ESTRACK, 10, cc, ro2, rt)$

Using both, TGO and MRO, with a ground station network consisting of BLK+ESTRACK+NASA DSN, the RWT can be increased to 1885.9 h while the EPT is 1569.1 h. Hereby, 117 out of 401 overflights are allocated on MRO.

Scenario 2b i: Allocation for both assets

$(MRO + TGO, EXM + RUS, BLK + DSN + ESTRACK, 10, cc, ro2, rt)$

When using the multiple lander solver, with a focus on the rover optimisation, to investigate the influence of splitting the overflights, the rover is serviced with 1890.1 h RWT and 1549.0 h EPT while the surface platform gets 1427.3 h RWT and 1477.4 h EPT. In this solution, 612 TGO and 117 MRO overflights are used. Furthermore, the rover can be serviced with enough data volume on every sol, while the platform requires more data volume on 27 % of the sols.

Scenario	RWT/h	$\overline{\text{RWT}}$/h	RRWT	$\overline{\lambda_{\text{FWD}}}$/h	$\overline{\text{EPT}}$/h	<4 h EPT	<6 h EPT	<150 MBit
2b	1885.9	9.4 ± 1.9	73%	3.6 ± 0.5	7.8 ± 1.5	0 %	5 %	0 %
2b i rov.	1890.1	9.5 ± 1.9	73%	3.6 ± 0.5	7.7 ± 1.6	2 %	7 %	0 %
2b i pla.	1427.3	7.1 ± 4.1	55%	3.9 ± 0.6	9.0 ± 5.4	2 %	20 %	27 %

Table 6.9: Summary of all variations of Scenario 2b

6.2.3 Scenario 3a

Scenario 3a: Desired Operations

$(MRO + ODYSSEY + TGO, EXM, BLK + ESTRACK, 10, cc, ro2, rt)$

Adding as well Odyssey as an option to the network, with the same constraints as MRO, increases the RWT further to 2058.6 h while the EPT is decreased to 1478.0 h. The reason for this can be found when looking at Fig. 6.27, revealing that the overflights of Odyssey can be perfectly used to fill the times where the TGO

has its overflights around noon and midnight. This leads to the usage of TGO, Odyssey and MRO overflights, even when constraining Odyssey's usage similar to the one of MRO. In numbers, 208 TGO, 21 MRO and 167 Odyssey overflights are booked.
Since Odyssey is not equipped with an Electra radio, the data rates on it are lower and therefore the orbiter

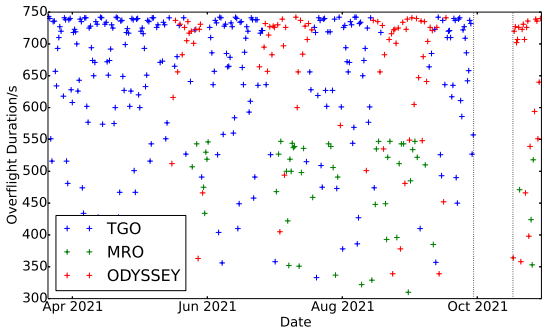

Figure 6.27: The overflights allocated on the different orbiters during the RSM, with the solar conjunction being between the black lines.

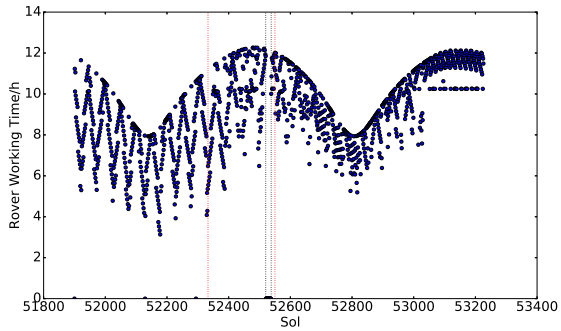

Figure 6.28: The RWT available on each sol in scenario 3a con., with the RSM being indicated by the red lines and the solar conjunction by the black ones.

should not be used if MRO can provide similar support. This is guaranteed by setting the cost factor to 20000 in total, leading to a RWT of 2020.3 h and an EPT of 1468.7 h with the key parameters in the table under 3a con.. The investigation of the data volume was hereby removed, since no correct model of Odyssey's relay radio and its data rates was available. For this scenario, 247 TGO, 51 MRO and 99 Odyssey overflights are used.

Scenario 3a i: Allocation for both assets

$(MRO + ODYSSEY + TGO, EXM + RUS, BLK + ESTRACK, 10, cc, ro2, rt)$
Solving the scenario for both landed assets leads to a similar picture for the rover, with 2014.9 h RWT and 1474.4 h EPT, and to 1395.5 h RWT and 1478.3 h EPT for the surface platform. With 580 TGO relay passes, 45 MRO ones and 104 Odyssey ones.

Scenario	RWT/h	$\overline{\text{RWT}}$/h	RRWT	$\overline{\lambda_{\text{FWD}}}$/h	$\overline{\text{EPT}}$/h	<4 h EPT	<6 h EPT
3a	2058.6	10.3 ± 1.8	70%	3.8 ± 0.8	7.4 ± 2.1	2 %	20 %
3a con.	2020.3	10.1 ± 1.9	78%	3.8 ± 0.8	7.4 ± 2.3	4 %	24 %
3a i rov.	2014.9	10.1 ± 1.9	78%	3.8 ± 0.9	7.4 ± 2.4	4 %	24 %
3a i pla.	1395.5	7.0 ± 4.2	54%	4.0 ± 0.8	9.1 ± 5.4	4 %	20 %

Table 6.10: Summary of all variations of Scenario 3a

6.2.4 Scenario 3b

Scenario 3b: Desired Operations

$(MRO + ODYSSEY + TGO, EXM, BLK + DSN + ESTRACK, 10, cc, ro2, rt)$
Allowing the usage of NASA DSN stations by all orbiters leads to an increase of the RWT to 2054.1 h and of the EPT to 1472.8 h. The reason for the increment is hereby similar to the one of scenario 1d and 2b.

Scenario 3b i: Allocation for both assets
$(MRO + ODYSSEY + TGO, EXM + RUS, BLK + DSN + ESTRACK, 10, cc, ro2, rt)$
The result, when sharing overflights, is similar for the rover with 2057.5 h RWT and 1462.5 h EPT while the surface platform is serviced with 1421.3 h RWT and 1491.6 h EPT.

Scenario	RWT/h	$\overline{\text{RWT}}$/h	RRWT	$\overline{\lambda_{\text{FWD}}}$/h	$\overline{\text{EPT}}$/h	<4 h EPT	<6 h EPT
3b	2054.1	10.3 ± 1.7	79%	3.6 ± 0.5	7.4 ± 1.8	1 %	19 %
3b i rov.	2057.5	10.3 ± 1.7	80%	3.6 ± 0.5	7.3 ± 1.8	1 %	21 %
3b i pla.	1421.3	7.1 ± 4.0	55%	3.9 ± 0.6	7.1 ± 4.0	2 %	17 %

Table 6.11: Summary of all variations of Scenario 3b

6.2.5 Scenario 3c

All landers and orbiters $(MRO + ODYSSEY + TGO, EXM + MRB + MSL + NSY + RUS, BLK + DSN + ESTRACK, 10, cc, ro2, rt)$
To provide a sufficient solution for all assets at Mars using all orbiters around it, while respecting the minimisation of agency cross-support, the following parameters were set in advance:

- Establishing an overflight using an orbiter from another agency is penalised with an extra cost factor of 10000.
- Establishing a pass with a ground station of another agency is penalised with and extra cost of 500.
- Rovers are provided with a cost factor of 10000 for the loss of an hour of RWT or EPT, respectively.
- Surface platforms are provided with a cost factor of 100 for the loss of an hour of RWT or EPT, respectively since they are not relying on daily command updates.
- The operational constraints are kept as the desired ones determined in scenario 1a and confirmed by scenario 1c.
- Working and planning constraints are assumed to be similar to the one of the ExoMars RSP rover.

With these constraints, the key parameters in Tab. 6.12 can be achieved. When investigating the relay passes booked on the different orbiters in Fig. 6.29, a pattern can be spotted from the point on where all orbiters are available. There it can be seen, that TGO is allocated more often every ≈ 48 d. During these times its passes are well aligned with dawn and dusk of the ExoMars RSP assets, leading to it being used for every overflight by those two assets. In between TGO is only used by RUS, since it has not so demanding constraints regarding RWT and EPT. This leads as well to RUS not having optimal RWT when investigating Fig. 6.30. However, it can be seen that the assets of the ExoMars RSP mission have a huge advantage during the RSM regarding the RWT, since Martian summer in the northern hemisphere is spreading the time with daylight and therefore the possible RWT. The seasonal influence can be as well spotted when comparing the MSL RWT with the one of EXM. Even though MSL is provided with Odyssey overflights, which are nearly perfectly aligned with its dawn and dusk, the RWT available for it during the RSM is 330.1 h less than the one for EXM. Furthermore, it can be seen that all rovers can be serviced on a lot of sols with the maximum possible RWT while the surface platforms are a bit more constrained since they are only serviced by the relay orbiters of their own agencies.

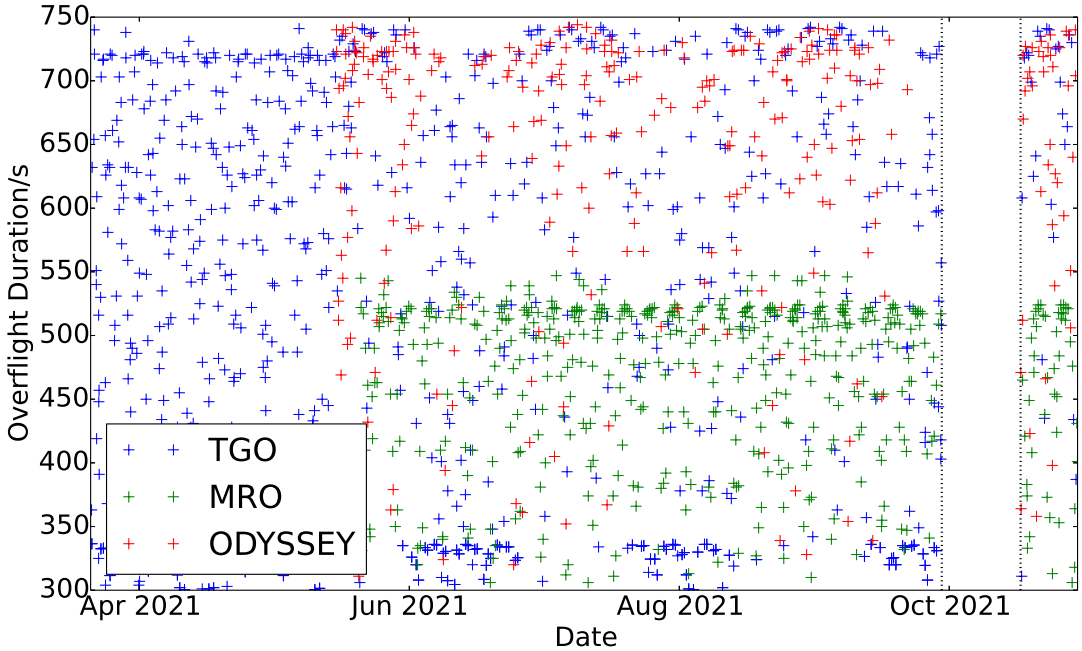

Figure 6.29: The relay passes allocated on the different orbiters and their durations, with the time of the solar conjunction being between the black lines.

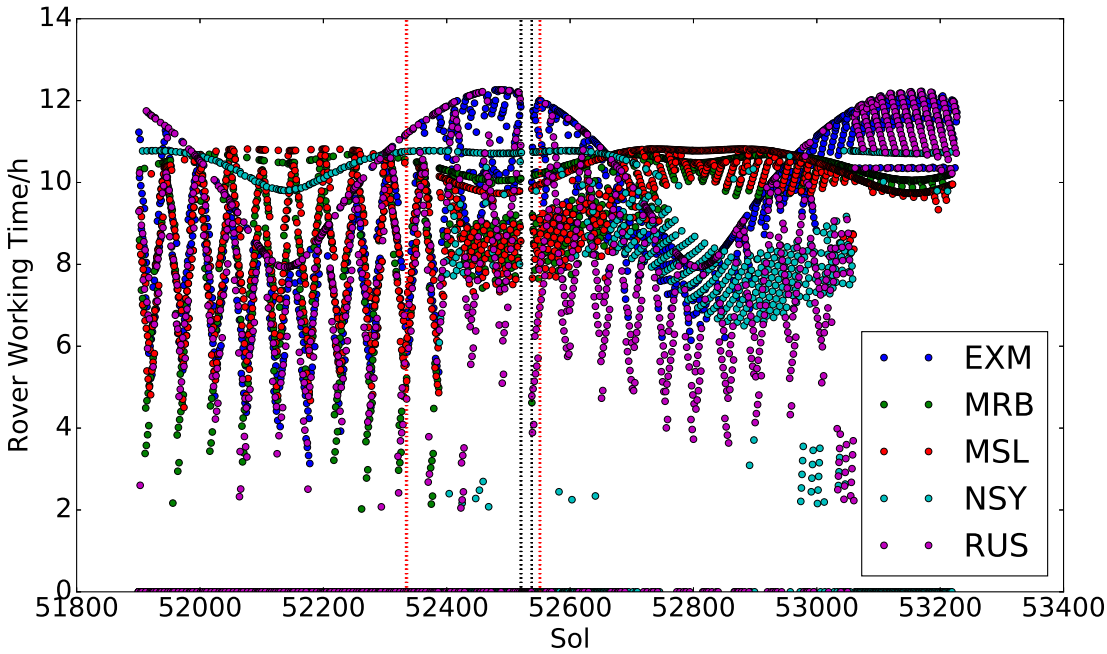

Figure 6.30: The RWT available for the different assets on every sol. The red lines are indicating the borders of the RSM, while the black ones are showing the borders of the solar conjunction.

Scenario	RWT/h	$\overline{\text{RWT}}$/h	RRWT	$\overline{\lambda_{\text{FWD}}}$/h	$\overline{\text{EPT}}$/h	<4 h EPT	<6 h EPT
EXM	2057.5	10.3 ± 1.7	80%	3.6 ± 0.5	7.3 ± 1.8	1 %	21 %
RUS	1421.3	7.1 ± 4.0	55%	3.9 ± 0.6	8.9 ± 5.2	2 %	17 %
MSL	1727.4	8.6 ± 1.3	81%	3.5 ± 0.4	7.8 ± 1.0	0 %	9 %
MRB	1737.2	8.7 ± 1.8	79%	3.5 ± 0.4	7.8 ± 2.0	0 %	13 %
NSY	701.2	4.2 ± 4.9	30%	3.8 ± 0.9	12.2 ± 7.3	5 %	12 %

Table 6.12: Summary of Scenario 3c

6.3 Comparison to 2018 launch

Solving scenario 1e for the 2018 launch date 1810.0 h RWT and 1566.9 h EPT can be provided for the rover and 1449.6 h RWT and 1574.0 h EPT for the surface platform. A summary of the key parameters can be found in the first column of Tab. 6.13 for the rover and in the second column for the surface platform.
Solving scenario 1e for the 2020 launch date provides 1736.3 h RWT and 1419.0 h EPT for the rover and 1318.0 h RWT and 1466.0 h EPT for the surface platform. A summary of the key parameters can be found in the third column of Tab. 6.13 for the rover and in the fourth column for the surface platform.
Comparing the key parameters, the scenarios in the different years seem to be nearly the same. The only difference are the absolute values for RWT and EPT and the average RWT for the rover. The average RWT being higher during the 2020 RSM can be explained, since the mission arrives later during Martian spring. Therefore, the time of sunlight on each sol is longer. The reason for the absolute values being higher during the 2018 RSM is that the solar conjunction is only partially in the RSM, while the 2020 RSM contains it completely. This leads to ≈ 12 sols more on which working is possible during the 2018 RSM. This can be as well seen when comparing the RRWT. Since the sunlight during conjunction can not be used, the percentage during the 2020 RSM is smaller.

Parameter	2018 rover	2018 surface platform	2020 rover	2020 surface platform
RWT/h	1810.0	1449.6	1736.3	1318.0
$\overline{\text{RWT}}$/h	8.4 ± 2.4	6.7 ± 4.1	8.7 ± 2.3	6.6 ± 4.5
RRWT	70%	56%	67%	51%
$\overline{\text{EPT}}$/h	7.5 ± 3.2	9.2 ± 5.6	7.2 ± 2.5	9.6 ± 6.2
$\overline{\lambda_{\text{FWD}}}$/h	3.9 ± 1.0	4.0 ± 1.0	4.1 ± 0.9	4.1 ± 0.9
$\overline{\lambda_{\text{RET}}}$/h	1.5 ± 0.7	1.5 ± 0.8	1.5 ± 0.8	1.5 ± 0.9
< 4 h EPT	5 %	5 %	5 %	3 %
< 6 h EPT	30 %	27 %	23 %	28 %
$< 150 \frac{\text{MBit}}{\text{sol}}$	4 %	31 %	2 %	38 %
data volume/ $\frac{\text{MBit}}{\text{sol}}$	371 ± 129	216 ± 90	379 ± 116	201 ± 83

Table 6.13: A comparison of the key parameter between the 2018 launch date and the 2020 on for rover and surface platform

7 Conclusion & Outlook

From the results in Sec. 6 several operations- and overflight-planning-strategies can be derived. For better traceability, the conclusions are sorted similarly to the results, from which they are drawn.

7.1 Overflight Pattern

From the results for the overflight elevation, it can be derived that the driving constraints for relay operations are the overflight patterns of the satellites over the landers, since they are providing the constraints on the RWT depending on their distance to dawn and dusk. Therefore, the best way to maximise the RWT and EPT is to have a satellite with an orbit dedicated to provide an overflight close to Martian dawn and one close to dusk, as performed by Odyssey for MRB. This way the RWT can be maximised. Since the orbit of the TGO can not be altered, due to its scientific mission, the number of orbiters used should be increased to increase the number of overflights. Furthermore, the requirement of a minimum elevation of 10 degrees to communicate with the rover shall be tested extensively during operations, since the possibility of shrinking the minimum elevation required would provide a high number of extra overflights. Even though the data volume of those would be quite small, the extra forward link opportunity would provide an additional degree of freedom. Finally, the usage of MRO and Odyssey as relay orbiters should be considered, since there overflights are timed close to dawn and dusk at Oxia Planum.

7.2 One Orbiter Scenarios

7.2.1 Scenario 1a

$(TGO, EXM, BLK + MLG)$
From this scenario and all its sub-scenarios, it can be seen that in a lot of cases even the MLG+BLK network can provide sufficient support to the mission by providing a RRWT of up to 60% and an EPT longer than 4 h in a lot of cases. Furthermore, it can be seen that all margins have a stronger influence on the EPT. This originates from the fact that the RWT is mostly fixed by the overflights of the satellite over the rover and can only be altered within the restrictions of the consecutive overflights. The only impact on the RWT originates from that fact, or from skipping a complete sol.
Furthermore, it should be noted that allocating nearly all passes for the rover leads the requirement of returning 150 Mbits of data to be fulfilled on every sol.
All this leads to the conclusion that this network can be used as a basis for the mission, but it has to be supported by other antennae to reach sufficient key parameters for this mission since the gap between the MLG and BLK visibility can lead to extensive forward link and return link latencies. Finally, it can be concluded that the key parameters are extremely sensitive to the timing of the ground station passes. Therefore, the overflights shall be booked with priority.
From the operational approach it is recommended to require the following margins:

A submission deadline to allow necessary preparation of commands to take place since it is demanded by ESOC

The confirmation of commands to immediately know if the commanding succeeded, to allow planning to take place even during Martian daylight when the sol is lost due to commanding failure.

The Retransmission of Files to counter eventual failures on the uplink chain, since this margin costs on average half an hour EPT, but could save a whole sol of RWT.

The following ones were neglected:

Ping since it is somewhat included in the retransmission of files.

Prime Uplink is reckoned to be an acceptable risk of not having it, because of its little extra use, essentially only in case of full pass failure which is guaranteed to be below 5% of the passes and is typically much less.

Operational approaches respecting these margins are referred to as desired operations.

7.2.2 Scenario 1b

$(TGO, EXM, ESTRACK)$
When investigating the numbers for this scenario , it can be shown that it provides sufficient support in most cases although there are some issues when Mars is situated in the northern hemisphere, due to the shortened visibilities for ground stations in the southern hemisphere. This is the most critical phase of operations since this time leads to the highest latencies in the network. That phase could be alleviated using a ground station located at a longitude between MLG and NNO, e.g. GDS, which is investigated in scenario 1d.
Furthermore, it can be shown that loading the scenario with bookings from other missions leads to a considerable decrement of RWT. Therefore, either other stations have to be added, which provide visibility during some of the bookings for which e.g. BLK is a considerable option, or the mission has to have priority when it comes to ground station booking. This is owing to the fact that the actual booking time and not only the duration impacts the key parameters of this mission. As a result from this scenario the further investigated scenarios contain as a minimum all ESTRACK stations and BLK as ground station network. This is as well the minimal advised option for operations.

7.2.3 Scenario 1c

$(TGO, EXM, BLK + ESTRACK)$
Investigating the operational margins for this ground station network reveals that the reasoning for those does not change with the ground station visibilities available. Therefore, the desired operations approach can be confirmed using this scenario as a countercheck to 1a. In addition to that, it can be seen that this scenario provides even sufficient support when the ESTRACK network is loaded. However, it shall be noted the same reasoning as for scenario 1b applies when Mars is in the northern hemisphere. Therefore, the impact of adding NASA DSN is investigated in scenario 1d. Moreover, the possibility of providing a downlink or uplink on passes which are dedicated as forward links or return links, respectively, should be taken if they can be provided on the same ground station as the required data link. This way, the cost is just the extension of the ground station time and not an extra hour for preparing a station. Hereby, downlinks should be preferred, since they allow to receive hints on possible contingencies earlier and allow planning to resolve them.
Furthermore, the uneven distribution of overflights between rover and surface platform of 79%:21% has to be countered, to allow both to return approximately the same amount of data. Doing this, the requirement of the return volume should be as well tried to be fulfilled. Therefore, an investigation of a possible overflight sharing is done in scenario 1e and multiple orbiters are introduced in scenario 2 and 3 trying to increase the return volume as well as the RWT and EPT.
Finally, it is shown that the loss cost for EPT and RWT should be kept equal to avoid an undesired behaviour of the switching of the forward link to sunlight. This could be resolved when equipping the solver with a global optimisation approach.

7.2.4 Scenario 1d

$(TGO, EXM, BLK + DSN + ESTRACK)$
Adding the NASA DSN stations as a costly option to the scenario leads to GDS being used in the cases when Mars is situated in the northern hemisphere to cope with the shortened visibilities of MLG and NNO. Furthermore, when loading scenarios with bookings on the ESTRACK stations, CAN is used as well to cope with the ones made on NNO. Therefore, it should be considered to add GDS to the baseline ground station network to resolve performance issues around May 2021. Moreover, it should be considered adding CAN to the baseline if the RSP mission does not get priority on the ESTRACK stations. Finally, MAD should be added if the RSP mission has neither priority on the ESTRACK, nor on BLK.

7.2.5 Scenario 1e

$(TGO, EXM + RUS, BLK + ESTRACK)$
Sharing the overflights between the assets of the RSP mission allows it to reach the return volume requirement for both landed assets on average. However, on multiple sols it is not reached which makes it necessary to think about prioritisation of the returned data to cope with those cases, especially since all overflights which can be provided by the TGO are allocated by the two assets. Another possibility is to add additional orbiters which is investigated in the scenarios 2 and 3. It is however not possible to use remaining overflights, since no idle ones remain.
Furthermore, implementing the overflight sharing and allocations for the surface platform into the optimisation process alters the performance of the solution of the rover only slightly when keeping the optimisation for the rover a priority for the solver. If this is not done, the key parameters suffer considerably, due to skipping complete sols. Since the surface platform is not as dependent on having dedicated commands for each sol, because it does not move as the rover, it shall be considered to optimise all overflights for the rover, but share every overflight longer than 10 min with the surface platform. This way basic support can be provided to both landed assets while the rover can be steered using dedicated commands for each sol. The time allocated to the rover during shared overflights should be reviewed to reach an equal distribution of the data volume as well as the minimum time required for an overflight to be shared. This should be done during operations as soon as more reliable numbers are available for the data volume.
Regarding acquiring extra downlinks and uplinks, the shared overflights should be served first with those since this would provide flexibility to both assets. Hereby the same applies as for scenario 1c. They should only be allocated if they fit on the same ground station pass to avoid booking extra configuration times. Furthermore, downlinks should be preferred in this case as well, for the same reason as in scenario 1c.

7.2.6 Summary

For the operations, with just having the TGO as a relay orbiter the rules for assigning the relay passes are quite straight forward:

- Overflights longer than 10 min are shared
- Overflight closest to dawn is assumed to be the forward link for the rover
- Overflight closest to dusk is assumed to be the return link for the rover
- If one of the rules above forces the forward link to be shifted to daylight or the return link to be shifted to night the assignment of forward link and return link is strictly propagated for several sols with a period of ≈ 12 h to avoid multiple switching.
- The remaining overflights are allocated to the surface platform in alternating order of being forward link and return link

For forward links, the operational margins of receiving a confirmation of the commands sent and a retransmission possibility should be respected, as well as the deadline set by ESOC for the delivery of the commands. Even respecting these margins, it is recommended to upload commands for two sols on every forward link. This could counter the problem of loosing a complete forward link. If it is not lost the commands for the current sol can be simply overwritten with the new ones.
The ground station allocation for these overflights, respecting as well the operational margins, are made the following way:

- An uplink ends one OWLT after the start of a forward link to capture the arrival of the commands on the orbiter.
- The start of the uplink is chosen such that all operational margins and some extra margin for the transmission fit into the resulting pass duration.
- If an occultation avoids the communication within this uplink window, the pass is shifted to the past until the communication can take place.
- A downlink starts one OWLT after the end of a return link since this is the first point were all data can be returned.
- The end of the downlink is chosen such that the required transmission fits into the resulting pass duration.
- If an occultation avoids the communication within this downlink window, the pass is shifted to the future until the communication can take place.

Since the performance of the relay link depends hardly on the timing of the ground station passes, a nearly gapless ground station coverage should be provided on which relay orbiters have booking priority. Therefore, the minimum recommended ground station network is ESTRACK+BLK with GDS being a valuable option to add. The different possibilities of ground stations bookings with unlimited visibilities following the rules mentioned above can be seen in Fig. 7.1.

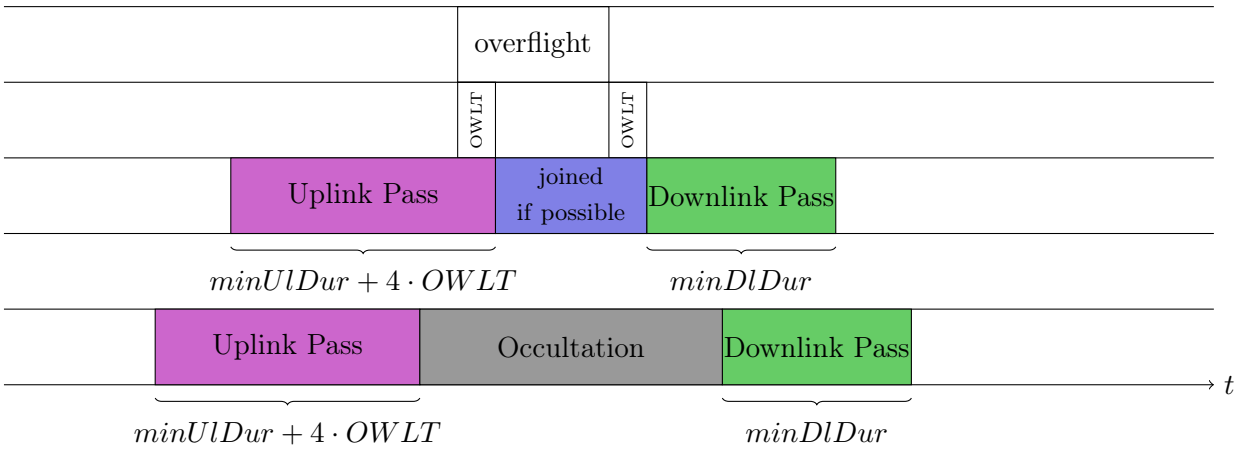

Figure 7.1: The different ways of allocating ground station passes for an overflight sketched on a timeline, with downlinks indicated in green, uplinks is purple and occultations in grey. The first line shows the overflight and the second indicates the OWLTs for the signals to travel. The third line shows the desired ground station allocation and the fifth one, the one, when an occultation occurs during the overflight.

In every scenario, the ground station passes booked need to be extended to provide the 6 hours of tracking the TGO requires. This satisfies the choice of keeping the cost for ground station allocation a lot lower than the ones for losing RWT or EPT.
Finally, it can be seen that up to 68% of the theoretically achievable RRWT is provided to the rover. Comparing

this with 69%, which is an approximate upper boundary, it can be concluded that the locally optimal solution of the solver is close to the globally optimal one.

7.3 Multiple Orbiter Scenarios

7.3.1 Scenario 2a

$(MRO + TGO, BLK + ESTRACK)$
When adding MRO as another orbiter, it can be seen that the solution gets more flexible, since the solution space is increased. Even when restricting its usage to cases were more than one hour of RWT or EPT can be gained leads to using it in roughly a quarter of the cases. Therefore, it shall be considered to use MRO, especially in the cases were the TGO overflights are unfavourable since MRO's sun-synchronous orbit keeps the overflight pattern stable with quite desirable timings. Finally, it can be seen that the data return requirement is nearly fulfilled every sol for the rover. On the other hand, it should be considered to book extra passes for the surface platform to fulfil its requirement as well.
However, it is not recommended to optimise the overflights, with the cost factors of the surface platform being equal to the rover, since this impairs the rover's key parameters strongly. It would be better to add an additional stage to the solver, which checks the data volume on every sol and adds relay passes or changes the ratio in which passes are shared, if necessary for an asset to fulfil its return volume requirement. This should, however, be decided upon during operations when accurate information on the return volume is available.

7.3.2 Scenario 2b

$(MRO + TGO, BLK + DSN + ESTRACK)$
The reasoning is similar to the one of scenario 1d. Adding NASA DSN to the network decreases the cases with adverse amounts of EPT drastically. Furthermore, it can be assumed that relay passes booked on a NASA orbiter will be most probably handled using NASA DSN stations. Therefore, it should be considered to add those stations first and afterwards NASA orbiters. For the data volume the same as for scenario 2a applies. An extra check, if it is fulfilled, should be added as new step to the solver and extra relay passes should be added, if it is not fulfilled.

7.3.3 Scenario 3a

$(MRO + ODYSSEY + TGO, BLK + ESTRACK)$
Adding as well Odyssey as an orbiter the solution gets even more flexible since the solution space is further increased. However, it has to be taken into account that Odyssey has no Electra radio. Therefore, it should be only chosen if it is really demanding since a return link using Odyssey has to be supported by another orbiter to have a high enough data volume. Therefore, an even higher cost factor for it might be applied when the data volume is found too be to critical.

7.3.4 Scenario 3b

$(MRO + ODYSSEY + TGO, BLK + DSN + ESTRACK)$
The reasoning on this scenario is the same as for scenario 2b. The amount of passes with undesired EPT is decreased. Furthermore, it can be assumed that NASA orbiters will most likely use their ground stations and therefore adding NASA DSN before adding NASA orbiters seems reasonable.

7.3.5 Scenario 3c

(Overall Solution)
With this scenario, it is shown that the solver is capable of solving the whole problem of the Mars Relay Network for all landed assets and all orbiters in circular orbits. Furthermore, it can distinguish between landers and orbiters of different agencies, only establishing agency cross-support if it is pressing. Therefore, it can be concluded that the solver can provide a basis for an automatic solution for the Mars Relay Network allocations, which, if extended with the capability of accessing the relay links of orbiters in elliptical orbits, data rates for all orbiters and global optimisation capabilities, could be even optimal. Finally, it can be seen that the RRWT for all rovers is essentially the same even though MRB has a dedicated satellite with a sun-synchronous orbit just optimised for relay requirements. Therefore, the solver can be assumed to provide nearly optimally solutions for all rovers only wasting 11.5% of the theoretically possible RWT, which is quite small given the limited solution space and on average 3.5 h of latency on every forward link which might cut into the RWT.

7.3.6 Summary

It can be seen, that the performance of a solution increases with every extra orbiter considerably. Therefore, it should be considered using as many orbiters as possible and as well assessing the relay capabilities of the orbiters in elliptical orbits. However, it is recommended to allow the usage of NASA DSN before adding extra orbiters, since the full advantage of the new orbiters is only available if a gapless ground station coverage is provided and the NASA orbiters would most probably use those stations anyway. The allocation of the the ground station passes remains hereby the exact same as for the one orbiter case.
Furthermore, it should be considered to restrict the usage of foreign orbiters since they always come at a price. The actual choice of the cost factor should be performed after the terms of cooperation with other orbiters is agreed on, but a good rule is to allow the usage only if one hour of EPT or RWT can be gained. In addition, the usage of a sun-synchronous orbiter allows to omit the switching of the pattern, since it provides its overflights alway around dawn and dusk. Therefore, the local optimal solution can be assumed to be close to the global optimal one, which is well confirmed by the RRWT being up to 80 %.

7.4 Conclusion

Reviewing the tasks in the thesis assignment, a solver is provided to resolve the problems stated in Chapter 3. This solver is not only minimising the latencies and the station booking times in the network, but provides as well the possibility to investigate different operational approaches. For these, the results show that it is most reasonable to choose confirmation of commands, the possibility of retransmitting corrupted files and the delivery deadline of two hours demanded by ESOC as the operational margins for transmitting the relay information up to the spacecraft. This way, the files are available at the orbiter operations centre early enough to be carefully preprocessed and prepared to send them to the spacecraft. Furthermore, it is assured that failures during the transmission are acknowledged, since the confirmation of commands is always received at the ground station. In addition, it is possible to resolve failed file transmission by resending corrupted chunks of the file, if necessary. However, it is recommended to uplink commands for two sols on every forward link to provide a backup for failed forward links. The backup commands should be the overwritten if new, dedicated commands arrive for a sol on the next forward link. If not, the backup plan can be used. This way a certain safety against complete pass failures is provided.
Furthermore, the ground station bookings were investigated and it could be shown that it should be considered to provide priority to the bookings of this mission since the performance of the relay link depends heavily on the timing of the passes. In addition it was shown, that it is beneficial to book extra downlink and uplink possibilities, even on forward links and return links, respectively, to provide additional information to the lander operations centre. Hereby, the allocation of the ground station passes should follow the rules stated in

the summary of the one orbiter scenarios.
For the timely allocation of the overflights for the one orbiter scenarios, it can be concluded, that the overflight closest to dawn should be allocated for the rover as forward link and the one closest to dusk as the return link for it. The point where the forward link changes from Martian night to Martian day should be selected carefully and the switching should be only performed once every 48 sols to provide a solution close to global optimum. Furthermore, all passes which are longer than 10 min should be split, such that the data return volume on the sol is equal between the surface platform and the rover. The allocation for the surface platform is then made such, that the passes are allocated alternating as forward link and return link.
This solution is extended to evaluate the possibility of using multiple orbiters. Regarding this, it can be concluded that as many orbiters as possible should be used, since it is shown that every extra orbiter increases the solution space for the solver drastically. Moreover, it can be seen that sun-synchronous orbiters can provide a drastic increase in RWT, especially when their overflights are aligned close to dawn and dusk. To not overstrain other agencies, it is however recommended only to use foreign orbiters if more than one hour of EPT or RWT can be gained and for surface platforms only to provide enough data return volume.
In addition, the solver was equipped with the capability to solve the problem as well for multiple landed assets and is shown to provide good key parameters for all of them.
Finally, it can be seen that the RRWT provided is always close to the theoretically best value. From that it can be concluded that the solver, even though searching for local minima, provides a result which is close to the global optimum.

7.5 Outlook

Among the things, which could not be concluded by this thesis is the assessment of the relay capabilities of orbiters in elliptical orbits. To investigate these, the related orbit files are required which could not be provided for this thesis. However, the structure of the solver provides an easy plugin possibility for these. Furthermore, this would offer the possibility of having a lot more accurate elevation and azimuth profiles, making a better analysis of the data volumes available.
Moreover, the solver is working in a straight way by finding local minima. A further enhancement would be, to provide a solver which can as well find global minima using e.g. variations of the initially found solution. In addition, colliding ground station allocations, due to serving multiple landed assets, can be solved more favourably as well. Both processes are however making the solver more complex and resource demanding. Therefore, they should only be considered when covering shorter periods than the ones evaluated in this thesis.

8 Bibliography

[1] Risto Pellinen, Paul Raudsepp, Michel Blanc, and William V. Boynton et al. *Towards Mars! Extra*. Raud Publishing, 2 edition, October 2006.

[2] Wikipedia. Mars. Internet, May 2016. https://en.wikipedia.org/wiki/Mars.

[3] B.G. Lee and J.D. Porter. The design and implementation of the viking mission. In *Annual Meeting and Technical Display Incorporating the Forum on the Future of Air Transportation; 13th; Jan. 10-13, 1977; Washington, DC*, pages 1–8, January 1977.

[4] C. D. Edwards, A. Barbieri, E. Brower, P. Estabrook, R. Gibbs, R Horttor, J. Ludwinski, R. Mase, C. Mc Carthy, R. Schmidt, P. Theisinger, T. Thorpe, and B. Waggoner. A martian telecommunications network: Uhf relay support of the mars exploration rovers by the mars global surveyor, mars odyssey, and mars express orbiters. In *55th International Astronautical Congress; 4-8 October 2004; Vancouver, BC; Canada*, pages 1–6, October 2004.

[5] N.Salerno, L. Simone, D. Gelfusa, V.Nanni, and MG. Campagna. X-deep space transponder (xdst) design report. Technical report, Thales Alenia Space, February 2015.

[6] LSSWG, J.L. Vago, and D.Rodionov. Exomars - 3rd landing site selection workshop - final report. Technical report, ESA, December 2015.

[7] I. Musso D. Bussi, P. Pognant. Rover to rocc communication scenario analysis assessment with the new tgo 373:30 frozen orbit. Technical Report 3, ALTEC, November 2014.

[8] P. Baglioni. Exomars rover requirements document. Technical report, ESA, July 2013. Issue 5, Rev.0.

[9] ESA. Exomars mission (2020). internet, May 2016. http://exploration.esa.int/mars/48088-mission-overview/.

[10] ESA. Exomars rover. internet, October 2015. http://exploration.esa.int/mars/45084-exomars-rover/.

[11] KKN. Adron-rm neutron detector for exomars project. internet, June 2016. https://np.cosmos.ru/ADRON-RM-en.html.

[12] ESA. The exomars rover instrument suite. internet, May 2016. http://exploration.esa.int/mars/45103-rover-instruments/.

[13] ESA. Exommars 2020 surface platform. internet, October 2015. http://exploration.esa.int/mars/45084-exomars-rover/.

[14] NASA Goddard Institute for Space Studies Dr. Michael Allison. Mars24 sunclock — time on mars, December 2015.

[15] David Evans. Ladybird guide to spacecraft operations (book one). ESOC Lecture, 2016.

[16] Comptes rendus de la 17e cgpm (1983), 1984.

[17] ESA. Network map. internet, December 2015. http://www.esa.int/spaceinimages/Images/2013/01/Network_map.

[18] ESA. New norcia - dsa 1. internet, April 2016. http://www.esa.int/Our_Activities/Operations/Estrack/New_Norcia_-_DSA_1.

[19] ESA. Cebreros - dsa 2. internet, April 2016. http://www.esa.int/Our_Activities/Operations/Estrack/Cebreros_-_DSA_2.

[20] ESA. Malargüe - dsa 3. internet, April 2016. http://www.esa.int/Our_Activities/Operations/Estrack/Malarguee_-_DSA_3.

[21] JPL. Dsn complexes. internet, April 2016. http://deepspace.jpl.nasa.gov/about/DSNComplexes/#.

[22] Sven Grahn. The soviet/russian deep space network. internet, 1996. http://www.svengrahn.pp.se/radioind/Russdeep/Russdeep.htm.

[23] Wikipedia. List of radio telescopes. internet, 2016. https://en.wikipedia.org/wiki/List_of_radio_telescopes.

[24] A. Dementiev A. Antipenko A. Pushkarev V. Yazykov I. Puchinin B. Sapozhnikov V. Titenko I. Molotov Y. Gorshenkov N. Dugin G. Tuccari A. Stepanov V. Saurin M. Nechaeva. Bear lakes radio astronomy station. internet, October 2006. http://lfvn.astronomer.ru/radio/bearlakes/blras/.

[25] M. Schagerl W. Steiner. *Raumflugmechanik: Dynamik und Steuerung von Raumfahrzeugen*. Springer, 2004.

[26] ESA. Trace gas orbiter at mars. internet, November 2015. http://www.esa.int/spaceinimages/Images/2015/11/Trace_Gas_Orbiter_at_Mars.

[27] ESA. Exomars on its way to solve the red planet's mysteries. internet, March 2016. http://www.esa.int/Our_Activities/Space_Science/ExoMars/ExoMars_on_its_way_to_solve_the_Red_Planet_s_mysteries.

[28] ESA. Trace gas orbiter instruments. internet, March 2016. http://www.esa.int/Our_Activities/Space_Science/ExoMars/Trace_Gas_Orbiter_instruments.

[29] N. Chamberlain, R. Gladden, and K. Bruvold. Maven relay operations concept. In *Aerospace Conference, 2012 IEEE*, pages 1–11, March 2012.

[30] National Aeronautics and Space Administration-Goddard Space Flight Center. Maven mission overview. Internet, July 2015. http://www.nasa.gov/mission_pages/maven/overview/index.html.

[31] C. D. Edwards, P. R. Barela, R. E. Gladden, C. H. Lee, and R. De Paula. Replenishing the mars relay network. In *2014 IEEE Aerospace Conference*, pages 1–13, March 2014.

[32] NASA/JPL. Nasa - mars reconnaissance orbiter over the martian landscape. internet, June 2005. http://www.nasa.gov/mission_pages/MRO/multimedia/MRO_image.html#.V2KYClfqo_U.

[33] NASA/JPL. Mro overview. internet, July 2015. http://mars.nasa.gov/mro/mission/overview/.

[34] ESA. A little help from friends. internet, June 2016. http://www.esa.int/Our_Activities/Operations/A_little_help_from_friends.

[35] ESA. Fact sheet. internet, January 2015. http://sci.esa.int/mars-express/47364-fact-sheet/.

[36] NASA/JPL. Odyssey overview. internet, June 2016. http://mars.nasa.gov/odyssey/images/odyssey/timeline/MOI-badge_br.jpg.

[37] NASA/JPL. Odyssey overview. internet, July 2015. http://mars.nasa.gov/odyssey/mission/overview/.

[38] NASA/JPL. Tgo_electra_backtoback_cmdseq_20150419.xlsx. internal communication, April 2015. E-Mail from JPL.

[39] RF Team. Tgo x and uhf telecommunication design report. Technical report, Thales Alenia Space, April 2016. Issue 5.

[40] David Weighton. Space communication. University Lecture, 2015.

[41] S. Hurst. Rover vehicle uhf link budget report. Technical report, Astrium, June 2013.

[42] ESA. Rosetta operations engineer. internal communication, June 2016.

[43] J. Y. Leung. *Handbook of Scheduling: Algorithms, Models, and Performance Analysis*. SCRC Peess, 2004.

[44] Prof. Dr. Peter Brucker. *Scheduling Algorithms*. Springer, 5 edition, October 2006. Version 7.1.1.

[45] A. Makovsky, P. Ilott, and J. Tylor. Mars science laboratory telecommunications system design. Technical report, JPL/NASA, November 2009.

[46] C.A. Lewicki, J.A. Krajewski, and P.A.Ilott. Phoenix mars scout uhf relay-only operations. Technical report, JPL/NASA, 2006.

[47] S. Hurst, A. Bull, and B. Boyes. Uhf communication system analysis report. Technical report, Astrium, July 2013.

[48] Jan Karel Lenstra, AHG Rinnooy Kan, and Peter Brucker. Complexity of machine scheduling problems. *Annals of discrete mathematics*, 1:343–362, 1977.

[49] Wikipedia. Gravitational constant. Internet, May 2016. https://en.wikipedia.org/wiki/Gravitational_constant.

[50] Klaas Vantournhout. Exomars tgo, flight dynamics eventfile, interface control document. Technical report, ESA, November 2015.

[51] G. Wilson, I.Shaw, M.Niezette, and H.Dreihahn. Ems interface control document. Technical report, ESA, March 2014.

Glossary

BLK is a Roscosmos deep space antenna near Mosow, Russia. 7–9, 28, 29, 49, 51, 54, 55, 57, 58, 62, 67–70

booking refers to the allocation of ground station tracking time by a mission. 39, 40, 87

CAN is a NASA DSN deep space antenna in the Canberra Deep Space Communication Complex near Canberra, Australia. 7, 9, 58, 69

CEB is an ESTRACK deep space antenna near Madrid, Spain. 7–9, 58, 87

downlink is defined as the transmission of data from a satellite to a ground station. 6–8, 10, 11, 23, 27, 29, 30, 39–42, 44–46, 56, 57, 60, 68–70, 72, 87–89, 95, 96

DSN short for Deep Space Network, refers to the ground stations, which are capable of providing a datalink between an operations centre and a satellite in deep space.. 7, 9, 26, 29, 57, 58, 62, 63, 68, 69, 71, 72, 79, 80, 98

Electra a NASA software defined radio. 11–13, 16, 30, 44, 63, 71, 97

ESOC is short for European Space Operations Centre. Located in Darmstadt, Germany, handles it the controlling of several ESA satellites. 2, 6, 8, 9, 24, 27, 30, 33, 39, 67, 70, 72, 79

ESTRACK is short for ESA tracking station network. Refers to the ESA network of ground stations, providing a datalink between operations centres and satellites. 7–9, 19, 26, 28, 29, 33, 51, 54, 55, 57, 58, 62, 68–70, 79, 80, 87, 98, 101

Eventfile provides the geometrical events, determined by the ESOC flight dynamics office, occurring during a mission, in the form of a XML document. This is in described detail in sec.9.6.1. 7, 13, 19, 23, 33, 34, 39, 48, 92, 96, 98

EXM abbreviation used for the rover which shall be landed within the ExoMars RSP mission. 20, 27, 64, 66, 87

ExoMars is a joint ESA-Roscosmos Mars exploration program. iii, 1, 3, 7, 8, 11, 21–23, 49, 64, 79–81

forward link is defined as the transmission of data from the landers operations centre to the lander. 10, 22–26, 39, 41, 43–45, 50–60, 67–70, 72, 73, 87, 88, 95, 96

GDS is a NASA DSN deep space antenna in the Goldstone Deep Space Communication Complex in the Mojave desert,California, USA. 7, 9, 57, 58, 68–70

KLZ is a Roscosmos deep space antenna near Mosow, Russia. 7–9

lander a machine stationed on the surface of an extraterrestrial body. iii, 1, 13, 15, 16, 21, 23–26, 33, 39, 44, 67, 72, 87, 96

MAD is a NASA DSN deep space antenna in the Madrid Deep Space Communication Complex near Madrid, Spain. 7, 9, 58, 69

MAVEN short for Mars Atmosphere and Volatile Evolution Mission, a Mars orbiting NASA satellite, situated in an elliptical orbit with an inclination of 75° and an altitude between 150 and 6200 km. 11, 12, 87

MEX short for Mars Express, an ESA Mars orbiting satellite, situated in an elliptical orbit with an inclination of 86.9° and an altitude between 330 and 10530 km. 12, 87

MLG is an ESTRACK deep space antenna near Malargüe, Argentina. 7–9, 28, 49, 51, 54, 55, 58, 67–69, 87

MRB abbreviation used for the NASA Opportunity rover. 27, 66, 67, 72

MRO short for Mars Reconnaissance Orbiter, a Mars orbiting NASA satellite, situated in a sun-synchronous slightly elliptical orbit with an inclination of 93° and an altitude between 255 and 320 km. 11, 12, 22, 30, 31, 35–37, 60–63, 67, 71, 87

MSL abbreviation used for the NASA Mars Science Laboratory rover. 27, 64, 66

NASA DSN short for NASA Deep Space Network, refers to the ground station network of NASA, operated by JPL, providing a datalink between an operations centre and a satellite in deep space.. 7, 9, 26, 29, 57, 58, 62, 63, 68, 69, 71, 72, 79, 98

NNO is an ESTRACK deep space antenna near New Norcia, Australia. 7–9, 55, 58, 68, 69, 87

NSY abbreviation used for the NASA surface platform, which shall be landed on Mars in 2018.. 27, 66

Odyssey a Mars orbiting NASA satellite in a sun-synchronous circular orbit with 400 km of altitude and a 93° inclination. 12, 20, 22, 30, 31, 37, 62–64, 67, 71, 87

overflight refers to all situations, where the line of sight between an orbiter and a lander is above the minimum elevation, which is necessary to communicate. iii, 1, 2, 13, 15, 19, 21–23, 27, 30, 34–37, 39–43, 45, 46, 48–52, 54–64, 67–73, 87, 89, 95, 96

Planview file provides the bookings of all spacecraft on all ESTRACK stations in a limited time range in a XML document. This is in described detail in sec.9.6.2. 9, 19, 23, 33, 34, 39, 48, 93, 101

return link is defined as the transmission of data from a lander to its operations centre. 10, 22–26, 39, 41, 43–46, 50, 51, 59, 60, 67–73, 87, 88, 95, 96

rover an asset landed (or which shall be landed) on Mars which can move over the its surface. 1, 3, 16, 21–27, 29, 30, 35, 39, 40, 43, 44, 46, 50, 51, 55, 57, 59–64, 66–69, 71–73, 79, 80, 85, 88

RRWT The percentage of RWT used compared to the theoretically available one where the Sun is high enough to work.. 23, 51, 53, 55, 57, 58, 60, 62–64, 66, 67, 71–73

RSM short for Reference Surface Mission, indicating the minimum time period in which the rover is required to work. 21, 23, 30, 33, 43, 49, 51, 52, 54, 56, 58, 59, 61, 63–66, 88, 89

RSP is short for Rover and Surface Platform mission, which is part of the ExoMars program. 3, 7, 8, 10–12, 21–23, 27–31, 46, 49, 64, 69, 79, 80

RUS abbreviation used for the surface platform which shall be landed within the ExoMars RSP mission. 27, 64, 66

scenario marks a certain frame in which the problem of relaying data from and to Mars has to be solved. A detailed description of possibilities can be found in sec.3.. 21, 23, 25, 28–31, 34, 47, 49, 51–55, 57, 63, 66–73, 88, 89, 91–98

sol describes the analogy of Earth's day on Mars. 21, 24, 28, 35, 43, 49–53, 55–57, 59–62, 64, 66–73, 87, 88

surface platform an asset landed (or which shall be landed) on Mars, with a fixed location. 1, 3, 21, 25, 26, 30, 44, 46, 51, 59–64, 66, 68–71, 73, 80, 85

TGO short for Trace Gas Orbiter, an ESA satellite orbiting Mars, which is part of the ExoMars program. 1, 7, 11, 12, 22, 28, 30, 31, 34–36, 41, 44, 49, 51, 56, 57, 60–64, 67, 69–71, 87, 98

uplink is defined as the transmission of data from a ground station to a satellite. 6–8, 23, 24, 27–30, 39–45, 50, 51, 54–57, 60, 68–70, 72, 87–89, 95, 96

Acronyms

ADR Adaptable Datarates. 11, 12

AOS Acquisition of Signal. 10, 99

CRC Cyclic Redundancy Check. 16

EPT Earth Planning Time. 2, 21–26, 29, 42, 44–46, 49–64, 66–68, 71–73, 88, 96, 97

ESA European Space Agency. 1, 3, 7, 11, 12, 33, 79–81

FSPL Free Space Path Loss. 10, 16

IMU Inertial Measurement Unit. 11, 12

ITU International Telecommunication Union. 8

JPL Jet Propulsion Laboratory. 11, 16, 30, 80

$LMST$ Local Mean Solar Time. 4, 5

LOS Loss of Signal. 10, 99

$LTST$ Local True Solar Time. 4, 5, 34–37

MTC Coordinated Mars Time. 4, 5

NASA National Aeronautics and Space Administration. 7, 11, 12, 16, 60, 71, 72, 79, 80

OWLT One Way Light Time. 4, 6, 7, 16, 17, 28, 39–42, 45, 52, 55, 70, 89, 95

ROCC Rover Operations Control Centre. 24, 45

Roscosmos Russian Space Agency. 1, 3, 7, 11, 79

RWT Rover Working Time. 2, 4, 21–26, 29, 42–46, 49–68, 71–73, 80, 87–89, 96, 97

TT Terrestrial Time. 4

TT&C Telemetry, Tracking and Command. 16, 17

UHF Ultra High Frequency. 3, 11

UTC Coordinated Universal Time. 4

List of Tables

List of Figures

9 Appendix

9.1 Appendix A - Table of Constants

$r_{\mathrm{M,eq}}$	$6792.4\,\mathrm{km}$	[2]
$r_{\mathrm{M,po}}$	$6752.4\,\mathrm{km}$	[2]
T_{M}	$24\,\mathrm{h}\ 37\,\mathrm{min}\ 22\,\mathrm{s}$	[2]
M_{M}	$6.4171 \times 10^{23}\,\mathrm{kg}$	[2]
G	$6.674 \times 10^{-11}\,\frac{\mathrm{N\ m^2}}{\mathrm{kg^2}}$	[49]

9.2 Appendix B - CD Content

MA_Joerdening.pdf	The digital version of the thesis
src-Folder	Containing the JAVA source code written during the thesis. This is however not the complete tool, owing to the reason that some underlying classes can not be published for legal reasons.
evaluation-Folder	Containing the Python scripts used to evaluated the produced data
Scenarios-Folder	Folder containing all scenarios produced during the thesis using the naming convention from Sec. 9.5.
windowTool.jar	A compiled version of the tool with its graphical user interface.
consoleTool.jar	A compiled version of the tool for command line calls.

9.3 Appendix C - Usage of the Tool

In order to use the tool, Java8, including JavaFX, and Python, with its side packages numpy and matplotlib, have to be installed.
After installing those, the tool can be started and provides a multiplicity of ways to interact with it. However, each time it is used the interaction can be divided in four subgroups which are described in the individual subsections. The first step is to load data into the tool, described in Sec. 9.3.1. Afterwards, the scenario can be viewed, as explained in Sec. 9.3.2. Simultaneously, the run configurations for the solver can be changed and the can solver be started, described in detail in sec. 9.3.3. Finally, the assessment of the results can be done, described in Sec. 9.3.4.

9.3.1 Loading Data

After launching the tool, a toolbar is shown on its right side. This contains, inter alia, the four buttons shown in Fig. 9.1(a), which can be used to load data into the tool. Of those four buttons the lower two are disabled, since, in the beginning, a scenario basis has to be fed to the tool to which additional data can be added later on.
The two options now are either to load an Eventfile or loading an already existing scenario using the related buttons.
Pressing the button for loading an Eventfile a file chooser opens accepting both, .EXM and .xml files. The file filter for switching between the two extensions can be changed at the bottom of the file chooser. After loading the Eventfile it is recommended to save it as a scenario, since loading scenarios is a lot faster than loading Eventfiles. This can be done by pressing the *"Save Scenario"* button and entering an arbitrary name for it.
When deciding to load a scenario on the other hand a dialog opens listing all the scenarios previously stored in the *"./Scenarios"* folder.

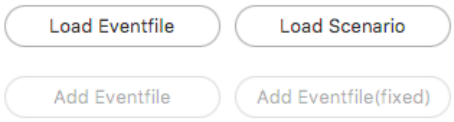

(a): The four buttons available, when starting the tool, two of them being disabled

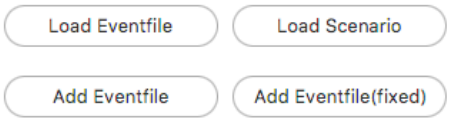

(b): All four buttons being available after a scenario was loaded to the tool.

Figure 9.1: Buttons available for loading data into the tool

After performing one of the steps mentioned above, the two other buttons become available as visible in Fig. 9.1(b). These buttons allow to add additional data to the scenario to e.g. perform a solution for multiple orbiters. The two options are required, since the way of deriving possible relay opportunities is different for orbiters in a circular orbit and the ones in elliptical orbits. For the circular orbits the elevation and azimuth propagation can be calculated from the Eventfile data, while the ones in elliptical orbits can not be predicted using the data available. Therefore, those in elliptical orbits have to be loaded using the button stating that fixed elevations are used. This way the times where the orbit is above ten degrees elevation from the landers perspective are added and no derivation of the actual propagation of elevation and azimuth is done, leading to those periods not being altered when altering the minimum required elevation in the lander options.

9.3.2 Viewing Scenarios

After loading a scenario, the timeline changes and looks similar to the one in Fig. 9.3(a). The upper third is split into enough rows to show all the landers in the scenario. Above this the local true solar time of the first lander is shown. Furthermore, daylight is indicated, by light orange and possible working time by darker orange. In order to see any events, a check tree is provided on the right side as shown in Fig. 9.2. Here the different options can be activated an deactivated to keep the overview while investigating the different scenarios. Activating them fills the scenario as indicate in Fig. 9.3(b).

In addition to those imports, a Planview file can be loaded to simulate bookings on the scenario made by other missions. This can be performed by clicking the *"Load Planview File"*. Afterwards, a dialog shows all missions in the Planview file and the ones checked are added as bookings to the scenario depending on the mission type chosen to the mission name's right.

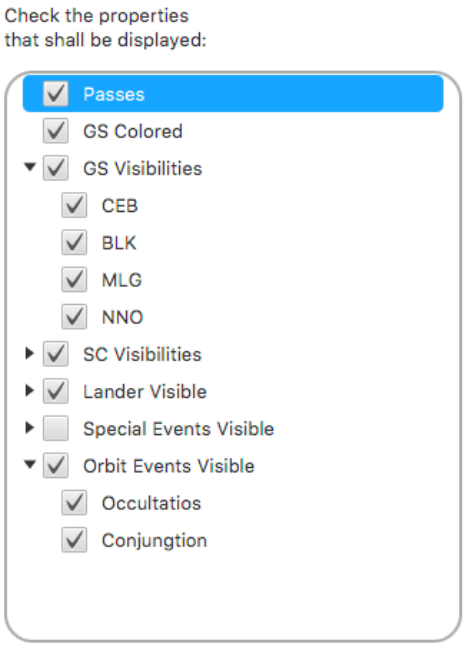

Figure 9.2: The different view options for the scenarios

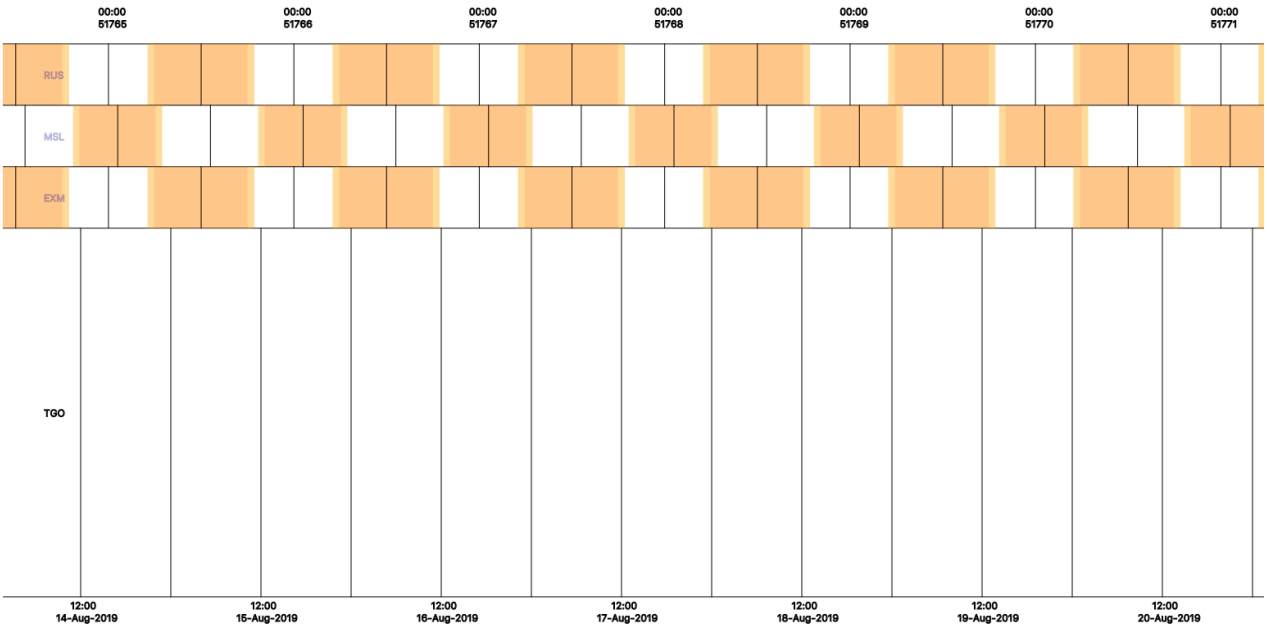

(a): The timeline view after loading a scenario

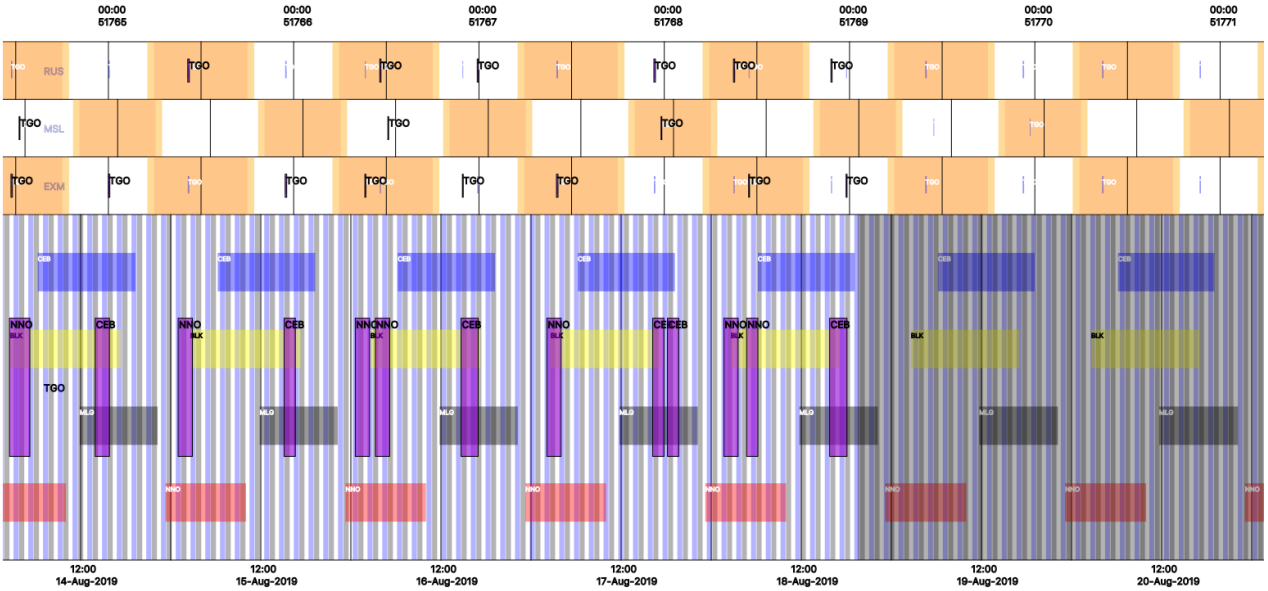

(b): The timeline view after selecting properties which shall be shown

Figure 9.3: The different looks of the timeline

9.3.3 Configuring and Running the Solver

After loading a scenario, different run configurations can be made for the solver, using the lower tool bar of the program. In this, the left window, shown in Fig. 9.4(a), provides global options which alter the reasoning on all assets. The different options are:

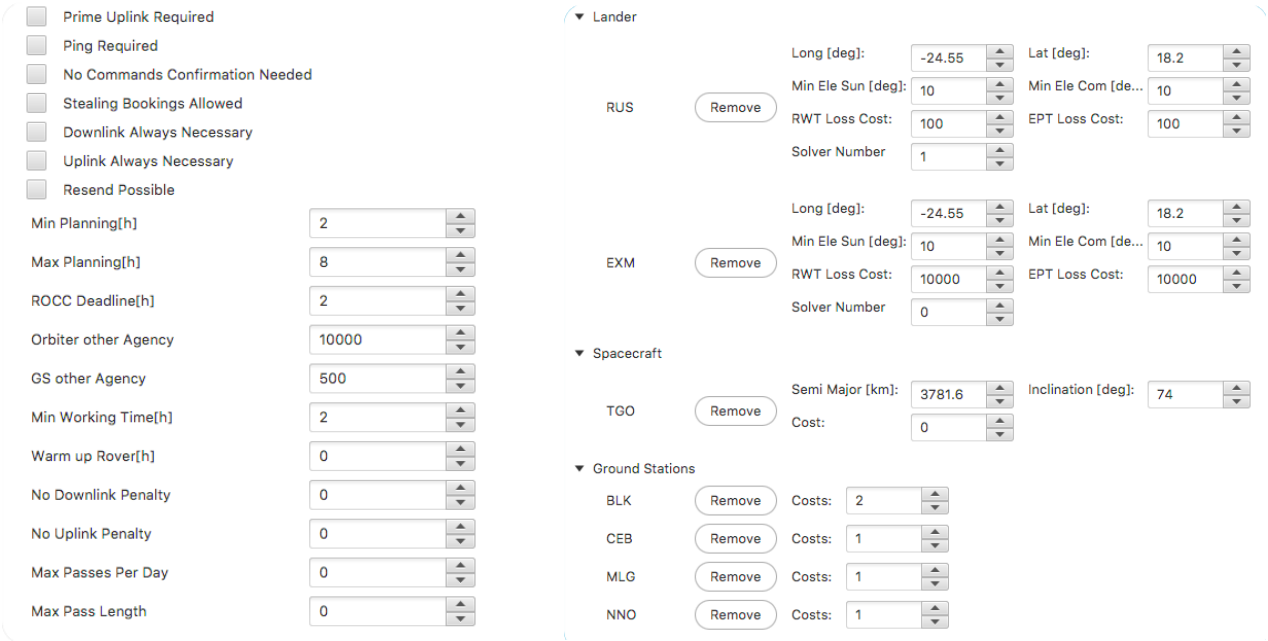

(a): The global solver options available in the tool

(b): The individual solver options available in the tool

Figure 9.4: Run configuration options of the tool

Prime Uplink Required states that a backup uplink opportunity has to be provided

Ping Required extends all uplink passes by two OWLT to provide the possibility of checking that the spacecraft is available using a command.

No Commands Confirmation Needed removes the necessity for the solver to stretch uplink passes by two OWLT to receive a confirmation of the commands sent.

Stealing Bookings Allowed allows the solver to ignore bookings made by other missions.

Downlink Always Necessary allocates a downlink after every overflight to provide as well a data return with a low latency on forward links.

Uplink Always Necessary schedules uplinks for every overflight to provide every time an uplink with a low latency.

Resend Possible allocates enough ground station time to uplink the commands, receiving a confirmation and repeating the sending if an error occurs.

Min Planning [h] sets a constraint on the minimum time between the end of a return link and the deadline for the lander operations centre to deliver new commands.

Max Planning [h] sets the maximum planning time beneficial for the lander operations centre. If more is available, it is not respected in the cost function.

ROCC Deadline [h] sets a constraint on the time which is set to the lander operations centre to provide the commands in hours before the uplink.

Orbiter other Agency sets the penalty costs for using a relay orbiter of an another agency than the one of the landed asset served.

GS other Agency sets the penalty costs for using a ground station of an agency other than one of the served orbiter.

No Downlink Penalty adds the given penalty on the cost function for a forward link if no downlink is provided. This way it is possible to constraint the allocation of downlinks to the cases where they can fit into a certain number of ground station hours.

No Uplink Penalty adds the given penalty on the cost function for a return link if no uplink is provided. This way it is possible to constraint the allocation of uplinks to the cases where they can fit into a certain number of ground station hours.

Max Passes Per Day restricts the number of ground stations passes to this value. Zero implies no restriction.

Max Pass Length gives the solver a length in hours, to which it tries to extend passes. If the passes are longer, than the value given, it is ignored.

The right window on the other hand, shown in Fig. 9.4(b), offers solver options which only impact certain parts of the scenarios. It has three sub-trees:

Lander This tree shows all landers, offers the possibility to remove them from the scenario by pressing the related remove button and lists their individual options. Hereby, the following options can be altered:

- **Long [deg]** states the longitude of the lander in degrees. However, this only alters the local mars time and not the overflights, since those are defined by the Eventfile.
- **Lat [deg]** states the latitude of the lander. The same as for the longitude applies.
- **Min Ele Sun. [deg]** here the minimum elevation of the sun over the horizon required for the lander to be able to work can be altered. This alters the reasoning on the working time.
- **Min Ele Com. [deg]** here the minimum elevation required to communicate with an orbiter can be altered. This changes the duration of the overflight, unless loaded using the fixed elevation button.
- **RWT Loss Cost** shows the multiplication factor applied in the cost function on each lost RWT hour. The usage of this cost factor is explained in Sec. 5.3.1.
- **EPT Loss Cost** shows the multiplication factor applied in the cost function on each lost EPT hour. The usage of this cost factor is explained in Sec. 5.3.1.
- **Solver Number** specifies the order in which the landers are solved (lowest number first). If changing one, the program takes care, that each number is unique.

Spacecraft This tree shows all spacecraft in the scenario , offers the possibility to remove them from the scenario by pressing the related remove button and lists their individual options. Hereby, the following options can be altered:

- **Semi Major [deg]** states the length of the semi major axis of the spacecraft's orbit. Changing this alters the overflights of this spacecraft, if it was not loaded using the fixed elevation button.
- **Inclination [deg]** states the inclination of the spacecraft's orbit. Changing this, alters the overflights of this spacecraft, if it was not loaded using the fixed elevation button.
- **Cost** states the cost for allocating the spacecraft for an overflights. Changing this the spacecraft can be favoured in the solution. It is recommended to choose a value in the same order of magnitude as the RWT and EPT cost factors. This leads to an orbiter only being allocated if more than x hours of RWT or EPT are being lost. The usage of this cost factor is explained in Sec. 5.3.1.

Ground Stations This tree shows all ground stations in the scenario, offers the possibility to remove them from the scenario by pressing the related remove button and lists the cost for one hour of tracking. This cost factor allows to favour ground stations above others. The usage of this cost factor is explained in Sec. 5.3.1.

After setting the desired values the solver can be started by pressing the *"Run Solver"* button. If the scenario was loaded from the data system, one should bear in mind that the scenario has to be saved with a new name before running the solver. Otherwise the old results are overwritten.

9.3.4 Assessing the results

There are multiple ways to assess the results after the solver has been run. The easiest is to use the window in the middle of the lower tool bar. It allows to plot a subset of results by choosing them in the drop-down menu. Hereby the x-axis always marks earth dates and the y-axis hours or MBit in case of the data volume. *"Science"* refers to RWT, while *"Planning"* states the EPT. However, these charts are only provided to give a rough overview.
A lot more accurate data are provided when clicking the *"Show Graphs"* button in the right toolbar. This launches the python script *"./evaluationConsoleMultiple.py"* (or *"./evaluationConsoleMultipleWindows.py"* in case Windows is the operating system) and outputs a multiplicity of information to the user and the data system for easy usage in presentations etc. For this it is however required to install python and its side package matplotlib.
The last option is to export an OOF-file by pressing the *"Export OOF"* button. This outputs a file compliant with the OOF file definitions as of the 23.06.2016.

9.4 Appendix D - Extension of the Tool

Altering the Optimiser

Altering the optimiser and its reasoning is the easiest way in which the functionality of the tool can be changed. For that it is recommended to inherit from the *Optimizer* class and change the *getCheapestDownlink()*, *getCheapestUplink()*, *optimizeOrbiterGroundStationAllocationsForRelay()* and *findOptimizedSelectionOfRelay-Passes()* methods to accomplish the desired reasoning on the passes.
If the output of additional or other data is required, the functions in the ScenarioManager classes can be altered. Hereby, the *writeResults* function should be the only one being changed, since all other functions are required for the storing and loading of scenarios and should not be altered if it can be avoided.
If a change in the evaluation shall be done, the *evealuationMultipleConsole.py* and *evealuationMultipleConsoleNoShow.py* scripts are the things, that have to be changed (or the related Windows ones). The first one is hereby called, when the show graphs button is clicked in the GUI, the latter one is called when the tool is started in the console.

Altering the Radiation Patterns

If new radiation patterns for the assets' antenna gains become available, they can be saved in the *gains* property of the *Spacecraft* and *Lander* class respectively. The spacecraft gains should be an array of gains in 5° steps. The lander gains a two-dimensional array with 30° steps in azimuth in the first dimension and 10° steps in elevation in the second dimension. Alternatively, one can as well inherit from the respective class and override the *getGain()* method to return the right gain upon call.

Altering Gain-Data Rate Table If the gain-data rate table for the Electra radio changes or another relay radio shall be implemented, this can be reflected by altering the contents of the *dataRateMap* of the *Spacecraft*

class. If the spacecraft has no adaptable data rate, a new class, inheriting the *Spacecraft* class should be build and the *getDataRate* should overridden.

9.5 Appendix E - Scenario Naming Convention

In order to provide an easily accessible folder structure for the results after building and processing the scenarios and allowing scripted commands to the tool, a taxonomy for the scenarios was developed. It is defined as:

$$spacecrafts, landers, groundstations, minimum\ comms\ elevation, ops\ constraints$$

with the following possible values:

- *spacecrafts* is the abbreviation from the Eventfile of one or the alphabetically sorted sum of all orbiters available for relay communications in this scenario.
- *landers* is the abbreviation from the Eventfile of one or the alphabetically sorted sum of all landers, which have to be served in this scenario.
- *groundstations* is the abbreviation from the Eventfile of one or the alphabetically sorted sum of all ground stations, which can be used to receive or send data to an orbiter. Hereby, all ESTRACK stations can be abbreviated using $ESTRACK$ and the NASA DSN stations using DSN.
- *minimum comms elevation* is the value for the minimum elevation in degrees needed for communication with the orbiter from all the landed assets.
- *ops constraints* gives the operational margins, which have to be taken into the account by the reasoning in this scenario. The abbreviations used are the same as for the processing speed in Sec. 3.3.1 and are just sorted alphabetically and added comma separated.

The taxonomy for scenario 2a ii would be for example:

$$MRO + TGO, EXM + RUS, BLK + ESTRACK, 10, cc, ro2, rt$$

9.6 Appendix F - Files

9.6.1 Eventfile

The Eventfile provides the geometrical constraints on which every possible solution relies. It contains the visibility periods of all ground stations for the spacecraft, the visibility periods of all landers for the spacecraft, occultations of the spacecraft and when the spacecraft enters solar conjunction and leaves it. A detailed description of it can be found in the related ICD document [50], but a brief description of the different events shall be provided using examples from the TGO Eventfile. In all event files, every event has minimum 4 fields:

- id, giving a unique identification of the kind of event
- time, providing the time when the event occurs
- count, stating the amount of times, that particular kind of event occurred already
- duration, stating the time until the corresponding end event happens, or zero, if no corresponding end event exists

Ground Station Visibility

```
<aos id="A34H" time="2017-324T17:38:14.000Z" count="␣␣␣␣␣␣␣1"
duration="␣␣␣␣␣40971" ems:station="CAN" criteria="h_mask"
elevation="␣9" ems:rtlt="␣2277"/>
<aos id="A34T" time="2017-324T17:45:08.000Z" count="␣␣␣␣␣␣␣1"
duration="␣␣␣␣␣39379" ems:station="CAN" criteria="fix_el_mask"
elevation="10" ems:rtlt="␣2277"/>
<los id="L34T" time="2017-325T04:41:27.000Z" count="␣␣␣␣␣␣␣1"
duration="␣␣␣␣␣␣␣␣␣0" ems:station="CAN" criteria="fix_el_mask"
elevation="10" ems:rtlt="␣2274"/>
<los id="L34H" time="2017-325T05:01:05.000Z" count="␣␣␣␣␣␣␣1"
duration="␣␣␣␣␣␣␣␣␣0" ems:station="CAN" criteria="h_mask"
elevation="␣6" ems:rtlt="␣2274"/>
```

A ground station visibility is indicated by four events. Two are with respect to the horizon mask at the ground station and two with respect to 10° elevation. Latter one is included, since communication with a spacecraft is theoretically possible above the horizon mask, but a higher elevation decreases disturbances, due to surface based clutter. An id ending on H and the criteria "h_mask" indicate hereby, that the horizon mask is crossed and an ending on T or the criteria "fix_el_mask", that the fixed elevation mask was crossed. In both cases the related elevation is given in the equally named key. The entries are hereby starting either with AOS, which means, that the signal is acquired and a possible communication could follow this event, or LOS, which states, that signal will be lost at this point and that communication should end before. In addition to that, every AOS and LOS event contains a station tag, which specifies the station for which the event occurs. With these events, the useable communication can be taken from the fixed elevationAOS and the fixed elevation LOS.

Occultations

```
<occ id="POCS" time="2017-334T01:32:09.000Z"
 count="␣␣␣␣␣␣␣1" duration="␣␣␣␣␣␣␣␣37"/>
<occ id="POCE" time="2017-334T01:32:46.000Z"
 count="␣␣␣␣␣␣␣1" duration="␣␣␣␣␣␣␣␣␣0"/>
```

All occultations are indicated by two events, indicating the start and the end of the bodies being in the line of sight between Earth's centre and the spacecraft. Hereby the id ends on S, if the occultations start is indicated and on E for the end. The rest of the id provides the occulting body and the type of occultation. It can have the following values:

- POCx, if Phobos is the occulting body
- DOCx, if Deimos is the occulting body
- LTCx, if the moon is blocking the TC signal from a ground station. With an extra tag station, providing the related ground station
- LTMx, if the moon is blocking the TM signal from a ground station. With an extra tag station, providing the related ground station
- MOCx, if Mars is the occulting body
- MO2x, if Mars is the occulting body. It indicates the extra event of the line of sight between Earth's centre and the spacecraft being less than 200 km above Mars' surface.

Lander Visibilities

```
<vis id="AL00" time="2017-334T06:31:02.000Z" count="␣␣␣␣␣220"
duration="␣␣␣␣␣␣1032" lander="EXM" criteria="fix_el_mask"
elevation="00"/>
<vis id="ALHM" time="2017-334T06:31:02.000Z" count="␣␣␣␣␣215"
duration="␣␣␣␣␣␣1032" lander="EXM" criteria="h_mask"
elevation="00"/>
<vis id="AL10" time="2017-334T06:34:04.000Z" count="␣␣␣␣␣152"
duration="␣␣␣␣␣␣␣677" lander="EXM" criteria="fix_el_mask"
elevation="10"/>
<vis id="LL10" time="2017-334T06:45:21.000Z" count="␣␣␣␣␣154"
duration="␣␣␣␣␣␣␣␣␣0" lander="EXM" criteria="fix_el_mask"
elevation="10"/>
<vis id="LL00" time="2017-334T06:48:14.000Z" count="␣␣␣␣␣222"
duration="␣␣␣␣␣␣␣␣␣0" lander="EXM" criteria="fix_el_mask"
elevation="00"/>
<vis id="LLHM" time="2017-334T06:48:14.000Z" count="␣␣␣␣␣217"
duration="␣␣␣␣␣␣␣␣␣0" lander="EXM" criteria="h_mask"
elevation="00"/>
```

Each visibility of the lander can be indicated by up to six entries, since each visibility can have two different criteria either "h_mask" (corresponding to the id "ALHM") for indicating the crossing of the local horizon and "fixed_el_mask" for crossing a fixed elevation. Latter can have as well two different elevation values to indicate the crossing of the 0° (corresponding to the id "AL00") and 10° (corresponding to the id "AL10") elevation line.

Solar Conjunction

```
<con id="SE5S" time="2019-220T13:11:23.000Z" count="␣␣␣␣␣␣␣2"
duration="␣␣␣4280502"/>
<con id="ES5S" time="2019-230T15:04:04.000Z" count="␣␣␣␣␣␣␣1"
duration="␣␣␣2550742"/>
<con id="SE3S" time="2019-230T19:29:49.000Z" count="␣␣␣␣␣␣␣1"
duration="␣␣␣2526452"/>
<con id="ES3S" time="2019-236T23:58:17.000Z" count="␣␣␣␣␣␣␣1"
duration="␣␣␣1461475"/>
<con id="ES3E" time="2019-253T21:56:12.000Z" count="␣␣␣␣␣␣␣1"
duration="␣␣␣␣␣␣␣␣␣0"/>
<con id="SE3E" time="2019-260T01:17:21.000Z" count="␣␣␣␣␣␣␣1"
duration="␣␣␣␣␣␣␣␣␣0"/>
<con id="ES5E" time="2019-260T03:36:26.000Z" count="␣␣␣␣␣␣␣1"
duration="␣␣␣␣␣␣␣␣␣0"/>
<con id="SE5E" time="2019-270T02:13:05.000Z" count="␣␣␣␣␣␣␣2"
duration="␣␣␣␣␣␣␣␣␣0"/>
```

The solar conjunction is indicated by eight entries entries, providing the solar conjunction from both points of view described in Sec. 2.3.1.2. Ids starting with an S are indicating that the angle is measured from the spacecraft's point of view and the ones starting with E that the angle is measured from the Earth's point of view. The number in the id states the angle below or above which value in degrees the angle is falling or rising. The last letter is indicating if the angle is falling (S) or rising (E).

9.6.2 Planviewfile

The Planview file states bookings, which are made on the ESTRACK ground station network, which can be fed to the tool as an input. It contains the activity and tracking windows of every spacecraft at every station of the ESTRACK network. A detailed description of it can be found in [51], but a brief overview shall be given as well. Besides extra information a Planview file contains a lot of service session entries, which are the ones mattering for this thesis. Such a service session contains inter alia the following tags:

```
<service_session>
        <satellite_id>ROS</satellite_id>
        <ground_station>DSS-25</ground_station>
        <activity_start>2016-03-10T04:15:00.000Z</activity_start>
        <activity_end>2016-03-10T09:30:00.000Z</activity_end>
        <tracking_start>2016-03-10T05:15:00.000Z</tracking_start>
        <tracking_end>2016-03-10T09:15:00.000Z</tracking_end>
</service_session>
```

The satellite_id is used to determine the satellite booking the station which is indicated in the ground_station tag. The activity_start and activity_end give the times during which the ground station is unavailable for any other spacecraft.